A NEW PARADIGM TO STUDY NF- κB IN VIVO AND THE ROLE OF DIETARY PHENOLIC METABOLITES USING DROSOPHILA

SARA ISABEL GUERREIRO MOTA

A dissertation submitted in partial fulfillment of the requirements for the Degree of Masters in Biomedical Research (Specialization Area: Neurosciences) at Faculdade de Ciências Médicas | NOVA Medical School of NOVA University Lisbon

June, 2022

A NEW PARADIGM TO STUDY NF- κB IN VIVO AND THE ROLE OF DIETARY PHENOLIC METABOLITES USING DROSOPHILA

Sara Isabel Guerreiro Mota
Supervisors: Rita O. Teodoro, Invited Assistant Professor and Principal Investigator at CEDOC
Cláudia N. Santos, Principal Investigator at CEDOC

A dissertation submitted in partial fulfillment of the requirements for the Degree of Masters in Biomedical Research (Specialization Area: Neurosciences)

February, 2022

Part of the results of this thesis were presented in the following meetings:

Sara Guerreiro Mota, Cláudia N. Santos, Rita O. Teodoro. *"Infection and Nervous system: How infection influences neurons and glia".* NBR 5th Edition Welcome Ceremony – NMS, Portugal. 17th September 2021. [Oral Presentation]

Sara Guerreiro Mota, Cláudia N. Santos, Rita O. Teodoro. *"Infection, neural and glial function: Innate Immune mechanisms and food-derived metabolites as a neuroprotective strategy"*. 3rd NMS Symposium on Chronic Diseases and Translational Science. CEDOC - Portugal, 11th - 13th October 2021. [Flash talk]

Sara Guerreiro Mota, Cláudia N. Santos, Rita O. Teodoro. *"A new paradigm to study NF-kB in vivo using Drosophila melanogaster*". CEDOC Casual Friday. CEDOC - Portugal, 19th November 2021. [Oral presentation]

Sara Guerreiro Mota, Cláudia N. Santos, Rita O. Teodoro. *"Dietary phenolic metabolites and brain health: Increasing neuroprotection by reducing neuroinflammation"*. AIMS Meeting 2021. Portugal, 18th – 19th March 2021. [Poster]

Sara Guerreiro Mota, Cláudia N. Santos, Rita O. Teodoro. *"Infection and Synaptic Function: Innate Immune mechanisms and food-derived metabolites has a neuroprotective strategy."* 13.0 iMed Conference - Innovate Competition. Portugal, 7th- 9th October 2021. [Poster]

Sara Guerreiro Mota, Daniela Marques, Catarina Pinto, Cláudia N. Santos. *"Zoom on the link between diet and brain health: how phenolic metabolites modulate brain inflammation".* Licenciatura em Biotecnologia - Politécnico de Leiria, Portugal. 23rd March 2021. [Open class]

During the development of this thesis the following papers were published/submitted:

Carregosa, D.; Mota, S.; Ferreira, S.; Alves-Dias, B.; Loncarevic-Vasiljkovic, N.; Crespo, C.L.; Menezes, R.; Teodoro, R.; Santos, C.N.d. Overview of Beneficial Effects of (Poly)phenol Metabolites in the Context of Neurodegenerative Diseases on Model Organisms. Nutrients 2021, 13, 2940. https://doi.org/10.3390/nu13092940

Mota S., Santos C.N.d and Teodoro RO. A new paradigm to study NF- κ B in vivo using *Drosophila melanogaster* (in preparation).

ACKNOWLEDGEMENTS

In a period of severe challenges, with academic frustrations and an unprecedented pandemic, I am extremely delighted to have chosen to spend this phase in such an amazing place, with such wonderful people. I am truly grateful to every single person that every day lifted my spirit and encourage me to keep going, without whom this work would not be possible.

To begin, I would like to express my gratitude to both of my supervisors, Rita Teodoro and Cláudia Santos. To Rita, for always encouraging me to pursue new subjects and ideas, for all the funny and joyful moments, and for the prompt and endless availability to help me. Thank you for accepting me as your student, and because of that, I only hope I was able to make you proud. To Claudia, for welcoming me with open arms, for all the opportunities you provided and gave me, and above all, thank you for pushing me to think further and beyond. Hopefully, I was able to reach or exceed any expectations you had for me or my work. Thank you both, for being kind and caring, for all the help and support. For being wonderful persons and especially, for everything you taught me, and for being the greatest mentors I could have asked for.

I would like to express the deepest appreciation to all the members of the RT & CNS lab for all the advice, support, and scientific discussions. It was an astonishing journey and an even greater opportunity to be part of such incredible groups, different and amazing in every aspect, and for that, I will always be thankful. I would like to pay my special regards to Joana, for all the help you provided me, always with a smile, even when I asked for it non-stop. Your endless patience and for your never-ending kind words. To Joao, for all your generosity and help. For your unique sense of humor, which although sometimes I was not the first to get, at the end of the day, it always made me laugh. To Catarina, the best artist I know and my "laugh-not-to-cry buddy", for all the help, kindness, and support. For the breath-taking sense of humor, which without my days would have been much greyer. To Mariana, your practical, high-spirited, and contagious personality was always able to lift my mood. I hope you known, that there is no one that I rather flip stocks with, than the four of you. To Cátia, for your sympathy and encouragement whenever you came to the lab. To Diogo, for your fun and easy-going personality. For your promptitude and availability to help me and everyone around you always with a positive a cheerful mood.

I am deeply grateful to my friends, that supported me in the darkest and brightness phases of this journey. To Joana, who even far away, always found a way to keep in touch and cherish our friendship, which I hope to keep for many years to come. Thank you for the long laughs, the well-spent hours during the masters, and especially, for all your help and support during this period. To Miguel, my lifelong friend, with whom I have also shared this scientific journey since day one. Thank you for always earing me out, even when I talk non-stop for hours, and for everything you have ever done for me.

Lastly, but certainly not least, I would like to thank all my family for the support and encouragement. With a special thanks to my mother, with whom I could not have done this without. Thank you for always taking care of me, for your endless and unmeasurable love, for always being supportive, and for encouraging me every step of the way. But above all, thank you for all the sacrifices you have made, throughout your life, to ensure my happiness and success.

Thank you all, now and always.

ABSTRACT

Neuroinflammation is a common feature of neurodegenerative diseases. Although it is still not consensual if it represents the cause or consequence of the development of such pathologies, it is established that sustained pro-inflammatory glial responses can induce collateral damage in the host's nervous system. In fact, glial hyperactivation of innate immune pathways, such as Nuclear Factor kappa-B (NF-κB), can impair neuronal activity and promote neuronal loss, leading to long-term neurological impairments. Thus, the development of strategies to study and modulate glial NF-κB could enable the discovery of plausible therapeutic approaches to balance inflammation in the right direction, mitigating its deleterious effects. Akin to mammals, in *Drosophila melanogaster* the hyperactivation of NF-κB-like proteins, such as Relish, in glial cells has been demonstrated to cause neurodegeneration. Even though great progress has been made in this topic, many aspects regarding inflammation-driven neuronal loss as well as the ability of Drosophila glial cells to be immune responsive remain unclear and ill-defined

Recently, Low molecular weight (poly)phenols metabolites (LMWPM), which originated from fruit and vegetable human metabolism, such as Pyrogallol-sulfate, arose as promising candidates to control neuroinflammation, due to their described *in vitro* abilities to decrease neuroinflammatory markers and their pleiotropic and positive effects in several mammalian and invertebrate neurodegenerative models. Therefore, we aimed to understand the immune responsive ability of fruit flies' glial cells and to develop a method in which we could study the anti-neuroinflammatory ability of LMWPM.

In this study, we established a new paradigm to study *in vivo* NF-κB activation in Drosophila, in a neuroinflammatory context. We use a fused Relish-YFP protein transgene to track its activation upon exposure to gram- bacteria peptidoglycan, an inflammatory molecule known to activate Relish. Here, we identify, amongst the glial cells present in the peripheral nervous system, subperineurial and wrapping glia as immune responders and perineurial glia as non-responsive. Furthermore, we tested if our model was sensible to already known NF-κB inhibitors (such as Aspirin) and studied the anti-neuroinflammatory potential of Pyrogallol-sulfate. We show that Aspirin prevents PGN-dependent activation of Relish in glial cells. Moreover, we are the first to show that Pyrogallol-sulfate has anti-neuroinflammatory properties in a multicellular organism, since we observe that it inhibits Relish PGN-dependent activation in glial cells in 3rd instar Drosophila larvae.

In summary, our findings provide a new *in vivo* neuroinflammatory model to dissect the molecular and cellular mechanisms behind neuroinflammation in Drosophila, filling the gaps regarding the way the fruit flies' nervous system responds to inflammatory molecules. Additionally, our new method demonstrates the potential of Drosophila for the versatile and fast screening of potential anti-neuroinflammatory compounds, paving the way for the discovery of plausible new therapeutics for controlling neuroinflammation and mitigating the impact of neurodegenerative diseases.

Keywords: Drosophila; Neuroinflammation; NF-κB; Relish; Glia; Low molecular weight Polyphenol metabolites

RESUMO

A neuroinflamação constitui um dos fatores mais comuns em doenças neurodegenerativas. Contudo, ainda não é consensual se este processo representa uma causa ou se é uma consequência. Sabe-se, no entanto, que a ativação continua de mecanismos pro-inflamatórios induzem graves danos colaterais no sistema nervoso. Um exemplo destes mecanismos é a hiperactivação da via do fator nuclear kappa-B (NF-κB). Deste modo, o desenvolvimento de estratégias para estudar e modular a ativação do NF-κB poderia possibilitar a descoberta de novas terapêuticas de forma a controlar o processo inflamatório, impedindo os seus efeitos prejudiciais. Na *Drosophila melanogaster*, a ativação excessiva de factores de transcrição semelhantes ao NF-κB nas células da glia, como é o caso do factor Relish, também tem consequências nefastas.

No entanto, existem ainda muitos aspetos mal explorados, tais como os mecanismos e a forma pela qual as células da glia na mosca da fruta respondem a um insulto imunológico. Recentemente, os metabolitos fenólicos originados a partir do metabolismo humano de alimentos como as frutas e os vegetais, como o pyrogallol-sulfate, demonstraram possuir grande potencial neuroprotetor, sendo capazes de diminuir vários marcadores inflamatórios *in vitro.* Desta forma, estes compostos fenólicos podem ser candidatos promissores para o controlo da neuroinflamação e para a diminuição do impacto negativo que esta pode ter sobre o organismo. Deste modo, tínhamos como principal objectivo o desenvolvimento de uma estratégia para poder investigar não só a capacidade imunitária que as células da glia apresentam na mosca da fruta, como também o estudo do potencial anti-neuroinflamatório de compostos fenólicos. Neste trabalho estabelecemos um novo paradigma que possibilita o estudo *in vivo* da ativação do NF-κB num contexto neuroinflamatório usando as células da glia da Drosophila. Tomámos partido de Relish-YFP, a proteína Relish fundida com YFP, de forma a seguir a sua ativação após exposição ao peptidoglicano. De entre as células da glia do sistema nervoso periférico da Drosophila, identificámos as Subperineurial e Wrapping glia como capazes de responder a um estímulo inflamatório e as Perineurial glia como incapazes de o fazer. Adicionalmente, demonstramos que o nosso modelo é sensível e passível de ser modulado por anti-inflamatórios já estabelecidos, tal como Aspirina. Neste trabalho demonstramos ainda que o pyrogallol-sulfate possui capacidades anti-neuroinflamatórias num ser multicelular.

Em suma, os nossos resultados providenciam um novo modelo no qual é possível estudar as respostas neuroinflamatórias *in vivo* assim como averiguar quais são os mecanismos moleculares e celulares envolvidos na resposta neuroinflamatória da mosca da fruta. Adicionalmente, o nosso método inovador, permite demonstrar sem sombra de dúvida o potencial da Drosophila como modelo para a rápida testagem de potenciais compostos com interesse farmacêutico e com capacidade de regular a neuroinflamação que mais tarde podem ser testados noutros organismos ou usados para controlar ou mitigar o impacto das doenças neurodegenerativas.

Keywords: Drosophila; Neuroinflammation; NF-κB; Relish; Glia; Low molecular weight Polyphenol metabolites

INDEX

FIGURE INDEX

TABLE INDEX

LIST OF ABBREVIATIONS

ACP1: accessory protein 1

AG: Astrocytic glia

AMP: Anti-microbial peptide

BBB: Blood-brain-barrier

BNB: Blood-nerve-barrier

CG: Cortex glia

CNS: Central nervous system

DAMPs: damage-associated molecular patterns

DAP: meso-diaminopimelic acid

Dif: Dorsal-related immunity factor

Dl: Dorsal

Dredd: Death related ced-3/Nedd2-like caspase

ECM: extracellular matrix

EG: Ensheating glia

GNBP: Gram-negative binding protein

Gram -: Gram negative bacteria

Gram+: Gram positive bacteria

Iap2: inhibitor of apoptosis 2

IKAP: IκB kinase complex (IKK-αβγ)-associated protein

IL: interleukin

IL: interleukin

Imd: Immune Deficiency

IRAK: IL-1R-associated kinase

ISN: intersegmental nerve

IκB: inhibitor of NF-κB

LMWPM: Low molecular weight (poly)phenols metabolites

LPS: lipopolysaccharide

LPS: lipopolysaccharides

LTA: lipoteichoic acid

NF-κB: Nuclear Factor kappa-B

NIK: NFκB-inducing kinase

NL: Neuronal lamella

NMJ: Neuromuscular junction

PAMPs: pathogen-associated molecular patterns

PG: Perineurial Glia

PGN: Peptidoglycan

PGN: peptidoglycan

PGRP: Peptidoglycan receptor protein

PNS: Peripheral nervous system

PRRs: pattern recognition receptors

Psh: Persephone

Pyr-sulf: pyrogallol-sulfate

RIP: Receptor-interacting protein

ROS: Reactive oxygen species

SPG: Subperineurial Glia

Spz: Spätzle

TGFβ: transforming growth factor beta

TJ: tight junction

TLR: Toll-like receptor

TNF: tumor necrosis factor

TNFR: TNF receptor

TNFR: Tumor necrosis factor receptor

TRADD: TNFR1-associated protein with death domain;

TRAF: TNFR-associated factor

UAS: Upstream activating sequence

UAS: Upstream Activation Sequence

Ub: ubiquitin

VNC: ventral nerve cord

WG: Wrapping

1. INTRODUCTION

Every day, animals are exposed to threats and inflammatory cues, which inevitably affect the body's cells and organs, being the brain no exception. In the nervous system, upon the recognition of a potential threat, glial cells engage several immune mechanisms to cope and eliminate that hazard. However, while acute inflammatory responses are beneficial, due to their role in the removal of dying cells or pathogens from the brain, prolonged (chronic) inflammation has been implicated as a major factor underlying neurodegeneration, either promoting or accelerating neurodegenerative disease progression. Interestingly, systemic infections have been shown to potentiate neurodegenerative diseases and although it is becoming increasingly clear that infections can leave long term neurological problems, the mechanisms that underly this association remain elusive and ill-defined. Thus, there is an urgent need not only to find strategies to prevent and tame uncontrolled neuroinflammation, but also to study how inflammatory cues impact neuron-glia communication and drive neurodegeneration. In this work, we will address several questions regarding the impact that inflammatory cues have in the nervous system, as well as to study potential food-derived metabolites in controlling neuroinflammation using the Drosophila 3rd instar larvae peripheral nervous system.

1.1. The nervous system: a brief overview

The ability to adequately respond to external and internal changes is essential for complex animal life and behavior, and this capacity is highly dependent on the nervous system. The nervous system is required for the perception, integration and computation of a variety of stimulus along with the orchestration and transmission of the appropriate response either to the motor system or to visceral organs. Thus, the nervous system is responsible for a series of functions that go from the control of voluntary and reflexive movement and cognition, to the regulation of the functioning of vital organs (Luo, 2016).

The nervous system is normally subdivided in central and peripheral nervous system (CNS and PNS, respectively) (Fig. 1.1A). In the PNS, sensory neurons are responsible for converting external stimuli into electric impulses which are carried from the sensory organs towards the CNS. It is in the CNS that the information received from the periphery is integrated and processed before it is conveyed back through the PNS towards effector organs, which generates the appropriate motor or physiological responses to the sensory stimuli perceived.

These responses are possible due to a very special type of cells - the neurons. Neurons are polarized cells whose main function is to carry and propagate information through action potentials. Neuronal cells are connected through networks forming highly specialized connections between them. These connections are called synapses and it is in their function that relies the basis for the majority of vital functions. Hence, the way that this

communication is established, propagated, received and integrated is tightly regulated and optimized to achieve a given goal (Luo, 2016; Ovsepian, 2017)

Neurons are typically subdivided in three main cellular compartments: dendrites, soma and axons, which have several functions. Briefly, dendrites are cellular processes that are mainly responsible for receiving information, while the soma, also designated as the neuronal cell body, is where the nucleus is located and where most of the incoming information is integrated. The axon, is a long neuronal process that extends from the cell body, where action potentials are formed and travel to the terminal synapses to assure that the information is transmitted to another cell (Brunger et al., 2019; Luo, 2016).

The most predominant strategy to convey information from a neuron to another neuron is through the release of small chemical molecules called neurotransmitters. When an action potential reaches the pre-synaptic terminal, it depolarizes the membrane, leading to the opening of presynaptic voltage-gated calcium channels, and the fusion of synaptic vesicles with the plasma membrane. The fusion of synaptic vesicles releases neurotransmitters into the synaptic clef (the gap between the pre-synapse and post-synapse). These neurotransmitters then bind to membrane receptors that are present in the post synapse, located in close apposition to the presynaptic release sites (Brunger et al., 2019). The activation of post-synaptic receptors leads to the influx of ions in the cell, resulting in a transient alteration of the membrane potential, which can be depolarizing (in the case of excitatory transmission) or hyperpolarizing (inhibitory transmission). This change in membrane potential travels towards the cell body where it is integrated and can lead to an axonal action potential, which propagates along the axon and allows the information received to be carried through long distances. Additionally, multiple neurons can synapse either in the dendrite, the soma or in the axon of another neuronal cell giving rise to multiple ways of transforming or reinforcing a specific message. Nevertheless, chemical synapses are not the only way neurons can communicate. Communication can also be achieved through electrical synapses (Paolicelli et al., 2011). Electric synapses are based on the change of small molecules such as ions from one neuron to the next through gap junctions, channels that directly link the cytoplasm of the two adjacent neurons. But besides two neurons, a synapse can occur between a neuron and an endocrine, gastric or muscular cell (Alcamí & Pereda, 2019; Luo, 2016).

While neurons are the most studied cell type, the nervous system is composed by both neurons and glial cells. For many years, glial cells were viewed as the “glue” that held neurons together. It was believed that glia were a connective tissue whose only function was to provide trophic, metabolic and structural support to neurons. Consequently, their importance and role in health and disease was for many years overlooked.

In the recent couple decades, many studies have shown that glia are much more than just neurons’ side-kick. Glia are electrically non-excitable cells. However, they express a multitude of voltage-gated ion channels, membrane transporters, neurotrophic receptors and neurotransmitters which allows them not only to transmit but also to receive signals from and to neurons or other glial cells (Stevens, 2003). Thus, they are able to influence not only neuronal activity but also the development of the nervous system, independently of

neuronal control. As such, glial cells have been shown to have additional important roles that range from neural regeneration, development and plasticity, to immunity (Paolicelli et al., 2011; Subramanian et al., 2019; Wilton et al., 2019; Yang & Zhou, 2019)

In the human brain, glia outnumbers neurons and have different functions, morphologies and biochemical features among them. There are four major subtypes of glial cells in the vertebrate nervous system: The myelinating glia - Oligodendrocytes in the CNS and Schwan cells in the PNS-, Astrocytes and Microglia.

Myelinating glia are mainly responsible for providing insulation, wrapping axons with their cytoplasmatic extensions and producing what is denominated as myelin sheets. This insulation allows nerve impulses to be rapidly propagated along axons over long distances. Additionally, the formation of myelin is a plastic process, and it is highly dependent on several cellular, mechanical and chemical signals. Myelination can be modified by synaptic activity and experience-driven mechanisms. For instance, active neurons can release glutamate and growth factors that induce the formation of myelin sheets (Bonetto et al., 2020). In addition, this process is necessary for memory recollection since it has been shown that chemical inhibition of myelination during memory formation prevents memory recall (Pan et al., 2020).

Astrocytes possess long processes, whose end feet wrap around the blood vessels. They assist in the formation, regulation and development of the blood-brain barrier (BBB) by inducing and regulating the assembly of tight junctions (TJs) between endothelial cells. Moreover, and like most glial cells, astrocytes, are major sources of extracellular matrix proteins, adhesion molecules and neurotrophic factors having key roles in neuronal growth, development, communication and survival. They are able to regulate the release as well as clear the excess of glutamate, preventing glutamate toxicity and consequent neuronal death. Plus, astrocytes extend long cellular processes that can contact hundreds of thousands of synapses where they influence synaptic plasticity, modulating both pre- and post-synaptic regions. This is achieved through many mechanisms, amongst them is the astrocytic secretion of synaptogenic factors, that can have a positive or negative influence in synaptic function (such as Thrombospondin or Hevin)(Chung et al., 2015; Kucukdereli et al., n.d.; Liauw et al., 2008; Stevens et al., 2007).

Microglia are considered the resident immune cells of the nervous system and, just like other immune cells, they are able to trigger inflammatory responses to fight and eliminate a possible threat. Additionally, they are able to phagocytose damaged cells and debris upon injury or during development, assisting in neuronal remodeling and plasticity through the pruning of synapses during circuit development (Paolicelli et al., 2011; Stevens, 2003)

In fact, synapses are dynamic structures that can undergo rapid formation and elimination and, both astrocytes and microglia, have been shown to mediate synapse pruning (Paolicelli et al., 2011). In this process of synaptic pruning many mechanisms are recruited, being innate immunity no exception. One major example, is the selective recognition and elimination of synaptic connections coated with classical complement proteins (Stevens et al., 2007)(Chung et al., 2015)(Subramanian et al., 2019).

Thus, the communication between neurons and glial cells is tightly regulated in order to maintain proper functioning of the nervous system since, if it fails or becomes dysregulated it compromises many of the host functions. Every day, animals are exposed to both external and internal hazards, which might compromise neuron-glia communication, impair neuronal activity and function, therefore inducing irreversible damage. As such, the nervous system is a highly isolated and protected tissue and animals have developed numerous mechanisms to cope and eliminate possible threats.

1.2. The nervous system: A shielded tissue.

As previously mentioned, the nervous system and the communication between neurons and glia is essential to maintain all vital functions. Hence, to achieve proper neural function it is crucial to maintain neural homeostasis: ensuring both the delivery of nutrients to the brain as well as shielding it from neurotoxic agents or possible pathogens present in the blood.

To achieved this, the CNS is surrounded by a dynamic and selective barrier called the blood-brain barrier (BBB) (Fig. 1.1B) The BBB is composed by endothelial cells, pericytes and the endfeet of astrocytes. Endothelial cells have efflux pumps, specific molecular transporters and also form TJs among them. This creates a diffusion barrier that selectively controls the passage of the smallest polar molecules and macromolecules and prevents most-blood borne substances from entering the brain. Pericytes are embedded in the basal lamina and surround endothelial cells. They are known to regulate the formation and the development of the BBB through the integration of endothelial and astrocyte functions. Pericytes are also responsible for inducing the polarization of astrocyte endfeet and regulate the formation of TJs and vesicle trafficking in endothelial cells (R Daneman et al., 2010; Richard Daneman et al., 2010). Lastly, Astrocytes tightly wrap the vessel wall and are critical for the induction and maintenance of the TJ barrier. Additionally, astrocytes together with endothelial cells and pericytes are responsible for the formation of the basal lamina also called extracellular matrix (ECM). The ECM is an acellular layer that provides a physical barrier for the passage of molecules and peripheral cells. Problems in ECM integrity or dysfunctions in the cellular constituents of the BBB are often correlated with high BBB permeability, inflammation and higher hemorrhage probability (Blanchette & Daneman, 2015; Richard Daneman & Prat, 2015).

Likewise, this protection from external toxic agents also needs to be ensured in the periphery of the nervous system. The PNS is also shielded by the Blood Nerve-Barrier (BNB) which isolates the PNS from the peripheral blood (Fig.1.1C). The BNB although anatomically distinct, being composed only by perineurial cells (pericytes), endothelial cells and the ECM, serves the same function as the BBB. The BNB allows the entry of needed substances, maintaining the ionic balance and keeping out harmful substances or pathogens that would disrupt essential neural functions.

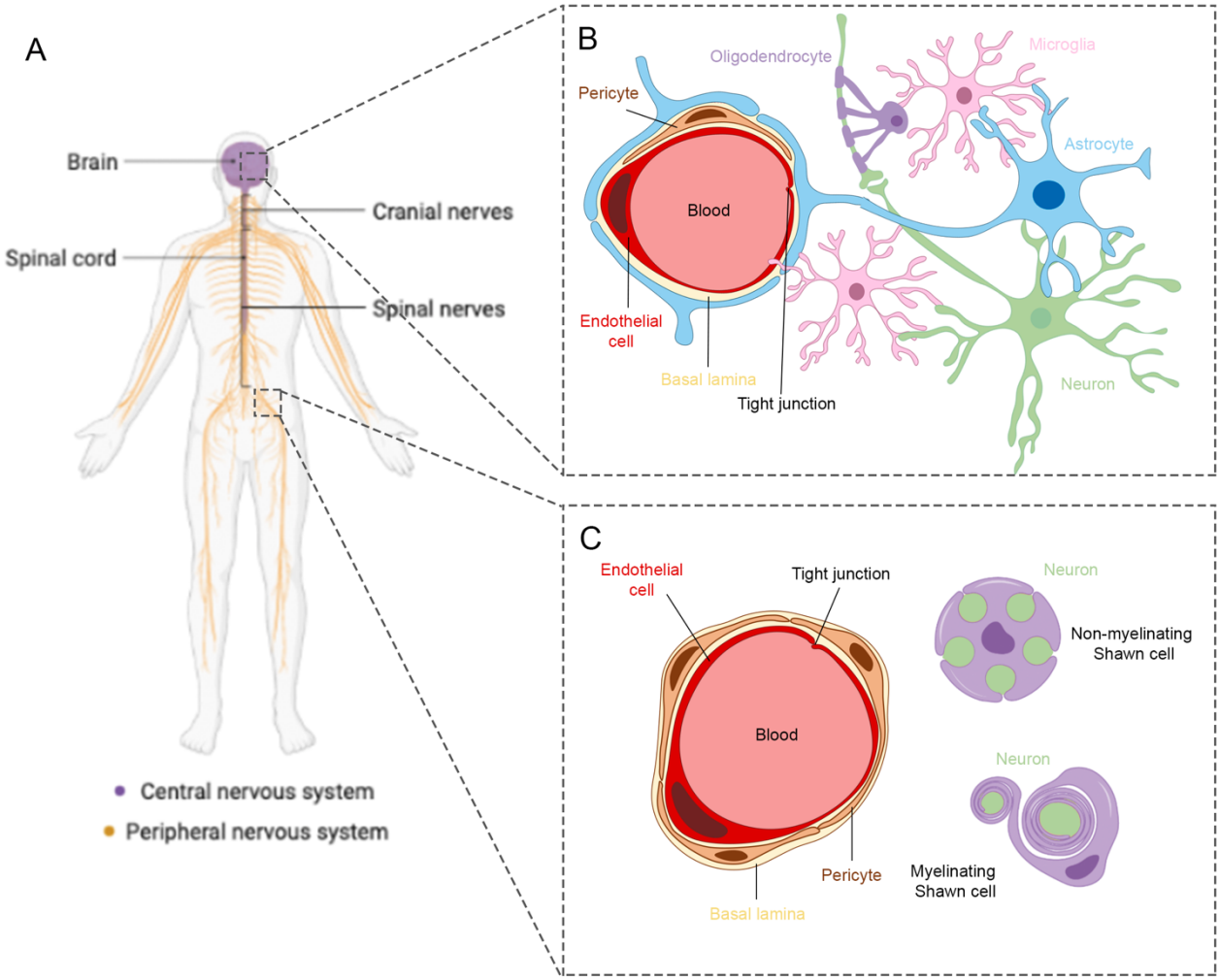

Figure 1.1 Schematic representation of the mammalian Blood-Brain-Barrier (BBB) and Blood-nerve-barrier (BNB). *(A) The nervous system is subdivided in central (brain and spinal cord) and peripheral (composed by peripheral nerves). Both the CNS and PNS are shielded from the blood by the BBB and BNB, respectively. (B) Schematic overview of the cellular environment of the BBB. The BBB is composed by: endothelial cells(red), pericytes(yellow), the end feet of astrocytes(blue) and the basal lamina (also known as ECM). Neurons(green), oligodendrocytes(purple) and microglia(pink) are also represented. (C) Schematic overview of the cellular environment of the BNB. The BNB is anatomical different from the BBB, being only composed by pericytes(yellow), endothelial cells(red) and the basal lamina. In the peripheral nervous system neurons(green) are wrapped by either myelinating or non-myelinating Shawn cells(purple). Endothelial cells, both in the CNS and PNS, form tight junctions among themselves that forms a paracellular barrier, which prevents the infiltration of external molecules, cells and pathogens into in the neuronal tissue. Thus, endothelial cells have specialized transporters (not represented) that allow the selective crossing of nutrients and other needed molecules. Pericytes are embed in the basal lamina and also play key functions in the formation and maintenance of BBB and BNB. Adapted from Biorender.*

Due to the presence of this barrier, the nervous system has been considered, for many years, to be an immune-privileged organ when compared to other peripheral tissues, since this barrier does offer resistance to peripheral immune cells. It was thought that peripheral immune cells were unable to penetrate the neuronal tissue due to the BBB. At a first glance, this would mean that this immune privilege would turn the brain into an immunological blind spot, increasing the risk of infection. However, over the years

increasing evidence has shown that rather than a pure immune-privileged site, the nervous system is always under active immune surveillance. Here, glial cells and the peripheral immune cells bi-directionally communicate to ensure the clearance of cellular debris, and to cope, restrain and eliminate invading pathogens. Still, a heightened neuroinflammatory environment is associated with detrimental effects. Thus, this so-called immune privilege rises not only from the existence of anatomical (such as the BBB) and physiological mechanisms, but also from immunoregulatory processes that tame and control immune responses avoiding destructive inflammation.

1.3. Active immune surveillance of the nervous system: Glial response to PAMPs and DAMPs

The recognition of pathogens is performed by pattern recognition receptors (PRRs) extensively expressed in microglia and peripheral immune cells. PRRs can recognize either pathogen-associated molecular patterns (PAMPs)- molecules frequently found and associated with microbial pathogens- or damage-associated molecular patterns (DAMPs)- molecules, cell components or proteins that are released during cell damage or death. These detection mechanisms emerged phylogenetically before adaptive immunity and are, therefore, considered part of the innate immune system. One of the most well-known forms of PRRs is the Toll like receptor (TLR) family. There are many types of TLRs that recognize different PAMPs and DAMPs (Fig. 1.2.) (Saijo & Glass, 2011)(Nguyen et al., 2016). When TLRs engage with PAMPs or DAMPs, a downstream signaling cascade is activated and culminates in the activation of the Nuclear factor kappa-light-chain-enhancer of activated B cells (NF-κB). NF-κB under normal conditions is arrested at the cytosol and upon activation (i.e.: the release from its inhibitor, IκB), it translocates to the nucleus where it regulates the expression of many genes (Fig. 1.2).

The engagement of TLRs in microglia induces the expression of pro-inflammatory mediators that contribute to the clearance and elimination of pathogens, aggregated proteins, unwanted damaged or infected cells. Plus, the secretion of pro-inflammatory cytokines and chemokines by activated neuroglia also increase BBB permeability and attract peripheral immune cells into the nervous tissue (Fig. 1.3.). These recruited peripheral immune cells have the main goal to provide assistance in the clearance of toxic insults or pathogens (Stankovic et al., 2016).

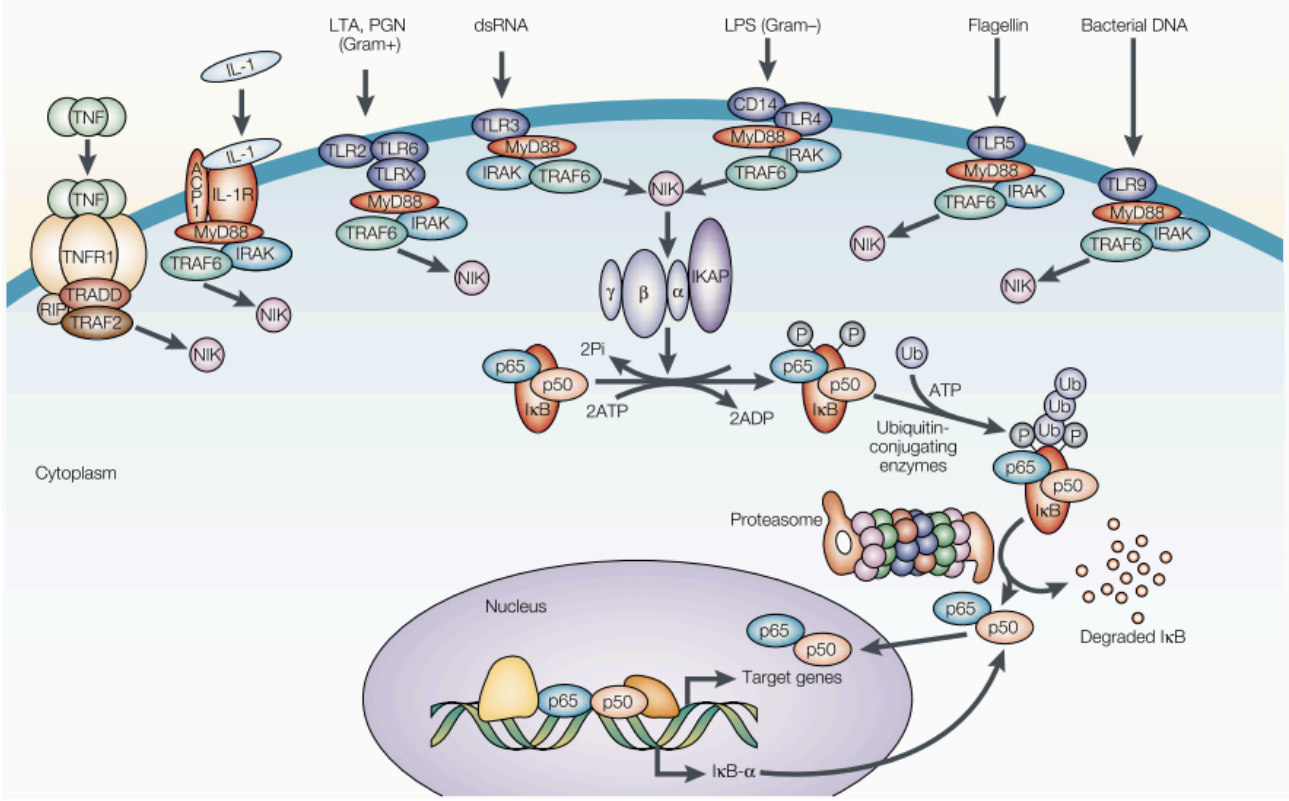

Figure 1.2 Simplified overview of TLRs family and pro-inflammatory signal-transduction pathways that recruit NF-κB. *The activation of TNFR or IL-1R- by TNF-α and IL-1, respectively - culminates in the activation of NF-κB. TLR2 recognizes the pathogen-associated molecular patterns that are produced by Gram-positive (Gram+) bacterial cell wall components such as PGN and LTA. TLR2 can form functional pair with TLR6 leading to signal transduction and cytokine gene expression. TL3 is able to engage in NF-κB activation upon recognition of viruses' dsRNA.TLR4, together with CD14, recognizes LPS from Gram– bacteria. TLR5 is able to recognize flagellin, the principal element of bacterial flagella. TLR9 binds bacterial DNA. All TLRs activate signaling pathways similar to those activated by IL-1, because they share a Toll/IL-1R homology domain that can interact with the adaptor protein MyD88. p50 and p65 are the two most common DNA-binding subunits of NF-κB, which have the ability to trigger the transcription of target genes that encode cytokines, chemokines, proteins of the complement system, enzymes, adhesion molecules, immune receptors and others. ACP1, accessory protein 1; Gram -, Gram negative bacteria; Gram+, Gram positive bacteria; IKAP, IκB kinase complex (IKK-αβγ)-associated protein; IκB, inhibitor of NF-κB; IRAK, IL-1R-associated kinase; LTA, lipoteichoic acid; LPS, lipopolysaccharide; NIK, NF-κB inducing kinase; PGN, peptidoglycan; RIP, receptor-interacting protein; TNF, tumour necrosis factor; TNFR, TNF receptor; TRADD, TNFR1-associated protein with death domain; TRAF, TNFR-associated factor; Ub, ubiquitin. From* (Nguyen et al., 2016)

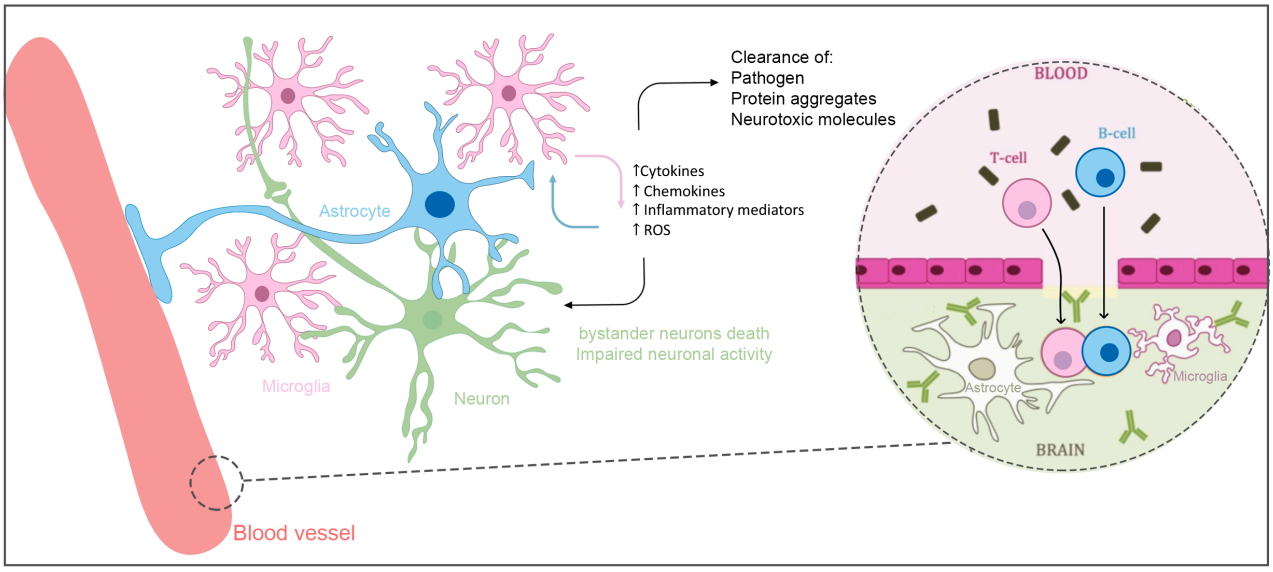

Figure 1.3. Simplified schematic of cellular interactions during neuroinflammation. *Microglia are considered the first line of defense in the CNS. Upon the activation of TLR receptors microglia secrete an array of pro-inflammatory cytokines, chemokines, ROS and NOS. This first response as the main goal to cope and eliminate pathogens, protein aggregates or other neurotoxic molecules. Additionally, the secretion of pro-inflammatory molecules from microglia activates astrocytes that also help in the immune response and in the reestablishment of neuronal homeostasis. Plus, cytokine and chemokine secretion increase BBB permeability and the penetration of peripheral immune cells in the nervous tissue. The invading peripheral immune cells have the main goal to help cope with the inflammatory hazard and the re-establishment of neuronal homeostasis. Both neuroglia and peripheral immune cells can have pro- or anti-inflammatory functions, which are regulated through an intracellular feedback mechanism and contact-dependent/independent intercellular crosstalk. These simultaneous functions have the goal to eliminate the toxic hazard and to minimize the detrimental impact of a heighted neuroinflammatory environment. However, if immune activation persists it may impair neuronal activity and induce neuronal death.*

1.4. Neuroinflammation: When things get out of control

During the course of neuroinflammation, both the responses of glial cells and immune cells are simultaneously coordinated to protect tissues from secondary damage caused by overactivation of inflammation. All these mechanisms are usually sufficient to deal with a toxic agent. However, when overloaded, these mechanisms become detrimental inducing harm to the host. A clear example is the NF-κB activation in glia: NF-κB regulates many important cellular functions which can be interpreted as protective - with roles in tissue repair – or as detrimental - since its hyperactivity has been extensively associated with neurodegeneration.

In contrast to acute inflammation, that lasts from a few hours to a few days, in which the system is able to resolve and reset homeostasis, chronic neuroinflammation can last from months to years.

As previously mentioned, TLR activation in microglia represents the first line of defense against diverse pathogens. However, it also contributes to CNS damage. The engagement

of microglia TLRs and their subsequent activation is shortly followed by astrocytic activation. In fact, chronic neuroinflammation is mainly defined by the consistent hyperactivation of neuroimmune cells (microglia and astrocytes), their transformation to pro-inflammatory active states and the positive continuous engagement that they establish among themselves and with peripheral immune cells. Microglia display different phenotypes and morphologies in both the healthy and the diseased brain (Fig. 1.4). In normal conditions microglia cells have a surveillance phenotype, characterized by their highly motile processes and the continuous monitorization of the neuronal environment. Under acute or chronic activation, microglia cells are activated, losing their surveillance phenotype and their ramified morphology. Upon activation, microglia switch into an amoeboid-like structure that responds according to the nature of the stimuli. During the course of inflammation, microglia can actively transition between different states (M1 and M2). They can behave as neuroprotective cells, known as the M2 phenotype, playing immune resolving and anti-inflammatory functions, through the release of anti-inflammatory mediators (such as IL-10; transforming growth factor beta (TGFβ) and glucocorticoids)(Yang & Zhou, 2019).

As previously mentioned, both pro- and anti-inflammatory responses can be simultaneously activated (Matias-Guiu et al., 2020)(DiSabato et al., 2016). However, in chronic neuroinflammation, the neurotoxic phenotype of microglia (M1) is persistently activated, which blocks their ability to circumvent inflammatory damage, feeding instead a vicious cycle of toxicity. Neurotoxic microglia secrete an array of pro-inflammatory cytokines (such as IL-1β and TNF-α) and reactive oxygen and nitrogen species (ROS, NOS), which are mainly regulated by NF-κB. The continued release of these molecules eventually impair neuronal activity and promotes neuronal death (Nguyen et al., 2016)(Matias-Guiu et al., 2020).

Similar to M1/M2 interchange, astrocytes also exhibit beneficial and detrimental phenotypes during the course of inflammation (Yang & Zhou, 2019). The secretion of pro-inflammatory cytokines, by microglia, results in the activation of astrocytes, which acquire a neurotoxic A1 phenotype. A1 astrocytes contribute to the death of neurons and oligodendrocytes, whereas A2 astrocytes promote neuronal survival and tissue repair (Yang & Zhou, 2019). As previously mentioned, the release of pro-inflammatory cytokines also triggers peripheral immune cells invasion in the neuronal tissue. Akin to acute inflammation, recruited peripheral immune cells have the primer goal to re-establish tissue homeostasis, helping in the elimination of pathogens and tissue repair. However, the sustained activation and recruitment of peripheral immune cells, that also secrete neurotoxic and pro-inflammatory molecules, further engage neuroglia and enhances neuronal death. A clear example of one feed-forward mechanism between neuroglia and peripheral immune cells is based on the release of TNF. TNF- α released either by glia or peripheral immune cells, binds to TNFR in both microglia and astrocytes. This further promotes the expression of TLR2 in microglia and astrocytes, reinforcing NF-κB activation and the expression of pro-inflammatory and neurotoxic molecules. This microglial–astrocyte crosstalk and amplification of inflammatory responses further enhances the damage of bystander neighbor neurons and it is thought to be one of the major

contributors to neurodegeneration(Glass et al., 2010; Hammond et al., 2018; Saijo & Glass, 2011; Stevens, 2003; Yang & Zhou, 2019).

To briefly summarize, there are many types of persistent cues that can promote continuous inflammatory responses and the induction of the neurotoxic phenotype of glial cells. These cues can be either environmental factors (e.g., xenobiotics, toxins and pathogens), or endogenous factors (e.g., protein aggregates) that are perceived by the immune system as "stranger" or "danger" signals (Fig. 1.4). The prolonged exposure to these factors triggers an inflammatory response that establish feed-forward loops, between neuroglia and peripheral immune cells, that overwhelm normal resolution mechanisms. In such situations, both microglia and astrocytes lose their ability to change from pro-inflammatory to neuroprotective phenotypes, becoming unable to perform immune resolving functions and promoting neuronal loss.

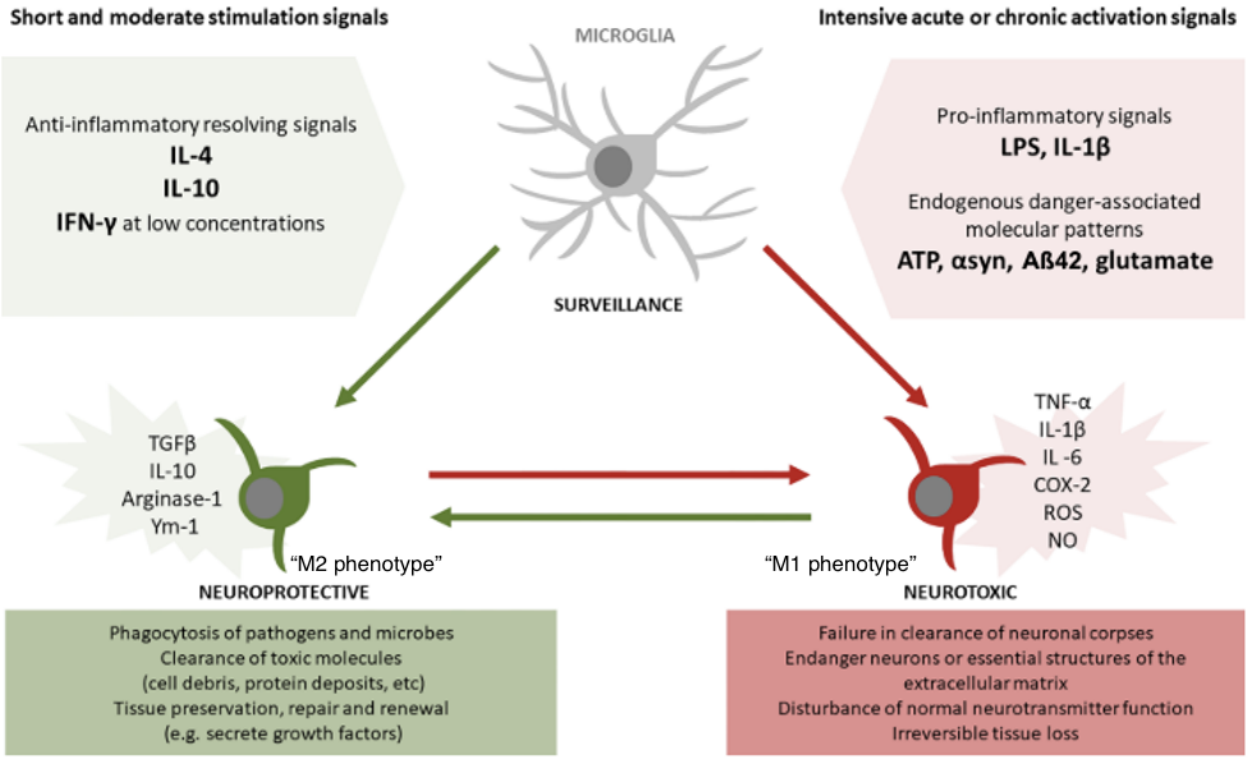

Figure 1.4. Microglia cell phenotypes. *Microglia in normal conditions are at resting surveillance state (gray ramified). Upon recognition of different signals, they become activated and transformed into neuroprotective (green amoeboid) or neurotoxic (red amoeboid) phenotypes. The neuroprotective phenotype, known as M2, is mainly responsible for phagocytosis and for preserving neuronal tissue integrity. The neurotoxic phenotype of microglia, known as M1, produce several pro-inflammatory cytokines that induce peripheral immune cells penetration in the neuronal tissues and further engages microglia and astrocytes in an autocrine and paracrine manner. In chronic neuroinflammation microglia fail to switch from the neurotoxic to the neuroprotective phenotype. This inability induces the uncontrolled release of pro-inflammatory cytokines, ROS, NOS and other molecules that impair neuronal activity and induce the death of bystander neurons, culminating in irreversible tissue loss. IL, interleukin; IFN-γ, interferon gamma; LPS, lipopolysaccharides; αsyn, alpha-synuclein; Aβ42, amyloid beta 42; TGF-β, transforming growth factor beta; TNF-α, tumor necrosis factor alpha; COX, cyclooxygenase; ROS, reactive oxygen species. Adapted from* (Carregosa et al., 2019)

In the PNS, upon injury of peripheral nerves or recognition of potential hazards, there is what is normally designated as local nerve inflammation. Schwann cells maintain neuronal homeostasis and ensure neuronal insulation of the peripheral nervous system. Plus, they are active players in nerve regeneration and immunomodulation (Zhang et al., 2020)(Carr & Johnston, 2017). When nerves are injured, Schwann cells detach from damaged axons and rapidly de-differentiate into an immature-like form of Schwann cells. Despite the loss of contact with axons these cells are able to survive, re-proliferate, migrate, and provide a permissive environment for axonal regrowth (Fig. 1.5). Schwann cells are able to recognize external and endogenous threats and initiate a local immune response. For example, Schwann cells when infected with a pathogen induce the secretion of cytokines and chemokines. The release of these molecules locally increases BNB permeability and attract peripheral immune cells. Peripheral immune cells such as macrophages eliminate infected Schwann cells causing demyelination which can lead to neuronal death, thus having sometimes obvious nefarious effects (Carr & Johnston, 2017; Nocera & Jacob, 2020; Zhang et al., 2020). Chronic nerve inflammation can lead to long term neuronal death and it is in the origin of several peripheral neuropathies.

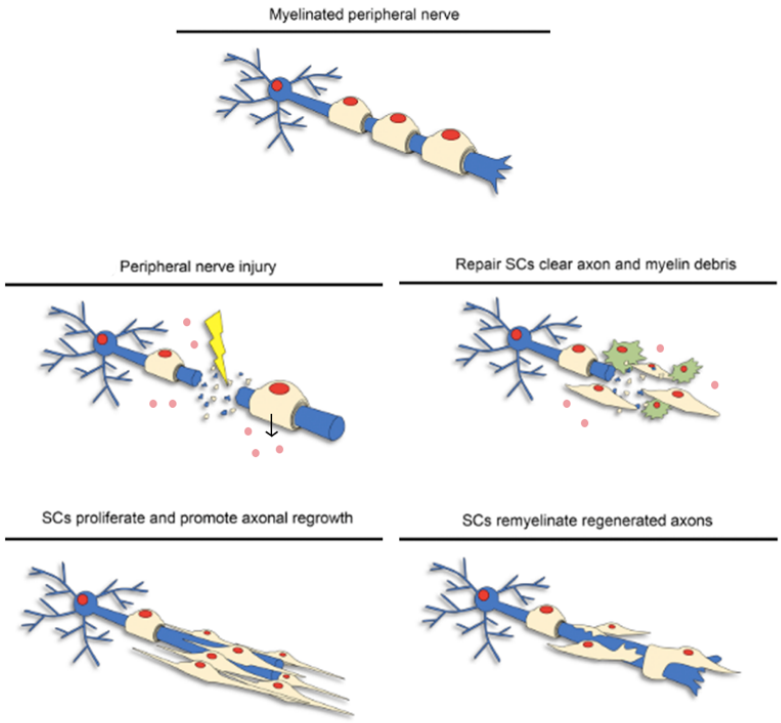

Figure 1.5. Peripheral nerve repair. *Upon injury, Schwann cells (SCs) (light yellow) trigger several molecular cascades that induce the secretion of cytokines, chemokines and other factors, which induce the recruitment of peripheral immune cells (green cells) and provide a premise environment for axon regeneration and re-myelination. SCs and peripheral immune cells are also responsible for the clearance of axon and myelin debris. Adapted from* (Nocera & Jacob, 2020)

Therefore, the balance between pro- and anti-inflammatory responses which is regulated through an intracellular feedback mechanism and contact-dependent/independent intercellular crosstalk between neuroglia and immune cells is of extreme importance, since its dysregulation is in the basis of neurodegenerative diseases both in the CNS and PNS (Nguyen et al., 2016).

1.5. Drosophila as a model system

Over the years, *Drosophila melanogaster* also known as the fruit fly provided critical insights into biological processes proving to be a powerful model system. Due to the remarkable conservation of genes and molecular pathways between fruit flies and mammals allied with less genetic redundancy (i.e., for the majority of genes, Drosophila will have one copy while humans will have a group of genes with the same function), it has been possible to address many biological and mechanistic questions, very difficult to tackle in vertebrates. This allied with many more advantages, addressed below, paved the way for major discoveries in Drosophila, in many fields of Biology.

In fact, since the times of the discovery of the role of chromosomes in heredity in Drosophila by Thomas Hunt Morgan (Morgan, 1915) and the discovery that irradiation induced an increase in the mutation rate in fruit flies by Hermann J. Muller (Muller, 1928), the tools to manipulate and control Drosophila genetics increased exponentially. Currently, researchers have a vast and comprehensive genetic toolkit with which is possible to manipulate the expression of every gene with precise spatiotemporal control and cell specificity. This toolkit ranges from cell-type-specific drivers to compound- or temperature-dependent driver lines. One of the most-well known systems that allow the manipulation of genes is the GAL4-UAS binary system (Fig. 1.6B). (Brand & Perrimon, 1993). GAL4 is a yeast transcription activator factor that can be expressed under the control of given promotor sequence, which will confer cell specificity. Once expressed the GAL4 protein can specifically bind to a UAS (Upstream Activation Sequence), an enhancer nucleotide sequence, allowing the transcription of a target gene localized under the control of the UAS. Additionally, lethal mutations or lines of interest can be kept over "balancer chromosomes". These are engineered chromosomes with multiple inversions that do not allow recombination between the two chromosomes preventing lethality and loss of the desired mutation or insertion. These balancer chromosomes additionally have a visible marker that allows the selection of the desired genotype without the need of sequencing the progeny which is less time-consuming. Another useful tool is the existence of gene-tagged transgenic lines, where the presence of a fluorophore can be used as a proxy for gene expression and protein localization. Moreover, the existence of additional binary systems (LexA-LexAop and QF-UASQF) allow the manipulation of different cell types simultaneously and independently. The use of these systems also allows the cell-specific silencing of a given gene, which permits the understanding of its function in that cell type. For example, the cell specific silencing of a certain gene, which can be achieved by the use of RNAi lines, allows the assessment of its direct effect in that specific cell type (e.g., in glia

or in neurons). Furthermore, this approach also grants the possibility to understand the role of that specific gene in complex animal behaviors. In addition, just like the role of a specific gene can be assessed by examining the phenotypic consequences of its removal, so can the role of a specific cell type (Venken et al., 2011). The silencing or removal of a specific cell, such as neurons, can be achieved through the expression of factors that prevent the release of neurotransmitters or through the expression of toxins that disrupt protein synthesis and promote cellular death, respectively. This astonishing precise and reproducible ways to manipulate the genome has contributed to many discoveries in neuroscience, namely in the understanding of the neuronal circuitry underlying complex behaviors as courtship (von Philipsborn et al., 2011) and sleep (Pitman et al., 2006).

Moreover, in Drosophila, answering specific questions can be much faster, easier and cost-effective when compared to other, more complex, model organisms. This is due to the fact that fruit flies are small living organisms with a relatively short life-cycle (around 10 days at 25◦C) (Fig.1.6A) and short lifespan (~2months). These organisms yield a large progeny with low rearing costs, which boost statistical relevance of the data obtained. In addition, fruit flies are very easy to manipulate and akin to what happens in higher organisms, they exhibit a multitude of complex behavioral phenotypes that allows complex questions to be addressed, including questions related with brain function and immunity (Arora & Ligoxygakis, 2020; Pitman et al., 2006; von Philipsborn et al., 2011).

Drosophila has also grown as a valuable model system in which to study immunity. A clear example of this is the Nobel-prize winning discovery of the Toll receptors and their role in the activation of an immune response against pathogens by Jules Hoffman and its co-workers which prompted the discovered, in mammals, of the Toll-like receptors and the similar mechanisms and molecules to initiate an innate immune response.

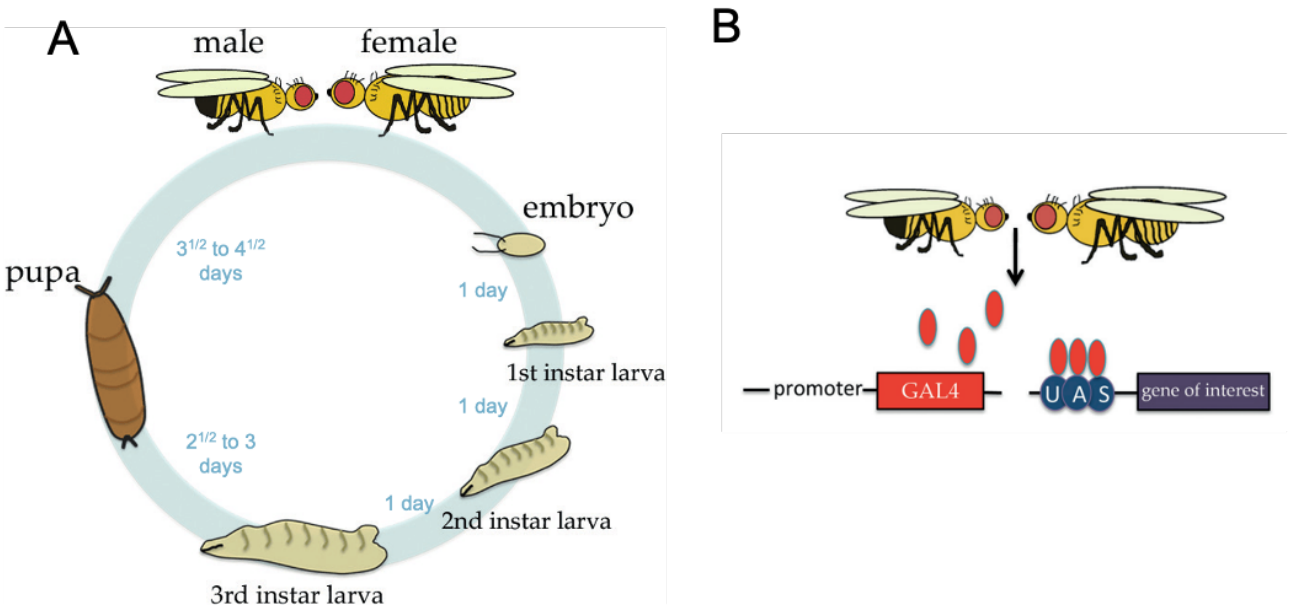

Figure 1.6. Drosophila life cycle and GAL4/UAS system. *(A) Fruit flies' complete life cycle lasts approximately 10 days at 25°C. Flies complete embryonic development as eggs before hatching as first instar larvae. Larvae eat, grow and molt through three larval instars. Upon reaching third instar larval stage, where they stay approximately for 3 days, they metamorphose during pupal stages, where adult forms are formed. Upon*

completing metamorphosis an adult fly hatch. (B) Scheme illustrating how to drive expression of a gene of interest in a tissue specific manner using the GAL4/UAS system. In this scheme, a female fly carries the transgene for the GAL4 transcription factor (red). The Gal4 is downstream of a tissue specific promoter region. If this female fly is mated with a male fly carrying another transgene in which a UAS (upstream activating sequence) is upstream of a "gene of interest," (purple), The offspring of these flies will have both Gal4 and UAS genetic constructs. In these flies, a tissue specific transcription factor will bind to the promoter region of the GAL4 transcription factor inducing the GAL4 expression. Since, the UAS sequence is the binding site for the GAL4 transcription factor, the Gal4 now expressed is able to bind to the UAS sequence. This binding allows the expression gene of interest. In this way, the gene of interest will only be produced in a designated tissue because of the specificity of the promoter placed upstream of the GAL4 transcription factor. Adapted from (Allocca et al., 2016)

1.6. Drosophila nervous system: simple yet powerful

Fruit flies have a nervous system with structural similarities to mammals, exhibiting a multitude of complex behavioral phenotypes that allows researchers to address questions concerning neuronal physiology and behavior, in both normal and disease conditions.

The Drosophila nervous system is also subdivided in CNS and PNS (Fig.1.7). In 3rd instar larvae the brain is composed by the lobes and the ventral nerve cord (VNC, the spinal cord analogue). Peripheral nerves extend from the VNC towards peripheral muscles, visceral and sensory organs (Kohsaka et al., 2012). Larvae are segmented into head, 3 thoracic and 8 abdominal segments. Each hemi-segment contains 30 muscles, 40 motor neurons and 42 sensory neurons (Landgraf et al., 1997). The abdominal segments A2 to A4 have been the most studied due to their stereotypical and well described morphology.

Akin to mammals, in Drosophila the nervous system is composed by both glial and neuronal cells. However, only 10% of the neural cells are glia (much less when compared to humans or other mammals). In Drosophila, there are 6 different glial subtypes: In the CNS there are cortex glia, astrocyte-like glia, ensheathing glia, perineurial glia and subperineurial glia. In the PNS there are perineurial, subperineurial and wrapping glia (a schematic of their organization is depicted in Fig.1.7C-D). Due to the vast molecular tools available in Drosophila, the different glial subtypes can be labelled or specifically manipulated with astonishing precision (Yildirim et al., 2019) .

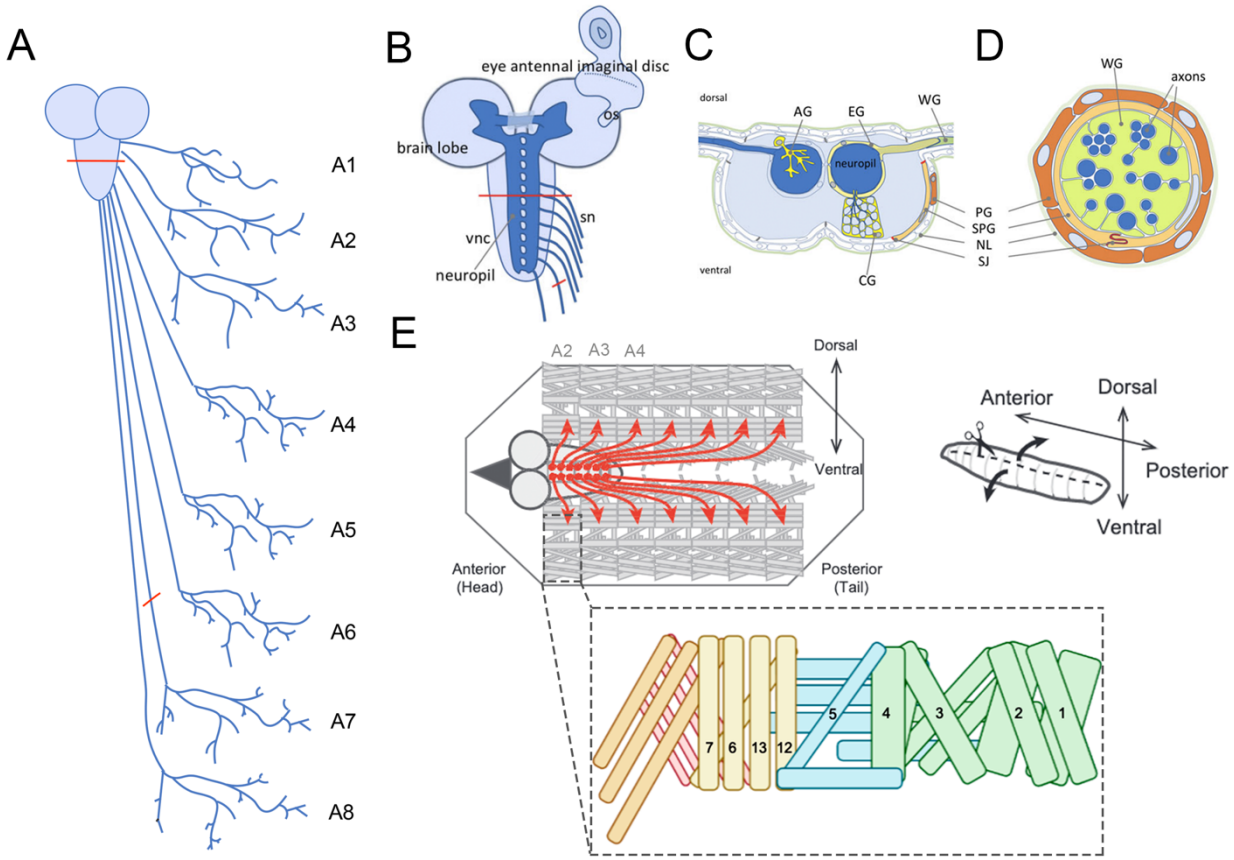

Figure 1.7. Schematics of the Drosophila 3rd instar larvae nervous system. ***(A)*** *Schematic view of a larval Drosophila nervous system (only the right side and abdominal hemi segments from A1 to A8 are represented). The CNS is composed by the central brain and the PNS is composed by peripheral nerves. Peripheral nerves can be subdivided in segmental nerves (SN) and intersegmental nerves (ISN).* ***(B)*** *Closer look to central brain. The central brain is composed by two brain lobes and the ventral nerve cord (VNC). It is to the VNC, more specifically into the neuropil, that all neurons project their axons and dendrites. Peripheral nerves, also denominated as segmental nerves (SN) due to their segmental organization extend from the VNC towards motor and visceral organs. From SN rise intersegmental nerves (ISN), from which motor and sensory neurons innervate their respective tissues. The red lines indicate the position of cross sections shown in (C) and (D). The eye antennal imaginal disc is a peripheral structure from which the eye develops and it is connected to the brain lobes via the optic stalk (os).* ***(C)*** *The CNS is metabolically separated from the larval hemolymph by a glial hemolymph-brain barrier. This metabolic barrier is made by two types of glia and a thick extracellular matrix called neural lamella (NL). The outermost layer of the blood-brain barrier is formed by the perineurial glial cells (PG), that do not contact neurons. Directly below PG lies the subperineurial glia (SPG). These cells establish a diffusion barrier through the formation of septate junctions (SJ). All neuronal cell bodies in the CNS reside in the cortex and are surrounded by cortex glia (CG). The neuropil, where all the synapses are located, is in close contact with astrocyte-like glial cells (AG). Both the neuropil and AG are surrounded by ensheathing glia (EG).* ***(D)*** *The PNS is also isolated from the potassium rich hemolymph. In peripheral nerves, PG and SPG are also responsible for the formation the hemolymph-nerve barrier. Wrapping glial cells (WG), are only found in the PNS and it is responsible for the insulation of the long axons of sensory and motor neurons.* ***(E)*** *Dorsal dissection representative image of the central nervous system and body wall musculature of a 3rd instar larva. Thoracic segments are not represented. Grey dashed line outline a schematic of a single hemisegment musculature. Adapted from* (Yildirim et al., 2019) *and* (Kohsaka et al., 2012).

Analogous with what occurs in vertebrates, the fruit fly's nervous system is isolated from the potassium rich hemolymph (the equivalent to the mammalian blood) by the Hemolymph-Brain-Barrier or Hemolymph-Nerve-Barrier (the homologous to the mammalian BBB and BNB, respectively) (Fig.1.7 C and D). These barriers are mainly comprised by 2 glial subtypes: perineurial and subperineurial glia, which cover the entire CNS and the majority of the PNS. Perineurial glia, together with hemocytes, are responsible for secreting carbohydrates, which form an acellular matrix layer called the neural lamella (NL), also a key constituent of the barrier. Both the NL and perineurial glia are the major contributors to the resistance of the penetration of big molecules in the nervous system. Although perineurial glia offer resistance to the penetration of molecules, they express an array of transporters that allow them to selectively transport needed proteins into the nervous system. Plus, throughout larval stages, in the eye imaginal disc, perineurial glia are able to divide and give rise to other glial types such as wrapping glia. This suggests that perineurial glia are also a multipotent glial source (Bauke et al., 2015; Rut Franzdóttir et al., 2009; Yildirim et al., 2019). To date, no morphological or molecular differences between CNS and PNS perineurial glia have been reported, being therefore assumed that these cells share similar functional properties in all parts of the nervous system. In close contact and positioned bellow perineurial glia are subperineurial glia. subperineurial glia are the main players in the formation of these barriers: they form auto-septate junctions, which makes a paracellular barrier to small toxins, hydrophilic molecules and some infectious agents, while allowing controlled intracellular transport of nutrients (Baumgartner et al., 1996). Additionally, subperineurial glia form gap junctions among themselves. This means that once a specific molecule or protein enters or penetrates the Drosophila BBB, it can be easily propagated and distributed throughout the whole nervous system. Subperineurial glia are on top and in contact with cortex glia in the CNS and wrapping glia in the PNS (Limmer et al., 2014; Yildirim et al., 2019). Thus, 3rd instar larvae peripheral nerves are surrounded by 3 different glial cell types: Perineurial glia, the outermost glial layer. Subperineurial glia that represents the second glial layer and wrapping glia, the innermost glial cell type and the one that is in closer contact with neurons. Wrapping glia are formed during embryogenesis and throughout larval development they do not divide, only growing in size to ensure complete axonal ensheathment and insulation (Yildirim et al., 2019). Wrapping glia do not produce myelin, instead they extend their membrane and enwrap the axons, resembling mammalian non-myelinating Shawn cells (the Remak fibers) allowing for the proper conduction of the nerve impulses (Kottmeier et al., 2020; Rodrigues et al., 2011; Stork et al., 2008; Yildirim et al., 2019). Additionally, it has been reported that wrapping glia also form gap junctions with subperineurial glia allowing the constant communication between these two types of glial cells (Das et al., 2018).

Perineurial, subperineurial and wrapping glia extend and enwrap axons reaching out to the neuromuscular junctions (NMJ). Here, a synapse is formed between motor neurons and the muscle, whose activation is responsible for muscle contraction. The Drosophila 3rd instar larvae NMJ is a highly stereotypic and plastic structure where alterations such as the addition or removal of synaptic connections are easily quantifiable. These characteristics

allow *in vivo* analysis of synapse formation and of the spatial and temporal mechanisms that regulate it (Fernandes et al., 2021). This synapse can also be used to study neuron-glia communication, since at the NMJ glial cells are in close contact and constant communication with the motor neuron. In contrast to wrapping glia, which stop at the bifurcation point where the motor neuron exits the bundle, perineurial and subperineurial glia extend beyond the hemolymph nerve barrier. Both of these glial subtypes extend cellular processes that cover some motor neuron branches, and also contact synaptic boutons and non-synaptic regions in the muscle. These cellular extensions have a wide range of morphologies which can change with neuronal activity and NMJ size (Brink et al., 2012). Additionally, at the NMJ, perineurial, subperineurial glia and the muscle are viewed as neuronal support cells since they are necessary to maintain NMJ homeostasis, clearing the neuronal debris induced by increased neuronal activity as well as engulf the excess of pre-synaptic boutons formed (Fuentes-medel et al., 2009). If this clearance function is inhibited, the motor neuron fails to develop properly and synapse growth is reduced (Fuentes-medel et al., 2009). Additionally, subperineurial glia during development are also able to clear and phagocytose dying neurons (Tasdemir-Yilmaz & Freeman, 2014). Thus, pointing towards the multitude of roles that these glial cells have in synaptic plasticity and development. However, their ability to trigger or circumvent inflammation is unknown.

1.7. How Drosophila fights pathogens: the innate immune system and its players.

All multicellular organisms are continuously exposed to pathogens and thus have evolved sophisticated and effective immune defense mechanisms to fight and eliminate these threats. While mammals and other vertebrates have developed two major types of immune response: the innate and the adaptive immune responses, invertebrates rely only on innate immunity to fight pathogens.

Fruit flies have a well-developed innate immune system to fight infection. Upon infection, flies trigger molecular immune mechanisms with the goal to eliminate pathogens, but this is not all. Fruit flies upon the recognition of infectious agents, also modify their behavior (avoiding feeding on contaminated food or reducing oviposition) with the primary goal to reduce the consequences of infection on themselves and on their offspring (Harris et al., 2018)(Masuzzo et al., 2020; Montanari & Royet, 2021).

Depending on the type of infection different immune mechanisms, which are shared with higher organisms, are mobilized. These mechanisms comprise: physical barriers and both cellular and humoral reactions (Fig.1.8).

The most important physical barriers are the cuticle and the epithelia (in the epidermis, intestinal walls, tracheas and the reproductive system). Both offer resistance to the penetration of microbes in the body cavity and can induce a localized immune response to eliminate pathogens (Lemaitre & Hoffmann, 2007; Tzou et al., 2000). This local immune response is based on the production and secretion of antimicrobial peptides (AMPs), that directly target pathogens and bactericidal ROS (Lemaitre & Hoffmann, 2007). When a pathogen reaches the body cavity both cellular and humoral reactions are mobilized.

The cellular innate response mostly relies in the strong phagocytic capacity of hemocytes (Drosophila blood cells). There are 3 types of hemocytes: plasmocytes, crystal cells and lamellocytes (Vanha-aho et al., 2016; M. J. Williams, 2007). Plasmocytes, resemble mammalian monocytes and/or macrophages. They are mainly responsible for phagocytosing pathogens or strange molecules along with producing and secreting AMPs. As for crystal cells, they play an important role in the coagulation of the hemolymph, melanization and wound healing. These cells are also able to promote the production of bactericidal ROS at the infection site, which further promotes the elimination of invading pathogens. The main function of lammelocytesis the encapsulation of large pathogens during infection or material recognized as non-self that are too large to suffer phagocytosis (Vanha-aho et al., 2016; M. J. Williams, 2007).

Humoral reactions, also denominated as the "immune systemic response" of fruit flies, mainly rely on the expression and secretion of AMPs by the fat body (the main immune organ of Drosophila and the equivalent of the mammalian liver) (Fig.1.8). These AMPs are released into the hemolymph, where they reach their most effective concentration (Arora & Ligoxygakis, 2020; Buchon et al., 2014; Hanson & Lemaitre, 2020; Lemaitre & Hoffmann, 1997, 2007). AMPs are structurally diverse and have a wide range of activities against bacteria (Defensins for gram-positive bacteria and Attacins, Cecropins, Drosocin and Diptericins for gram-negative bacteria) and fungi (Drosomycins and Metchnikowin) (Fig.1.8D) (Lemaitre & Hoffmann, 2007). The majority of these peptides are positively charged and are mostly attracted to the negatively charged pathogen membrane envelope. Upon encounter with the pathogen membranes, they are able to induce the formation of membrane pores and ultimately promote pathogen death (Hanson & Lemaitre, 2020). Furthermore, it is thought that the combined activities of different AMPs largely contribute to block the growth and spreading of invading pathogens. However, in some cases, the successful immune response relies only in a specific AMP. In addition to having different structures and activity spectra, these AMPs are differently expressed depending on the tissue and the pathogen, which confers some level of specificity to this response (Buchon et al., 2014; Lemaitre & Hoffmann, 1997, 2007; Tzou et al., 2000).

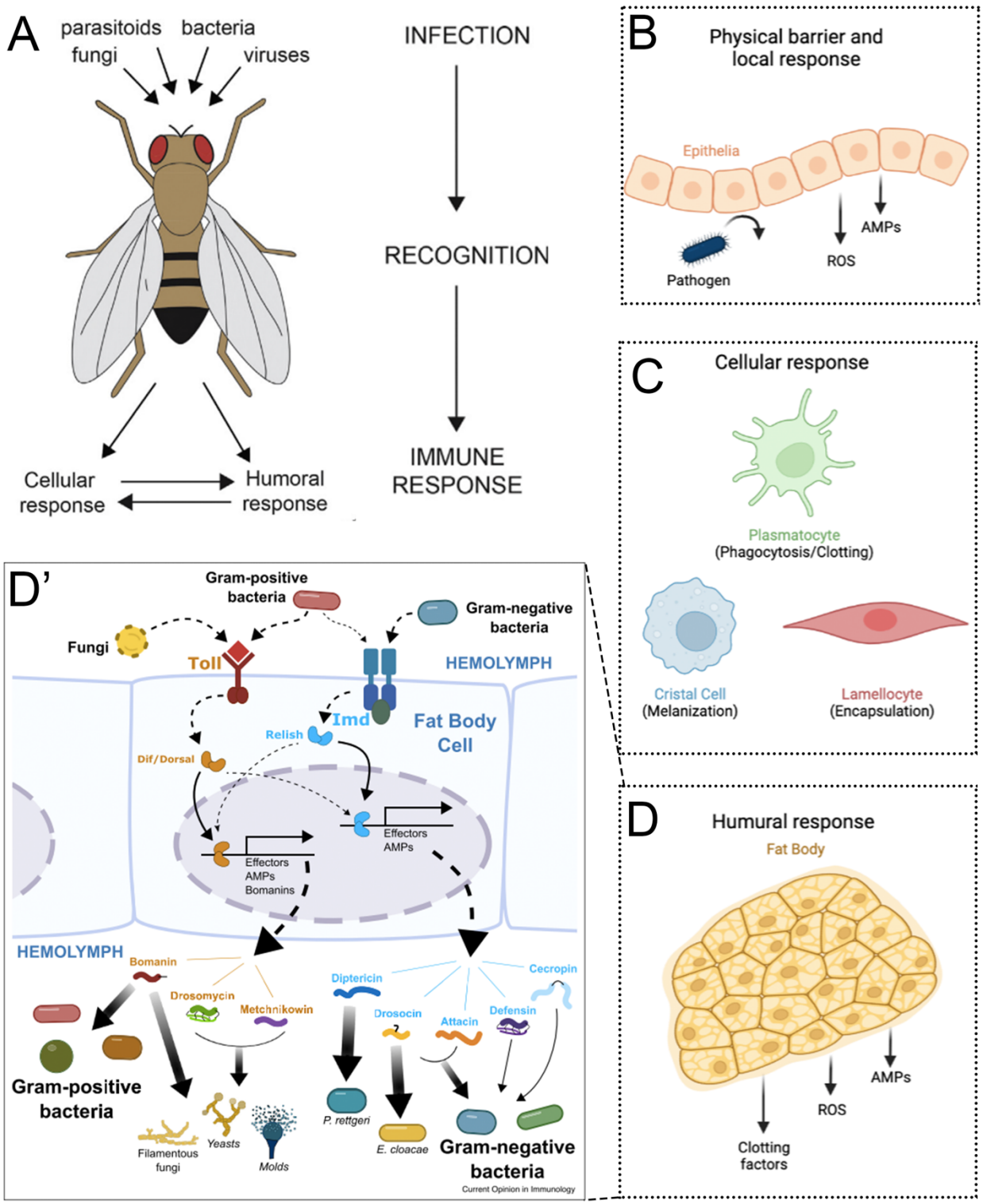

Figure 1.8. A simplified overview of the Drosophila immune response. Some processes depicted in the figure occur only in the larva or in the adult. *(A) Adapted from "cytokines in Drosophila immunity" (B) Epithelia in the epidermis, intestinal and reproductive tracks and tracheas can induce a local immune response when faced with pathogens. Additionally, they comprise physical barriers to the entry of pathogens in the body cavity. (C) Simplified overview of cellular immune response. The cellular immune response in Drosophila is mainly orchestrated by hemocytes – Drosophila blood cells. There are 3 types of hemocytes: Plasmocytes (green) mainly responsible for phagocytosis and clotting. Cristal cells (Blue) mainly responsible for myelinization. Lamellocytes (red) mainly responsible for encapsulation. Hemocytes are also able to produce molecules such as AMPs and ROS that directly target pathogens. (D) Humoral responsible mainly orchestrated by the fat body,*

the main immune organ of Drosophila and the equivalent to the mammalian liver. Upon recognition of pathogens the fat body induces an immune response producing several factors. Among the factor that this tissue secretes into the hemolymph are AMPs, ROS and also clotting factors (D') A zoomed in and simplified overview of the systemic antimicrobial response by the fat body. The recognition of certain pathogens leads to the activation of the Toll, Imd or both pathways. This leads to the downstream activation and nuclear translocation of Dorsal and Dif (orange), in case of the Toll pathway, and Relish(blue) in the case of Imd. Once in the nucleus this transcription factors are able to regulate the expression of AMPs. The Toll pathway regulates the expression of Bomain, Drosomysin and Metchnikowin. As for Imd, it regulates the expression of Diptericin, Drosocin, Attacin, Defensin, Cecropin. These effector peptides are release into the hemolymph and some show broad-spectrum importance against many pathogens (e.g., Bomanin, the combined action of Drosocin, Attacin, and Diptericin). Some processes depicted in the figure occur only in the larva, adult flies or both. See Adapted from(Vanha-aho et al., 2016) *and* (Hanson & Lemaitre, 2020).

In addition to the fat body, muscles have also been implicated in innate immunity in both vertebrates and invertebrates (Chatterjee et al., 2016). In adult *flies*, indirect flight muscles produce AMPs upon an immune challenge. If these muscles appear defective in function, flies fail to mount a potent humoral immune response (Chatterjee et al., 2016).

The expression of AMP genes and the other cellular mechanisms are highly dependent and regulated by two evolutionary conserved signaling pathways: the Toll pathway and the immune deficient (Imd) pathway, the homologous of the mammalian Toll-like receptors(TLR) and mammalian tumor necrosis factor (TNFR), respectively (Lemaitre & Hoffmann, 2007). Although in mammals both TLR and TNF pathways converge in the activation and nuclear translocation of NF-κB, in Drosophila Toll and Imd pathways do not appear to share any intermediate components. These two pathways regulate the expression of different AMPs and effectors due to the activation of different NF-κB like transcription factors – Dorsal and Dif, in the case of Toll, and Relish in the case of Imd. (Lemaitre & Hoffmann, 1997, 2007; Myllymäki et al., 2014)

Before the discovery of the innate immune functions of the Toll pathway, some of its players, including its NF-κB-like transcription factor - Dorsal, were mainly known from their roles in the establishment of the dorsoventral patterning during early embryo development (Steward, 1989). In innate immunity, Toll is mainly activated upon challenge with gram-positive bacteria or fungi. However, and unlike mammalian TLR, transmembrane Toll receptors do not directly bind peptidoglycan fragments but instead are activated by their ligand Spätzle (Spz), a cytokine like molecule. The direct recognition of bacteria, yeast or fungi is performed by Peptidoglycan Recognition Proteins (PGRPs; in this case PGRP-SA), Gram-negative binding proteins (GNBP) or through the cleavage of endogenous proteases. All these processes will give rise to an extracellular proteolytic cascade that gives rise to the Toll receptor ligand Spz. After, Spz binds to the Toll receptor and a signaling cascade that culminates with the nuclear translocation of Dorsal and/or Dif is triggered (pathway schematic is depicted in Fig.1.9). Once in the nucleus, they regulate the expression of several target genes such as AMPs (Bomain, Drosomycin and Metchnikowin) (Fig. 1.8 and Fig. 1.9) (Lemaitre et al., 1996).

In contrast with the Toll pathway, the activation of the Imd pathway is achieved through the direct binding of pathogen elicitors by PGRPs. For example, upon the recognition of

PGN fragments by PGRPs, a molecular cascade is triggered, which terminates in the activation of Relish. In normal situations, Relish is arrested at the cytosol and upon Imd activation Relish C-terminal (ANK repeats domain, which is the IκB homolog for Imd) is cleaved, allowing Relish to enter the nucleus and initiate the transcription of AMPs (mainly Diptericins, Drosocins, Attacins, Defensins and Cecropins) and other target genes (Fig. 1.8D' and Fig.1.9) (Lu et al., 2020; Maillet et al., 2008; Myllymäki et al., 2014)

The main PGRPs involved in the activation of Imd are PGRP-LC, PCRP-LE and PGRP-LA. Additionally, Drosophila encodes more PGRPs that can inhibit Imd activation, such as PGRP-LB and PGRP-LF (Lu et al., 2020; Maillet et al., 2008). These receptors are differently expressed in the organism and, depending on the tissue, they may have different functions and regulate more than one molecular mechanism, leading to different outcomes. Thus, pathogen recognition by PGRPs is an essential step to select the appropriate immune response as well as to regulate it.

Although many studies state that gram-negative bacteria activate preferentially the Toll pathway, whereas gram-positive activate Imd pathway, several other studies suggest a crosstalk where a pathogen can activate both. This double activation can be explained by the different accessibility of PGN. Since PGN from both gram-positive and gram-negative bacteria devoid of Wall teichoic acids are able to activate both Toll and Imd (Vaz et al., 2019).

Furthermore, both Toll and Imd are tightly regulated by extracellular and intracellular proteins to prevent harmful consequences of unwarranted activation. Akin to what occurs in humans and other higher organisms, in Drosophila, improper activation of the innate immune signaling pathways is highly associated with aging, inflammation and neurodegeneration (Badinloo et al., 2018; Y. Cao et al., 2013; Han et al., 2020; Kounatidis et al., 2017; Michelucci et al., 2018)

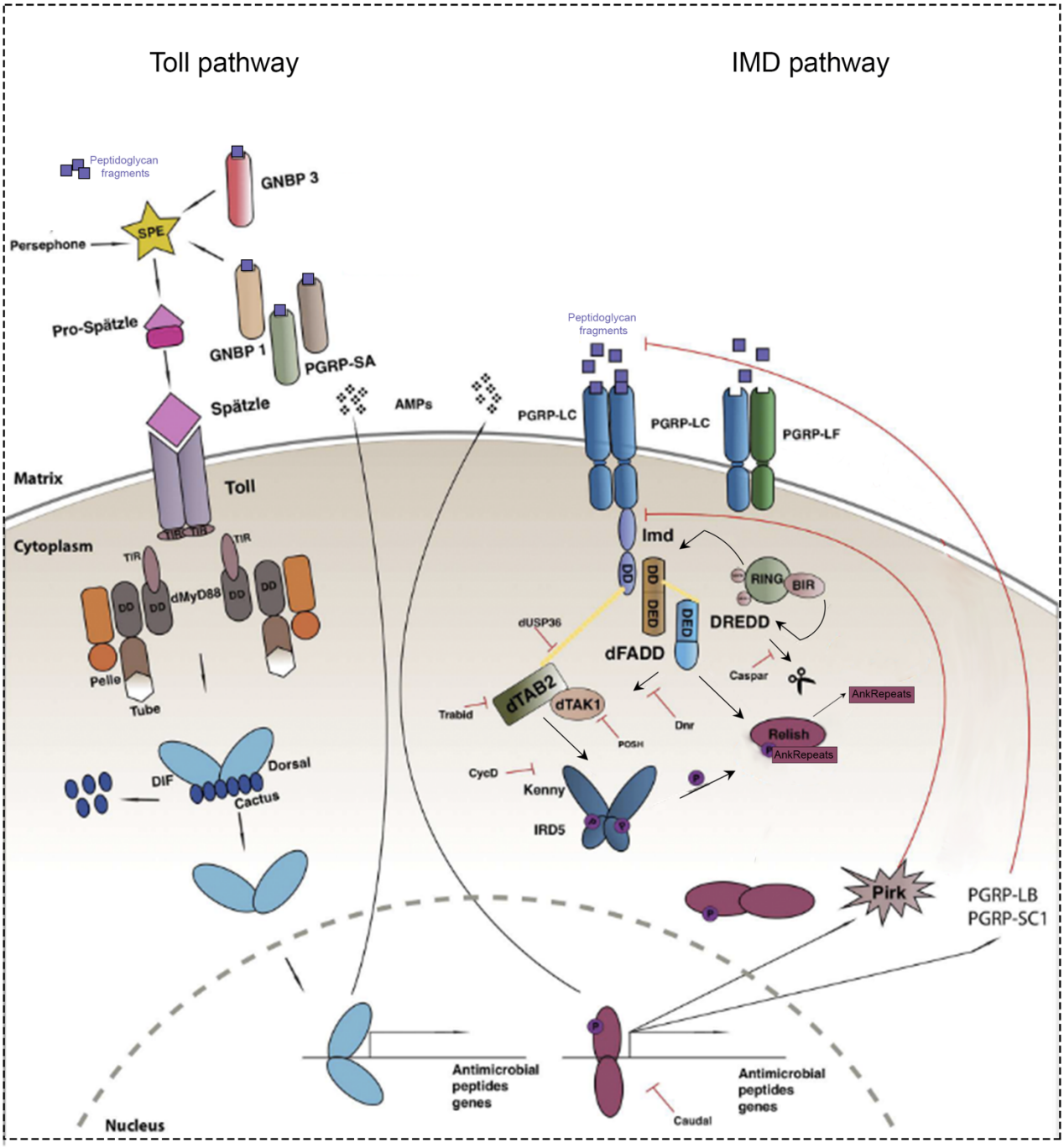

Figure 1.9. Simplified view of the NF-κB like signaling pathways*: The Toll pathway (Left) and the Imd pathway (Right). Toll pathway: The Toll receptor is activated upon binding with a cleaved form of Spatzle, which originates from the proteolytic cascades activated by secreted recognition molecules (PGRP-SA, PGRP-SD, GNBP1, GNBP3) upon the recognition of PAMPs such as PGN fragments. Spatzle binds as a dimer to Toll, thereby inducing its dimerization at the plasma membrane. This induces the recruitment of three intracellular Death domain-containing proteins, MyD88, Tube, and Pelle. Cactus, the NF-κB inhibitor, is then phosphorylated and then degraded by the proteasome. As a consequence, the Rel transcription factors Dif and Dorsal are released and translocate from the cytoplasm to the nucleus where they regulate the expression of several effector genes such as AMPs. Imd pathway: Imd pathway is directly activated by PGN fragments. Bacterial elicitors, mainly monomeric or polymeric DAP-type PGN, directly bind to PGRP-LC. This binding recruits the adaptor protein Imd. Imd then interacts with dFADD, which binds to the caspase Dredd. Relish is then phosphorylated by the IKK signaling complex (IRD5) which is itself thought to be activated by TAK1 and its adaptor TAB2 in an Imd-*

and dFADD-dependent manner. This then allows Dredd to cleave the ANK-repeats, the homologous to the mammalian IkB, and release Relish active domain. The Rel domain translocates to the nucleus, whereas the inhibitory domain remains stable in the cytoplasm. Once in the nucleus Relish regulates the expression of target genes, being amongst then several AMPs. Both the Imd and Toll pathways are tightly regulated by intracellular and extracellular regulators (not all are represented) Additionally, it is worth mentioning that not all PGN receptors are represented in this scheme.

1.8. The multiple neural roles of NF-κB: lessons from Drosophila

In Drosophila, similarly to mammals, glial cells are responsible for maintaining neuronal homeostasis. They play several functions that go from neuronal debris clearance to inflammation, the majority of which are regulated by Toll and Imd pathways (McLaughlin et al., 2019; Sonnenfeld & Jacobs, 1995; Tasdemir-Yilmaz & Freeman, 2014; Winkler et al., 2021). For example, the major receptor expressed in glia that coordinates neuronal debris engulfment is Draper, which expression increases when Spätzle (released from dying neurons) binds and activate the Toll6 receptor in glia. This activation leads to an increase in Draper expression, which is then used by glial cells to recognize "*eat-me-signals*" expressed by dying neurons (McLaughlin et al., 2019). This positive feedback ensures the proper clearance and engulfment of dying neurons, as well as neuronal debris (Arora & Ligoxygakis, 2020). Besides clearing debris, glial cells in fruit flies are also responsible for detection neurotrophic pathogens, upon which they engage in immune responses. Upon pathogen entry in the nervous system, glial cells recruit peripheral immune cells, whose primary goal is to eliminate the infectious agent. This process is dependent on the activation of Imd in glial cells, although the relevance of the different glia subtypes is not fully disclosed (Winkler et al., 2021).

Furthermore, Imd pathway is also linked to behavioral changes in fruit flies. As previously mentioned, fruit flies also modify their behavior in order to avoid the prolonged exposure to pathogens and their transmission to offspring, changing feeding preferences and avoiding egg laying. Some of these behavioral alterations are mediated via Imd, possibly by the recognition of pathogen elicitors by PGRP, expressed in sensory and octopaminergic neurons (Kobler et al., 2020; Masuzzo et al., 2020; Montanari & Royet, 2021) Furthermore, upon bacterial infection fruit flies increase sleep duration, which does not occur in Relish mutant flies. Additionally, some AMPs neural expression can enhance resilience to sleep deprivation, suggesting that Imd pathway has the ability to regulate complex behaviors (Kuo et al., 2010; Montanari & Royet, 2021; J. A. Williams et al., 2007)

While NF-κB is extremely important for survival, being indispensable for neuronal debris clearance, and limiting the damage that is imposed by pathogens, the responses triggered may sometimes come at a cost. In fact, the hyperactivation of NF-κB has been extensively linked with many neurological pathologies, including neurodegeneration. In fruit flies several studies show that sustained activation of NF-κB in glia alone translates into harmful consequences such as neurodegeneration, health and lifespan shortening (Kounatidis et al., 2017; Michelucci et al., 2018; Winkler et al., 2021). When an activated form of Relish is

expressed in glia, larvae show motor problems and never reach adulthood stages (Winkler et al., 2021). In addition, flies with hyperactive Imd display progressive neurodegeneration and reduced lifespan in a Relish-dependent manner (Y. Cao et al., 2013; Kounatidis et al., 2017; Petersen et al., 2013). In fact, forced expression of AMPs alone, reduces lifespan (Badinloo et al., 2018) and mimics neurodegenerative phenotypes which, most of the times, can be rescued by decreasing Relish activation in glial cells (Kounatidis et al., 2017)(Y. Cao et al., 2013). Additionally, it has also been demonstrated that during healthy aging there is an age-dependent increase in Relish activation, together with an increase in expression of its target AMPs genes, an increase in brain inflammation and neurodegeneration (Kounatidis et al., 2017). While reinforcing the idea that Imd dysregulation is involved in neuropathology, some of these studies also paved the way for the discovery of Imd roles in several neurodegenerative models. In fact, recent studies in *D. melanogaster* have linked Imd activation to disease progression (Han et al., 2020). For example, the inhibition of Relish activity has been demonstrated to decrease dopaminergic neuronal loss and motor defects in a Parkinson's disease model (Maitra et al., 2019).

Furthermore, accumulating evidence points towards the pleiotropic functions of several immune effectors and regulators, which also play indispensable roles in the nervous system, ranging from the control of neuronal activity, development and plasticity, to the regulation of complex behavioral outputs such as circadian rhythms (Masuzzo et al., 2020). In fact, while NF-κB inhibition in glia might ameliorate disease progression the same might not be true for neurons. In fruit flies, several key factors of immune signaling are indispensable for neuronal function and development. Toll pathway is necessary for correct CNS development and structural plasticity (McIlroy et al., 2013)(Montanari & Royet, 2021)(G. Li et al., 2020). Additionally, several canonical components of the Imd signaling pathway, namely Tak1 and PGRP-LC are required for homeostatic plasticity at the NMJ, a mechanism which operates to stabilize synaptic activity (Harris et al., 2018)(Harris et al., 2015).

All of these data are in agreement to what is observed in mammals, in which NF-κB also has pleiotropic roles in both glia and neurons (Table 1).

Table 1.1 Brief Overview of NF-κB pleiotropic roles in neurons and glia. Some of the Generalized NF-κB functions both in normal physiology and disease are described.

	Overview of NF-κB functions	
Cell type	Normal physiology	Disease/Hyperactivated states
Neuron	• Synaptic and structural plasticity (Harris et al., 2015; G. Li et al., 2020) • Learning and memory (Barajas-azpeleta et al., 2018) • Growth and development	• Neurodegeneration (Han et al., 2020)
Glia	• Immune Response (Winkler et al., 2021) • Dying neurons clearance (McLaughlin et al., 2019)	• Neurodegeneration/neuronal death (Kounatidis et al., 2017; Y. X. Li et al., 2018) • Locomotor defects and Shortening in lifespan (Kounatidis et al., 2017)

1.9. Low molecular weight polyphenols metabolites: a new strategy to control neuroinflammation.

Age related neurodegenerative diseases are thought to be triggered by multi-factorial events that accumulate throughout life. These pathologies have a significant projected rise in incidence and are among the most burdensome age-related chronic diseases, with both social and economic consequences and no expected cure. In fact, available therapies are far from ideal since the current treatments aim only at alleviating the symptoms. Thus, therapeutic or preventive strategies are urgently needed. A plausible therapeutic approach would rely on multi-ameliorating therapeutics including anti-inflammatory drugs able to decrease NF-κB activation in glia, which is known to increase throughout aging and exacerbate or potentiate age related neurodegenerative-diseases.

A balanced and Mediterranean diet has been associated with positive mood, healthy aging and decreased inflammation, neurodegeneration and cognitive decline (Carregosa et al., 2021; Miller et al., 2018; Nooyens et al., 2011; Psaltopoulou et al., 2013; Spencer, 2022). However, it still remains largely a mystery how dietary-derived metabolites can interact with cells, namely neurons and glia, to mediate these protective effects. However it is known that polyphenols, mainly flavonoids and phenolic acids from the diet can modulate NF-κB activation (Ines ; Figueira et al., 2017). Understanding the mechanisms by which these

metabolites reach and interact with cells in the brain to support neuronal function will be highly valuable to understand brain physiology and to be able to design diet-based therapies to promote healthy aging (Carregosa et al., 2021).

(Poly)phenols are a class of compounds that possess aromatic rings and at least one hydroxyl group. Flavonoids and phenolic acids represent the most biological relevant categories of (poly)phenols due to their high presence in dietary products and their ability to reach circulation. Additionally, it is important to keep in mind that upon ingestion the compounds present in dietary products are not the ones that will reach cells and tissues. After consumption, (poly)phenols in dietary sources are transformed into several metabolites being the most abundant the end-route low molecular weight (poly)phenol metabolites (LMWPM). The small metabolites are the product of metabolic and chemical reactions that occur along the digestive track and in the liver, by human metabolism and microbiota present in the gut (Fig.1.10).

These LMWPM tend to reach the circulation in much higher concentrations (10–30μM) than the original and bigger compounds present in food, being therefore more biological relevant and more likely to direct impact cells. Although these metabolites are able to reach the circulation it does not necessarily mean that they will influence the nervous system, this will be dictated by their ability to cross the highly selective BBB. Some studies have shown that indeed some of these compounds are able to reach the brain either in animal models or *in vitro* (Fig.1.11). (Carregosa et al., 2019; Ines ; Figueira et al., 2017)

Recently, it was observed that pyrogallol-sulfate (Pyr-sulf), a LMWPM resulting from the human metabolism of flavonoids, was able to cross the BBB and decrease NF-κB activation in microglia cells in *vitro*. This shows/reveals the great potential that it can have as a neuroprotective and anti-inflammatory compound (Ines ; Figueira et al., 2017). Still, a major unanswered question is whether this compound is able to inhibit neuroinflammation pathways in a multicellular organism, such as *Drosophila melanogaster*.

Akin to what happens in other organisms the supplementation of (poly)phenols in Drosophila is associated with positive effects such as an increase in lifespan, fecundity and locomotion improvements, not only in healthy conditions but also in genetic and chemical age-related disease models (Yi et al., 2021) (Carregosa et al., 2021). The use of fruit flies from a nutrition perspective in the screening of molecules or extracts with pharmacological potential has been rising, since Drosophila represents a substitute for *in vitro* approaches, also giving the advantage of mimicking the whole tissue and organismal responses, as well as being genetically amenable. However, and although informative, the majority of these studies overlook the precise potential and bioactivity of each individual LMWP, using extracts or (poly)phenol mixtures. Furthermore, the studies with dietary (poly)phenols and extracts do not take into consideration the fact that (poly)phenols might have low bioavailability in humans, together with their metabolism and transformation by human microbiota into LMWPM, before reaching circulation (Carregosa et al., 2021).

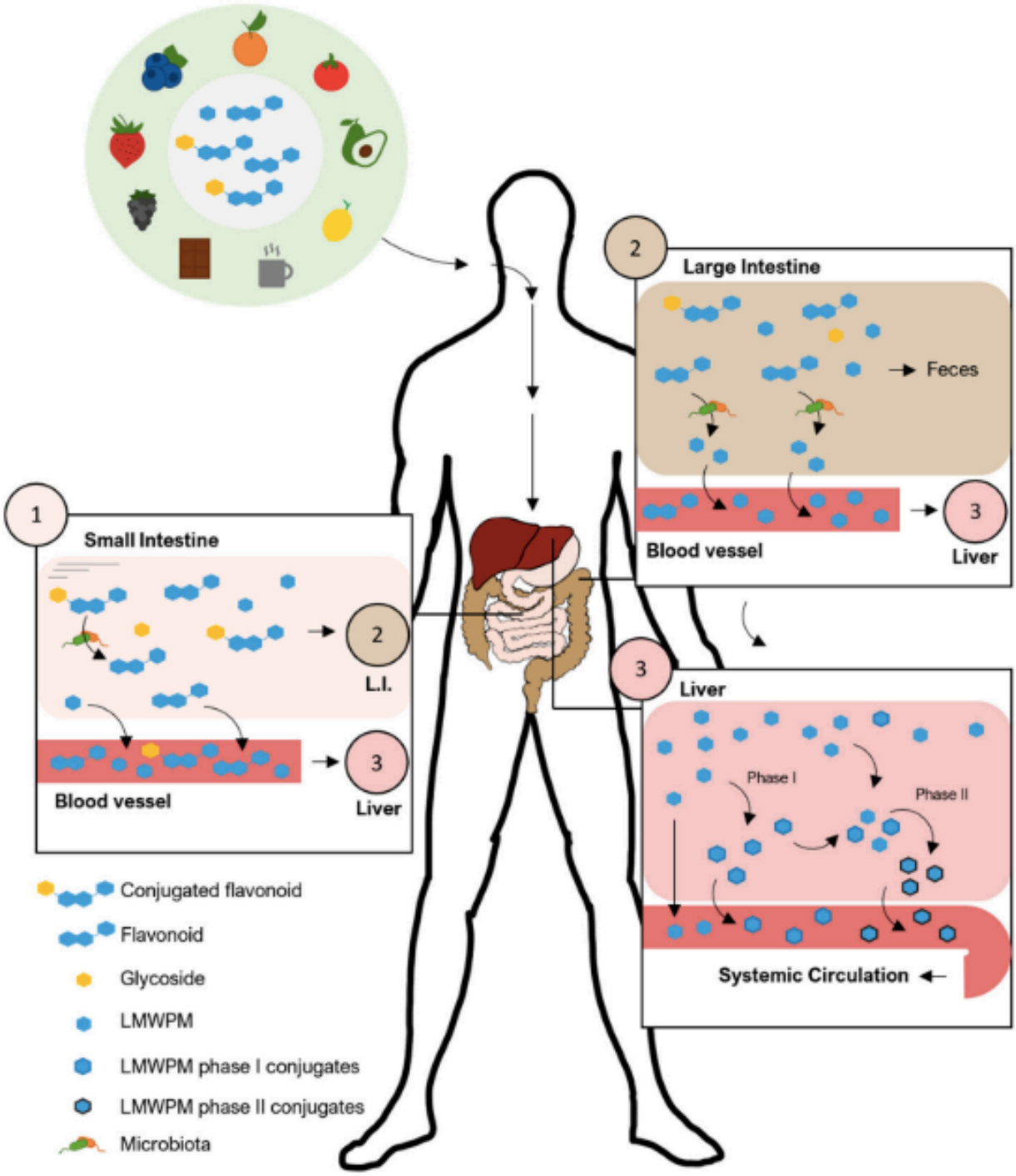

Figure 1.10 From dietary food sources to Low Molecular Weight Polyphenol Metabolites. *Some foods such as fruits and vegetables are very reach in (Poly)phenols. However, the polyphenols present in these dietary sources do not reach the circulation, or do so in very low concentrations. After consumption these (Poly)phenols are transformed: (1) In the small intestine, epithelial and bacterial enzymes remove sugar conjugates while absorption also occurs. (2) The majority of phenolic compounds travel to the lower part of the gut where microbiota catabolizes them into LMWPM. LMWPM are then absorbed into enterohepatic circulation. (3) LMWPM enter systemic circulation intact or undergo phase I and II metabolic reactions by intestinal and liver cells before reaching the circulation. LMWPM: low molecular weight (poly)phenol metabolites. L.I.:(large intestine). From* (Carregosa et al., 2021)

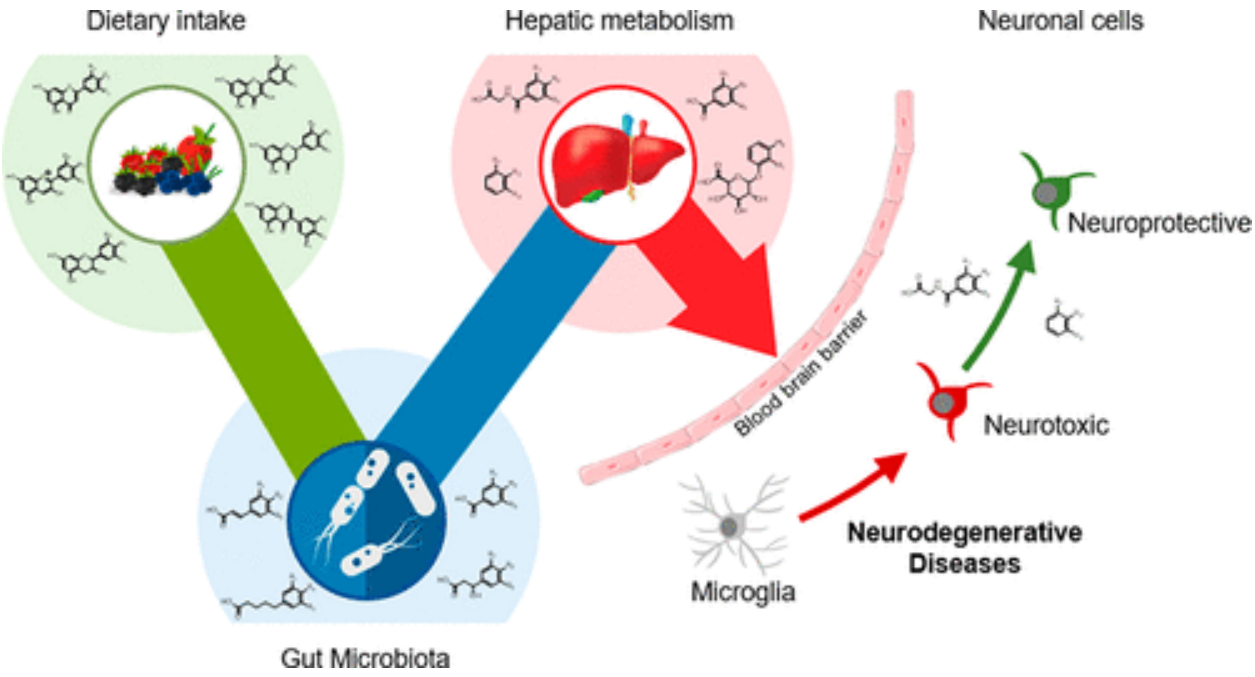

Figure 1.11. LMWPM journey to the brain. *Fruits and vegetables are food sources rich in (poly)phenols, upon ingestion parent compounds suffer alterations by microbiota(blue) and by the human metabolism (intestinal and hepatic, in red) giving rise to the Low molecular weight polyphenol metabolites (LMWPM). Therefore, the absorption and the blood concentration of parent (poly)phenols is very low when compared with their corresponding (poly)phenolic metabolites. Since LMWPM reach the circulation in much higher concentrations they represent much more promising candidates to overcome cellular barriers and reach target tissues, such as the brain. In fact, some studied point to the ability of some LMWPM to cross the able BBB (pink) and inhibit neuroinflammation in microglia, namely NF-kB activation.*

2. OBJECTIVES

Acute inflammatory responses are indispensable to eliminate pathogens or other toxic molecules, but, on the other hand, chronic inflammation induces neuronal loss as along with long term neurological consequences. Therefore, inflammatory responses need to be well balanced to avoid its detrimental activities.

In Drosophila the immune responsive ability of glial cells still remains ill-defined. However, akin to mammals the hyperactivation of NF-kB has been shown to be extensively linked to neurodegeneration. Thus, in this project my main goal was to develop a method in which we could easily assess glial response to inflammation, as well as to study the ability of candidate compounds for attenuating the hyperactivation of innate immune mechanisms involved in neuroinflammation.

Therefore, we had the following main objectives:

1. Assess if peripheral glia cells can respond to a peptidoglycan inflammatory insult.
2. Evaluate if PGN exposure induces any morphologic alterations at the NMJ.

3. Assess the consequences that the hyperactivation of NF-κB has in the peripheral nervous system.
4. Evaluate NF-κB inhibitors and LMW polyphenol metabolite's ability to attenuate NF-κB nuclear translocation in vivo.

3. METHODS

3.1. Fly stocks and husbandry

All flies used were raised and maintained on standard media or fresh yeast paste at 25°C, unless stated otherwise. All fly strains used are listed in Table 3.1.

Fly crosses from the appropriate stocks were performed in fly cages at 25°C, in which the plates with medium and the eggs laid were changed every 12 hours. 3rd instar larval collection was performed directly from the plates. Larvae were briefly washed in PBS1x before performing any experiment.

Table 3.1 Drosophila fly lines

Line	Description/Chromosome (Chr)	Source/Reference
w^{1118}	Wild Type	Bloomington Drosophila Stock Center (BDSC), #3605
Nrv2-GAL4	Wrapping glia driver/ 2nd Chr	BDSC, #6800
Repo-GAL4	Reversed polarity (Repo) is a Pan-glial transcription factor / 3rd Chr	BDSC, #7415
nSyb-GAL4	Pan-neuronal driver	BDSC, #19183
Bsg-GAL4	Perineurial and some Subperineurial glia driver/ 2nd Chr	Kyoto Drosophila Genetic Resource Center, #105188
UAS-CD4-GFP	Encodes CD4, a membrane protein tagged with a GFP under the control of UAS.	BDSC, #35836
UAS-CD8-GFP	Encodes CD8, a membrane protein tagged with a GFP under the control of UAS.	From Dr. Thomas Schwarz lab
UAS-Relish-YFP	Encodes Relish as a fusion protein with YFP under the control of UAS	Gift from Dr. Luis Teixeira (IGC)

UAS-H2B-YFP	Encodes, under the control of UAS, the histone H2B as a fusion protein attached to YFP which indicates nuclear localization / 3rd Chr	Gift from Dr. Catarina Homem (CEDOC)
Ppl-G4	Fat body driver. / 2nd Chr	BDSC #58768
Mhc-G4	Differentiated muscles driver / 3rd Chr	BDSC #55133
PGRP-LC – G4	Expresses of GAL4 under the control of PGRP-LC regulatory sequences. / 3rd Chr	BDSC #77776

For this study the following genotypes were recombined in the same chromosome: MdrG4,UAS-CD4-GFP; RepoG4,UAS-CD4-GFP and Nrv2G4,UAS-CD8.

3.2. Larval Dissection

Briefly, selected larvae were quickly rinsed in PBS 1x in order to remove any yeast paste remains, and were placed in a petri dish or a slide coated with Sylgard (a silicone elastomer SYLGARDTM 184 Silicone Elastomer, The Dow Chemical Company, USA). Larvae were dissected in HL3.1, a hemolymph-like solution known to preserve larval integrity and vitality (in mM: 70 NaCl, 5 KCl, 0.1 CaCl2, 4 MgCl2, 10 NaHCO3, 5 Trehalose, 115 Sucrose, 5 HEPES-NaOH, pH 7.3-7.4). The silicone elastomer present in the petri dish or slide allows the use of thin metal pins (Austerlitz Minutiens Insect Pins, Entomoravia, Czech Republic) or tissue glue (Gluture Topical Tissue Adhesive, Zoetis, USA) to immobilize the larvae. The head and tail of the larvae are pinned or glued, and an incision is made on the posterior region of the dorsal cuticle, using micro dissecting scissors. Larvae are then opened dorsally from the posterior to the anterior region. The 'flaps' created by the cuts are stretched and fixed either with metal pins or glue, exposing the body wall musculature and the central and peripheral nervous system.

For live imaging, the fat body and gut are fully removed maintaining the CNS and PNS intact and a cover slide is position on top of the dissect larvae using Silicone Vacuum Grease (BECKMAN) to fix it and to avoid squashing of the larvae. (Fig. 3.1)

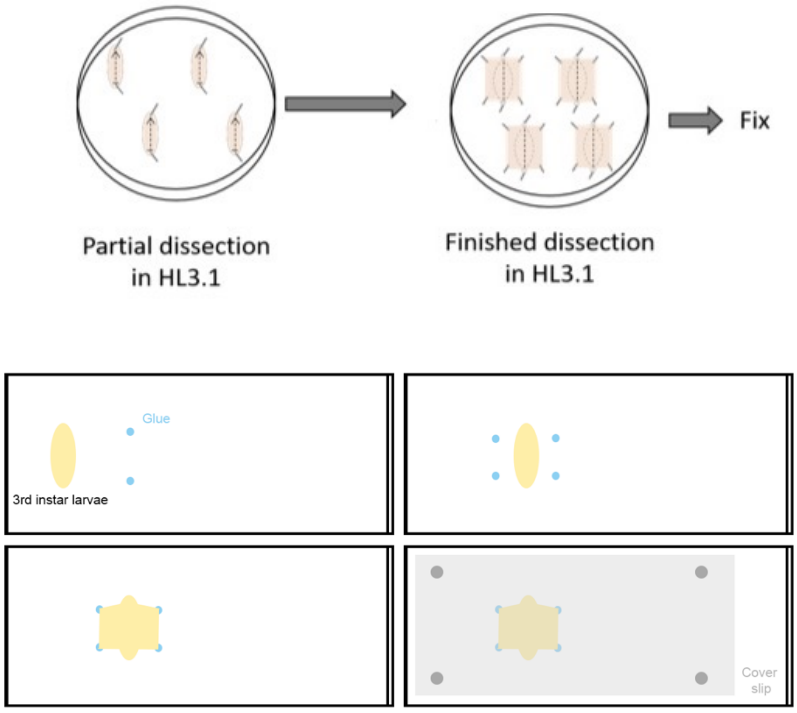

Figure 3.1 Workflow for fixed and live imaging - dissection protocol. *3rd instar larvae are washed in PBS. For fixed imaging (Top) larvae are dissected with the aid of thin metal pins and are then fixed. For live imaging (bottom) larvae are glued to a Sylgard-covered slide. Dissection is performed and flaps are also glued. Silicone Vacuum Grease (dark grey circles) are used to avoid squashing larvae upon cover slide (grey rectangle) positioning. All these processes are performed in HL3.1(not shown) to preserve larval integrity and vitality.*

For fixed imaging, after dissection, larvae are fixed with PFA (4% paraformaldehyde diluted in 1x PBS) at room temperature for 20 min, then thoroughly washed with PBS 1x to remove all the PFA. The gut and fat body is completely removed after fixation in order to allow visualization of the nervous system. Afterwards, larval fillets were extensively washed in 0,3%PBT (1x PBS + 0,3% Triton X-100) for membrane permeabilization and posterior immunocytochemistry.

3.3. Immunohistochemistry and Imaging

After fixation and tissue permeabilization, larvae fillets were blocked for unspecific antibody binding. Blocking was performed for 30 min – 1 hour with 5%NGS (Normal Goat Serum) dissolved in 0,3% PBT. Primary antibody incubation was performed at 4˚C overnight with agitation, in blocking solution (5% NGS in 0,3% PBT). Primary antibody is then removed and larvae fillets are washed an additional minimum of 3 times for at least 15 min each in 0,3% PBT. A secondary blocking is then performed. Secondary antibodies are incubated at RT, shielded from direct light, with agitation, for 2 hours. HRP staining (which

labels neuronal membranes in insects, including Drosophila) was performed with the secondary antibody. After secondary antibody incubation, larvae fillets are extensively washed in 0,3% PBT (at least 3 times, 15min each) before mounting. Larvae were mounted using DABCO mounting media (1,4-diazabicyclo[2.2.2]octane – DABCO, Sigma Aldrich, USA), and stored at 4˚C in the dark until imaging.

All antibodies used and respective concentration are listed in Table 3.2.

To label the neuronal membrane we used anti-HRP antibodies. These antibodies have been shown to label several neural-specific glycoproteins that are present in the central and peripheral nervous system of Drosophila and other insects (Snow et al., 1987; Yeh Jan & Nung Jan, 1982).

Table 3.2 List of Antibodies used in immunocytochemistry

Antibodies	Source / Identifier	Obs.
Mouse anti-Repo	Hybridoma Bank/ 8D12	Labels Reverse polarity (Repo) transcription factor which exists in the majority glial cells. Used at 1:30
Rat anti-Elav	Hybridoma Bank	Elav is a pan-neuronal marker (nuclear marker for post mitotic neurons). Used at 1:50
Mouse anti-DLG	Hybridoma Bank/ 4F3	Labels Discs Large Protein (DLG) present in mature post-synapses. Used at 1:250
Anti-HRP-conjugated A647	Jackson Immuno Research	Used at 1:500
Anti-HRP-conjugated A488	Jackson Immuno Research	Used at 1:500
Anti-HRP-conjugated Cy3	Jackson Immuno Research	Used at 1:500
Donkey anti-Rat A647	Jackson Immuno Research	Used at 1:500
Alexa Fluor 647 donkey anti-mouse	Jackson Immuno Research	Used at 1:500

Alexa Fluor RhRx donkey anti-mouse	Jackson Immuno Research	Used at 1:500
Alexa Fluor 488 donkey anti-mouse	Jackson Immuno Research	Used at 1:500
Hoechst		Binds to dsDNA specifically labelling the nuclei Used at 1:1000

For peripheral glia imaging the intersegmental nerve (ISN) of muscle 4 (m4) of abdominal segments A2-A4 were imaged. For Muscle or m6/7 NMJ visualization abdominal segments A2 and A3 were imaged.

3.4. Acute ex-vivo PGN exposure

Wandering 3rd instar larvae were selected and washed in PBS 1x to remove food remains. Larvae are dissected in semi-dissected in HL3.1. as previously described. After, the solution in which larvae are immersed is changed to HL3.1 containing 300ng/ml of *E.coli* PGN for 30 min. All experiments were done using either PGN from E. coli 0111:B4 (InvivoGen) or from E. coli K12 (InvivoGen). After 30 min of exposure to PGN, the solution was changed back to normal HL3.1 for another 30 min, unless stated otherwise. This last period is referred as post-infection period throughout this thesis. For fixed imaging, all incubations were performed at room temperature. For simplification PGN-exposed conditions are denominated as infected and non-exposed conditions are designated has uninfected controls

3.5. Fixed image analysis and statistics

Data was plotted and analyzed using GraphPad prism8. All data was tested for normality and statistical analyses were performed employing 1) if two conditions are being compared, unpaired t-test (if the data is normally distributed) or Mann Whitney test (if the data does not present a normal distribution); 2) when comparing more than two conditions A-NOVA was used as the statistical test (parametric or non-parametric, depending on the normally of the data). In plots data are represented as mean± standard error of mean (SEM)(if parametric tests are employed) or as median±SEM (if non-parametric tests are used). Along the text data shown is represented as mean±SEM. All statistical analysis and respective P-values are shown in supplementary data.

Quantification of Nuclear Relish intensity

Nuclear intensity of Relish was measured using Image J/Fiji. A region of interest of the nuclei (ROI) was taken using the channel with nuclei labelled (with Repo only used for glial cell nuclei or höescth to label all nuclei). Nuclear region was automatically selected with

the wand tool. The area and mean intensity were measured using the measure tool (Analyze-Measure). Additionally, the mean intensity of cytosolic Relish was also quantified. The Nuclear Mean intensity was taken and dived by cytosolic mean intensity in order to normalize for possible differences in expression throughout development. This ratio between nuclear and cytosolic Relish was used as a proxy of Relish nuclear translocation. In each experiment data was normalized for the control. Repeated experiments were then combined. When comparing exposed and non-exposed PGN conditions, non-exposed was used has control.

Ghost boutons

Ghost bouton are presynaptic boutons that are characterized by the lack of postsynaptic specializations. When new ghost boutons are formed, they are thought to be immature and lacking postsynaptic specializations, and proteins such as Discs Large (DLG) and glutamate receptors. Ghost Bouton count was done manually using max-Z projections taking advantage multi-point counter plugin in Image J/Fiji. Ghost boutons are therefore identified by their morphology given by neuronal membrane (labelled with HRP) and the lack of the postsynaptic markers such as DLG, which normally surrounds mature pre-synaptic structures. These newly formed boutons can then undergo maturation and become fully functional synapses. However, ghost boutons may not mature and in that case, they either retract or are engulfed by muscles and glial cells.

Neuronal Debris

Presynaptic-derived "debris" is formed either in response to neuronal activity or throughout normal synaptic growth. The formation of these neuronal debris can be enhanced when high-frequency stimulation of motor neurons occurs. Neuronal debris was quantified by measuring its area and mean intensity.

The motor neuron along with ghost boutons were eliminated from max-Z projections. Debris area was quantified around the motor neurons through the usage of a binary image where the same threshold throughout conditions always applied. Neuronal debris mean Intensity was measured in the previous debris area identified. To the debris mean intensity it was subtracted the background mean intensity (a region in the muscle devoided of neurons and far from the motor neuron).

Glial morphology

It has been reported that glial cells at the NMJ are dynamic and play important roles in debris clearance (Das et al., 2018)(Fuentes-medel et al., 2009). To quantify changes in glial morphology at the NMJ we quantified the following parameters: overall area, number of processes and processes area. Glial Area was quantified through performing a binary image of the glial channel. Glial processes number were manually determined. Processes were

defined as branch terminations, excluding the main branch. Lastly, glial process area was also quantified by performing a binary image of the glial channel. However, we eliminated the main glial branch and glia membrane that fully covered neuronal non-synaptic regions, through the help of HRP (which labels the neuronal membrane) and the DLG (that labels the post synapse) and measure the remaining area corresponding to glial processes in synaptic active zones, or that extended to the muscle

3.6. Live imaging of Relish translocation to the nucleus and analysis

For infected conditions, larvae are imaged for 5 minutes (pre-infection) and then the solution is replaced by HL3.1 with 300ng/ml of PGN and then imaged for at least 45 min(infection). Uninfected controls followed the same protocol but always in HL3.1 without addition of PGN. All live-imaging experiments were performed using a Nikon/Andor Revolution XD spinning-disk confocal microscope equipped with an electron-multiplying charge-coupled device (EMCCD) camera (iXon 897). During acquisition temperature was maintained at 25°C. Images were acquired with a 40X Plan Apochromat VC Perfect Focus System (PFS) 1.3 NA oil-immersion objective (Carl Zeiss).

Quantification of Relish nuclear translocation dynamics

Analysis of Relish dynamics was performed using max-intensity Z projections in Image J/Fiji. Time-lapse images were made using selected time points from the videos. Florescence intensity of glial nuclei were taken throughout time. A Region of Interest (ROI) was delimitated for each nucleus present in the ISN and mean intensity was taken. The first mean intensity measurement was set to 1 and every other measurement was normalized to that initial state. Normalized mean intensity of each nuclei were plotted with at the Y axis and the time (hh:mm:ss) at the X axis. fluorescence intensity variations (ΔF) in the nucleus were calculated through subtracting the initial fluorescence intensity to the fluorescence intensity of minute 45 (considered the final time-point for all plots) after infection and divided by initial fluorescence intensity.

3.7. Gal4 expression patterns

Expression patterns of PGRLC-Gal4, MdrG4, NrvG4, BsgG4 in the nervous system were visualized with a bright nuclear fluorescent reporter, a histone tagged with YFP (H2B-YFP). For this, each of the Gal4 lines was crossed with UAS-H2B-YFP, 3rd instar larvae were dissected, fixed and stained as previously mention. Fixed and tissues imaged in a confocal microscope (Zeiss LSM 710).

3.8. Food preparation

In order to test the ability of potential Relish inhibitors, we cooked food containing different compounds, namely Aspirin and Pyr-sulf. Food was prepared as suggested by the manufacturer (Fisher scientific, USA – Jazz mix Drosophila food) and food-derived or chemical compounds were added when food reached 50°C (in order to avoid compound degradation). For control food no compound was added. For Pyr-sulf and Aspirin the desired amount was added to obtain a concentration of 50μM. All different types of food were dispensed to polystyrene petri dishes (VWR, Italy) (around 6ml for each petri-dish) and were left at room temperature to cooldown and solidify. During solidification all food was shielded from direct light since LMWPM are light sensitive. Food was then stored at 4°C in the dark until time of use.

4. RESULTS

When the nervous system is exposed to an infectious or toxic stimuli animals engage in a multitude of mechanisms to cope and eliminate it. However, in Drosophila how an inflammatory stimulus is perceived by the nervous system, which cell types are involved and how it leads to neuroinflammation is not completely known.

PGN, a major component of the outer membrane of bacteria, can be recognized by immune responsive tissues. Its recognition triggers the activation of Imd pathway, which leads to the nuclear translocation of the NF-κB like protein - Relish.

To study the processes and impact following an inflammatory cue in the peripheral nervous system of Drosophila 3rd instar larvae, we developed a new method which consists in the dissection of 3rd instar larvae and their exposure to PGN fragments from *E.coli* in HL3.1 (Hemolymph-like solution 3.1 - natural hemolymph mimetic). This method simulates an infection that would occur in the hemolymph. However, before assessing the response of peripheral glia or neurons to PGN exposure, we started by assessing if Imd was activated in previously described immune responsive tissues.

4.1. Acute PGN exposure induces an immune response in the larval fat body and muscles

The most common methods to perform infections in Drosophila are based in either the puncture of the cuticle with a needle previously submerged in a bacterial pellet, the injection of a bacterial or peptidoglycan suspension, or feeding in contaminated food (Tzou et al., 2000)(Tzou et al., 2002). Through these methods, NF-κB becomes activated and translocates to the nucleus of immune responsive cells such as the fat body (schematized in Fig. 4.1 A).

Since we developed a new method of infection, we first assayed, as a positive control, whether our method of PGN exposure could trigger an immune response in already described immune responsive tissues - namely the fat body(Bettencourt et al., 2004) and the muscles(Kierdorf et al., 2020)(Vanha-aho et al., 2016).

In order to test if an immune response in a living fat body tissue could be triggered by PGN exposure, we employed the Gal4-UAS transgenic expression system to express a Relish reporter protein (Relish fused with a yellow florescent protein, YFP, UAS-Relish-YFP) specifically in the fat body (under the control of PPL-Gal4). For non-infected controls we dissected the larvae and maintained them for 1h in HL3.1. For the infected condition (PGN exposed) we incubated dissected larvae for 30 minutes in HL3.1. with 300ng/ml of PGN followed by another 30 minutes in normal HL3.1. After this time period, larvae fillets were fixed as described in the methods and the fat body was then isolated. As a proxy of Relish activation and nuclear translocation we calculated the ratio between nuclear and cytosolic mean intensity, as described previously in the methods. We observed some variability in larvae tissue within infected conditions, with some nuclei with high levels of nuclear Relish and others with less (Fig. 4.1 B). Despite the variability within each animal all nuclei within the fat body tissue were quantified in the same manner. Our results show that the ratio between nuclear and cytosolic Relish increases in the fat body after PGN exposure (infected=1.18±0.33), when compared to the uninfected control (uninfected=0.10±0.13) meaning that this tissue is responsive to our acute method of PGN exposure (Fig. 4.1 B and C).

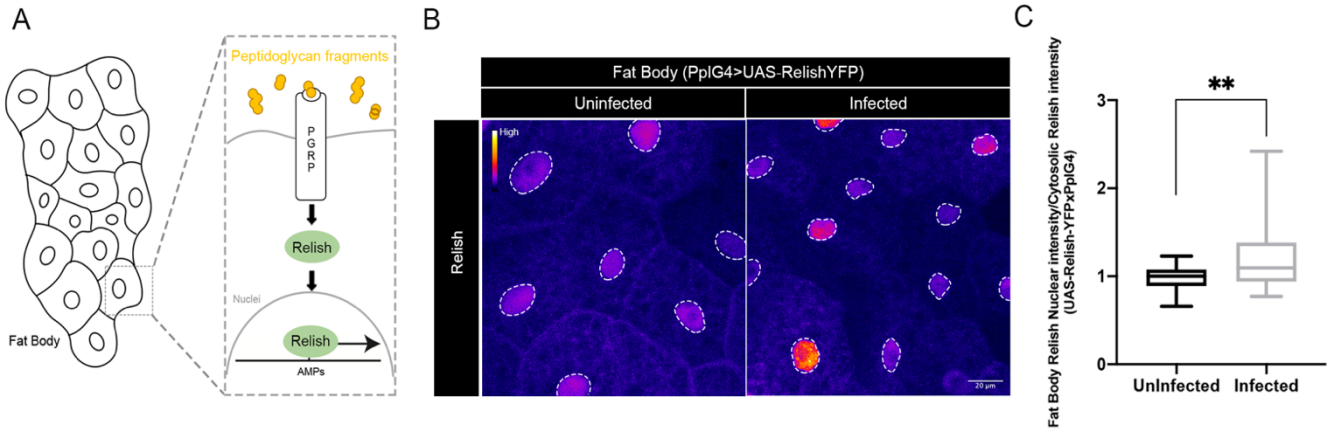

Figure 4.1 **Relish nuclear translocation in response to PGN exposure in the fat body.** *(A) Schematic of 3rd instar larvae fat body IMD activation in response to PGN (yellow) exposure. Upon recognition of PGN by PGRP, a signaling cascade is initiated and Relish (NF-κB like protein represented in green) translocates to the nucleus, where it regulates the expression of effector genes such as AMPs. (B) Representative images of PplG4>UAS-Relish-YFP larvae fat body tissue. Representative images Relish nuclear translocation in uninfected controls (non-exposed to PGN and remained 1 hour in HL3.1; left panel) and infected larvae (PGN exposed, 30 minutes of infection in HL3.1 with 300ng/ml of PGN plus 30 minutes post infection in normal HL3.1, right panel). Relish intensity is represented in fire color mode. Scale bar: 20 µm. (C) Quantification of the ratio between nuclear Relish and cytosolic Relish intensity in fat body cells of PplG4>UAS-Relish-YFP 3rd instar larvae. Uninfected controls (black, 0.10±0.13 ;n=61) and infected (grey, 1.18±0.33; n=58). **P<0.01 (non-parametric Mann-Whitney test). Data is represented in Whiskers plot with min and max values.*

In addition to the fat body, muscles have also been implicated in innate immunity and shown to be critical in pathogen fighting, in both vertebrates and invertebrates(Chatterjee et al., 2016). Therefore, we assessed if in muscles, Imd pathway could be activated upon PGN exposure. For this, we labeled the body wall muscles using Phalloidin and expressed UAS-Relish-YFP under the control of MHC-G4 driver (specific muscle driver) and assessed Relish nuclear translocation in muscles 6/7 of 3rd instar larvae (Fig. 4.2 A). We observed that upon PGN exposure, the ratio between nuclear and cytosolic Relish increases (infected=2.34±0.03), when compared to the control (uninfected=1.78±0.03) pointing to an activation of Relish after PGN acute exposure (Fig.4.2B).

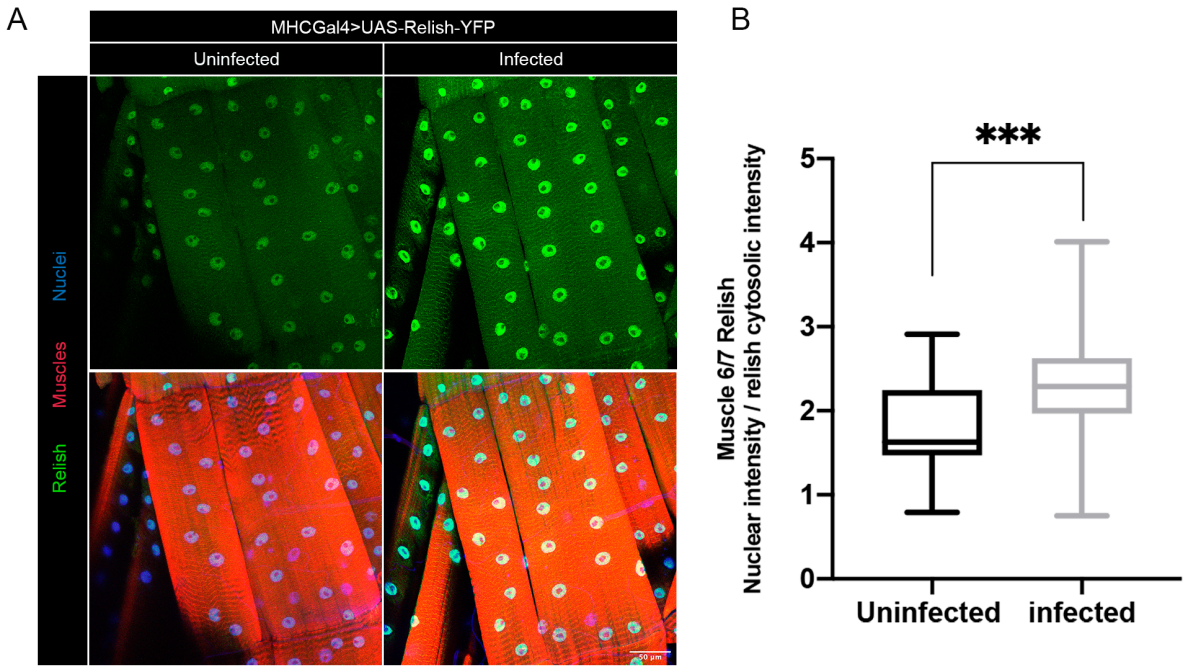

Figure 4.2. Relish nuclear translocation in response to PGN exposure in muscles 6/7. *(A) Representative images of MhcG4>UAS-Relish-YFP nuclear translocation in the muscles without PGN insult, uninfected (1 hour in HL3.1, left) and infected (30 minutes in HL3.1 with 300ng/ml PGN plus 30minutes in normal HL3.1, right) conditions. Relish is represented in green. Muscles are labeled with Phalloidin (red) and nuclei (blue) are labeled with Höechst. Scale bar: 50µm. (B) Quantification of nuclear Relish intensity divided by cytosolic Relish intensity in the muscles of MhcG4>UAS-Relish-YFP 3rd instar larvae. Uninfected controls (non-exposed to PGN- 1h in HL3.1, black, infected=1.78±0.03; n=255) and infected (30' infection plus 30' in normal HL3.1, grey, infected=2.34±0.03; n=385). ***P<0.0001 (non-parametric Mann-Whitney test). Data is plot in Whiskers plot with min and max values represented.*

4.2. Peripheral Glia response to an inflammatory insult

In Drosophila, glial IMD activation has been linked to neuroinflammation and neurodegeneration, but the molecular mechanisms and the relevance of the different glial subtypes involved are not completely understood(Kounatidis et al., 2017; Winkler et al., 2021). Thus, we asked whether PGN could activate Relish in peripheral glia. For this, we expressed UAS-Relish-YFP under the control of Repo-G4 (pan-glial driver) and analyzed peripheral glia Relish activation in infected (30' in HL3.1 with 300ng/ml of PGN plus 30' post-infection in normal HL3.1) and uninfected controls (non-exposed to PGN, 1h in HL3.1). Peripheral glial response to PGN was analyzed at the intersegmental nerves (ISNs) from segments A2-A4, at the point where the axons exit the bundle to innervate muscle 4 (as depicted in Fig.4.3A). Interestingly, our results revealed that the different peripheral glial cells at the ISN of m4 seem to respond differently to PGN exposure in terms of Relish activation. We observed that, while Relish increased in the nuclei in two glial cells upon PGN exposure, it did not increase in the third glia nuclei present in the ISN (as shown in Fig. 4.3B). Additionally, we also observed that PGN induced the formation of Relish cytosolic aggregates, forming puncta-like structures (Fig.4.3B, bottom panel). Despite noticeable differences in glia response to PGN, we decided to quantify all in the same manner and plot everything together, since we could not differentiate the cytosolic regions that belonged to each glial cell. Our results demonstrated that the ratio between nuclear and cytosolic Relish increased in infected larvae when compared to uninfected controls (uninfected=1.00±0.08 versus infected=1.72±0.07) (Fig.4.3C).

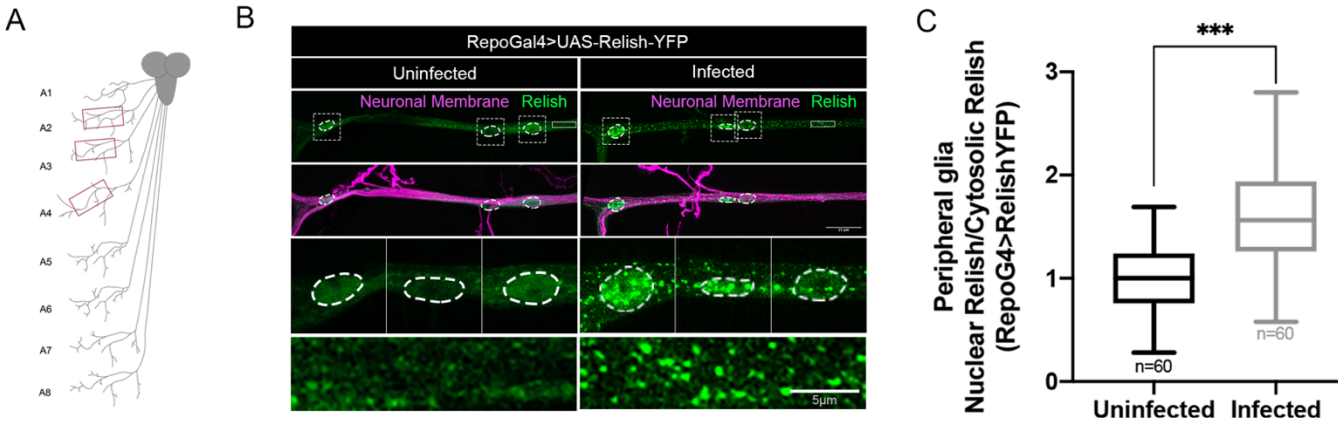

Figure 4.3 **Relish nuclear translocation in peripheral glia in response to PGN exposure.** *(A) Schematic of the left side of the PNS of 3rd instar larvae, only abdominal regions A1-A8 are represented. The CNS is also represented. Red rectangles represent the regions of ISN of muscle 4 where we acquired the images of peripheral glial response to PGN. (B) Representative images of peripheral glial Relish(green) translocation in uninfected(left) and Infected(right) of RepoG4>UAS-Relish-YFP larvae. Uninfected larvae are maintained for 1 hour in HL3.1. Infected larvae are exposed for 30 minutes to 300ng/ml PGN in HL3.1 and are incubated for an additional 30minutes in normal HL3.1 (post-infection). White dashed lines represent glial nuclei. White dashed squares (Top panel) indicate region magnified in the two bottom panels. The three nuclei present in the ISNs analyzed are identified from left to right with I,II and III, respectively. The bottom panel represents a magnification of the white dashed rectangles of the cytosol. Neuronal membrane is labelled with HRP (magenta). Scale bar: 25 µm or 5 µm. (C) Quantification of nuclear and cytosolic relish ratio. ***P<0.0001 (non-parametric Mann-Whitney test). n is represented in the graph. Data is plot Whiskers with min and max values.*

Next, we investigated whether these differences in glial response to PGN were due to differences in Relish translocation kinetics, and whether Relish puncta were motile or not. First, we performed the same infection protocol changing the post infection periods, fixed the larvae and assessed Relish translocation. Like previously described, infections were performed through exposing the larvae for 30' to 300ng/ml of PGN in HL3.1. Post-infections periods, where larvae are incubated in normal HL3.1 after PGN exposure, varied between 0 min, 30 min and 1h. Uninfected controls were maintained for 1h30 in normal HL3.1. We detected that until 1h30min after PGN exposure there are still differences in peripheral glial response: whereas Relish seems to be activated in two glia and increase in the nucleus, there is a third nucleus where Relish nuclear translocation does not occur (Fig.4.4A). Once again, we quantified Relish nuclear translocation in all glial cells in the same manner as previously described. Our data showed that nuclear and cytosolic ratio increases in 30' infected (1.91±0.13), 30'infected+30'post-infection (2.35±0.12) and 30'infected+1h post-infection(2.15±0.13) conditions when compared to the uninfected control (1,00±0.02). Additionally, the ratio between nuclear and cytosolic Relish in infected conditions do not appear different between them, suggesting that the response is mounted quickly after exposure to PGN and is sustained for at least 1h.

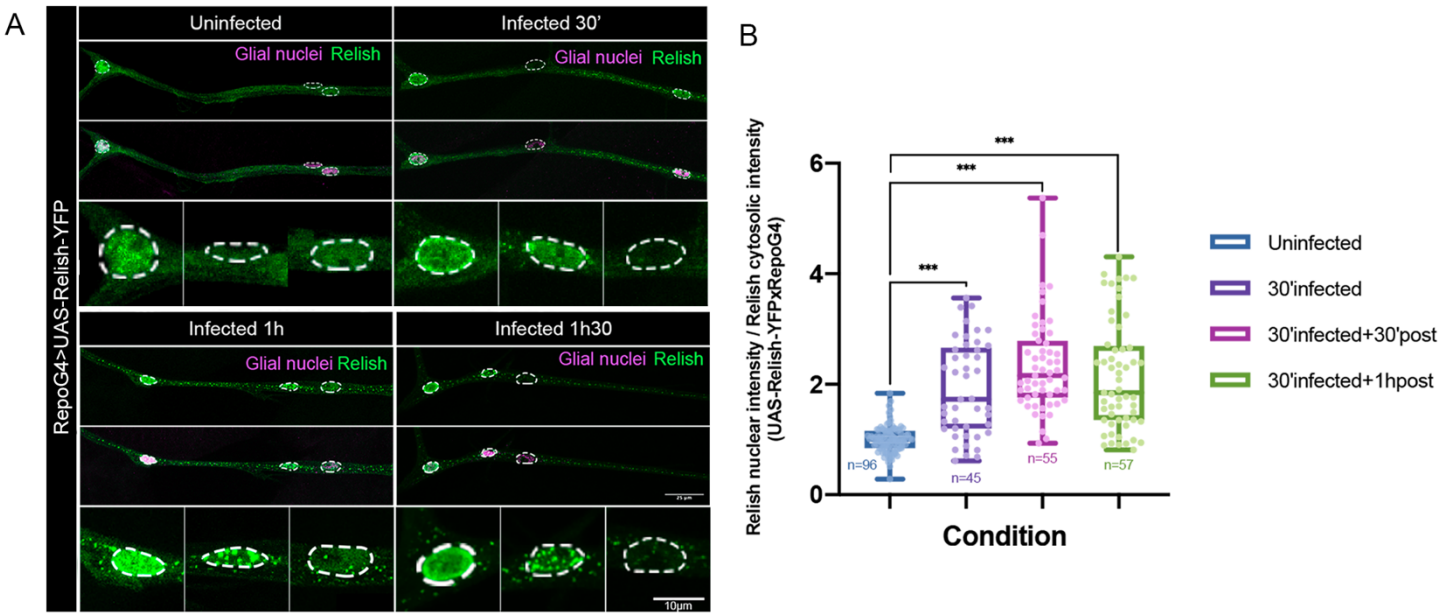

Figure 4.4 Different time points of Relish nuclear translocation in peripheral glia in PGN exposure. *(A) Representative images of Relish-YFP translocation. Top left panel represents uninfected control (1h30min in HL3.1). Top right panel represents 30' infected larvae (30' in HL3.1 with 300ng/ml of PGN). Bottom left panel represent 1h of infected larvae (30' exposed to PGN plus 30' post-infection incubation in normal HL3.1). Bottom Right panel represents 1h30 infected larvae (30' exposed to 300ng/ml of PGN in HL3.1 plus 1h of post-infection incubation in normal HL3.1). Relish is represented in green. Glial nuclei were labelled with Repo antibody (magenta). Scale bar is shown in the figure (scale bar=25 µm or 10 µm). (B)* Quantification of nuclear and cytosolic Uninfected = 1,00±0,03; 30'infected = 1,92±0,13; 30'infected+30'post = 2,35±0,12; 30'infected+1hpost = 2,15±0,13 Relish ratio. ***P<0.0001 (non-parametric Mann-Whitney test). n is represented in the graph. Data is plot Whiskers with min and max values.

To assess whether Relish puncta were motile as well as Relish nuclear translocation dynamics upon PGN exposure, we performed live imaging. Here, we expressed UAS-Relish-YFP under the control of Repo-G4 and imaged Relish-YFP dynamics, over time. Regarding Relish puncta, we observed that they were not motile and instead seem to be formed in response to PGN in a given place and increase in intensity overtime (Fig. 4.5 A). The other goal of the live experiment was to assess Relish nuclear translocation dynamics. To have an overview of Relish nuclear intensity changes in the first 45 minutes after PGN exposure, we plotted Relish nuclear intensity in each nucleus and compared the dynamics between uninfected and infected larvae. In infected conditions, we detected differences in glial response. Upon PGN exposure, nuclear Relish increased in two nuclei (nuclei I and II) and did not increase in the third (nuclei III) (Fig. 4.5 B, where Relish intensity is represented in heat map, and in Fig.4.5C, colored lines represent infected conditions). We also observed that within five minutes after PGN exposure (represented by the dashed line), Relish starts increasing in two glial nucleus (Nuclei I and II) (shown in Fig.4.5 C,) Regarding uninfected conditions, Relish did not increase overtime in the nuclei of any glia cell (nuclei I, II and III) (Fig 4.5 B and C, where black lines represent uninfected nuclear Relish intensity overtime).

To assess the variation between t=0min (uninfected/pre-infected) to t=45min (uninfected/infected) we calculated the variation of Relish mean fluorescence (ΔF). Our results show that upon PGN exposure, Relish increases in the first glial nuclei (infected=0.89±0.35) when compared to uninfected controls (0.02±0.05). Akin to what occurs in the first nucleus, the second glial nucleus is also responsive to PGN. In this nucleus, Relish increases upon PGN exposure (infected=0.70±0.26) when compared to uninfected controls (uninfected=0.02±0.09). Moreover, there is no significant variations in Relish mean intensity in the third glial nuclei when comparing uninfected to infected larvae (uninfected=0.10± 0.07 versus infected=0.22±0.10).

Repo is considered a pan-glial driver and it is described to be expressed in all peripheric glial. However, to verify that that these differences in response were not due to lack or different levels of expression in the different glia, we expressed UAS-H2BYFP (a histone tagged with YFP) under the control of Repo-G4 (Fig. 4.6). Like expected, YFP expression was present in the three glial nuclei analyzed (identified by an asterisk) and it showed equal expression strength. This means that Repo induces expression in the glia cells analyzed, and shows that the lack of response to PGN in the third nucleus is not a consequence of low Gal4 expression.

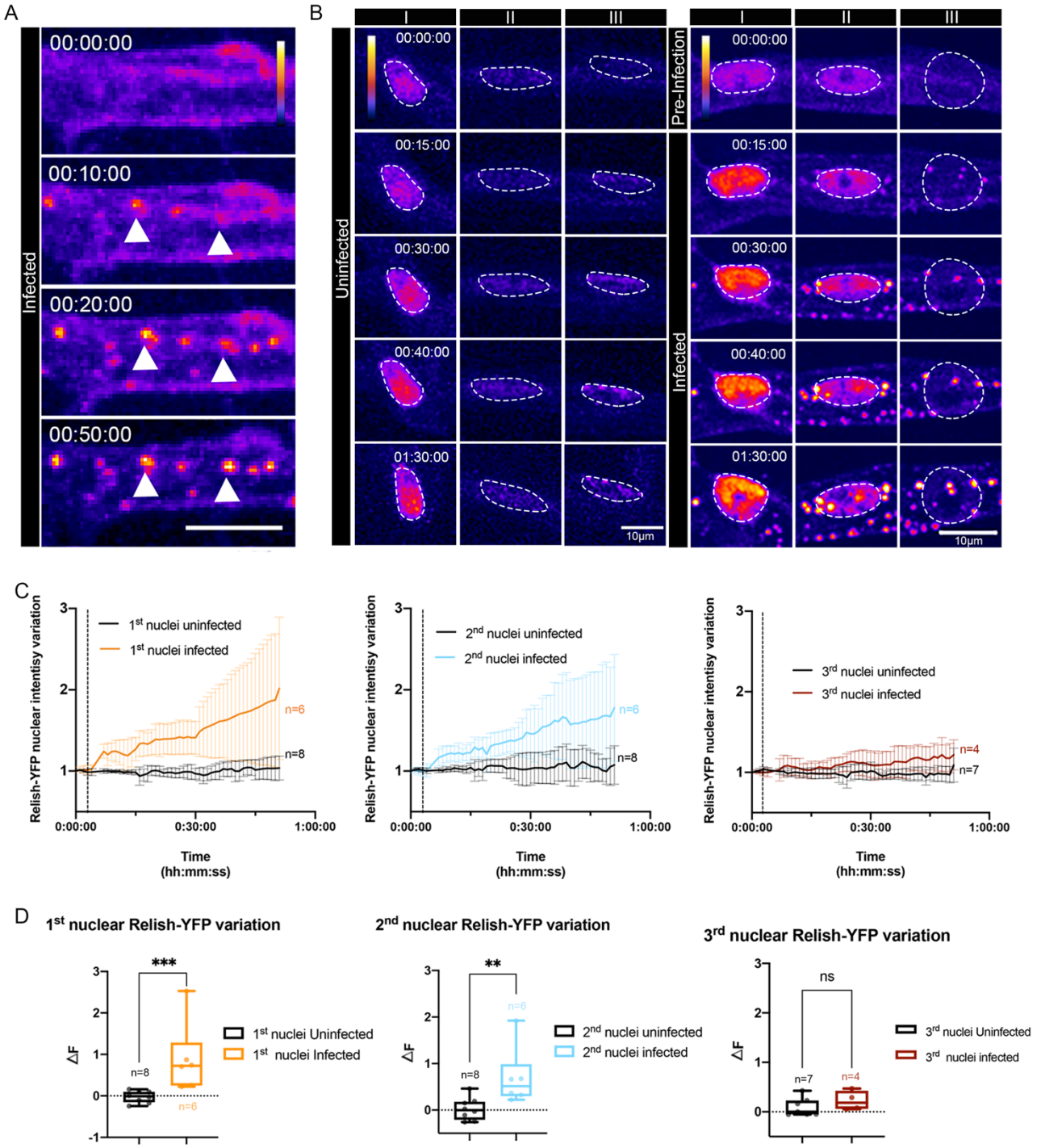

Figure 4.5 Relish dynamics in peripheral glia, in response to PGN exposure. *(A) Representative images of Relish cytosolic puncta formation in RepoG4>UAS-Relish-YFP larvae exposed to 300ng/ml of PGN inHL3.1 (B) Representative images of Relish nuclear translocation dynamics for 1h30min in the 3 peripheral glia non exposed to PGN (left panel) and exposed to PGN (right panel). Relish intensity is in fire heat map. Scale bar: 10µm (C) Quantification of nuclear relish intensity overtime in the 3 nuclei individually. Nuclei were divided taking in account position, morphology and type of response. (D) Variation of nuclear Relish intensity.* ΔF *is calculated between t=0min (time in which larvae were in normal HL3.1) and t=45min (45min uninfected or 45 after first contact with PGN for infected conditions). In the first graph is shown the florescence changes in* 1^{st} *nuclei in uninfected conditions (-0.02± 0.05, black) and infected (0.89±0.35, orange) Mann-Whitney test was used. In the second graph is shown the florescence changes in* 2^{nd} *nuclei in uninfected conditions (0.02± 0.09, black) and infected (0.70± 0.26, blue), Mann-Whitney test was used. In the third graph is shown the florescence*

*changes in the 3rd nuclei in uninfected conditions (0.10± 0.07, black) and infected (0.22± 0.10, red), Unpaired t test was used. **P<0.001, **P<0.01 Peripheral glial nuclei quantified were taken from ISN of m4 of segments A2-A4. n for each condition is shown in the graph.*

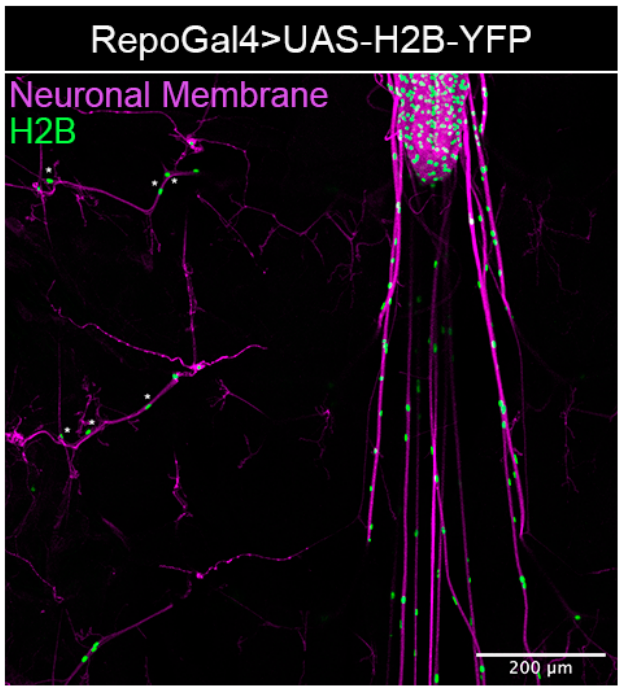

Figure 4.6. Repo-Gal4 driver line is expressed in the 3 glial nuclei present at the ISN that innervates m4. *Representative image of Repo-G4 nuclear expression patterns. H2BYFP (green) is expressed under the control of RepoG4. H2BYFP appears in the 3 nuclei in the ISN that innervates m4 (represented with an *). Neuronal membrane (magenta) was labelled with anti-HRP antibody. Scale bar: 200µm..*

Since cytosolic Relish puncta form and stay in place, we questioned the identity of these puncta. Knowing that Relish is a transcription factor, we hypothesized that those puncta could be Relish accumulation in a specific organelle, namely mitochondria. Since, NF-κB has been found inside mitochondria in several cells upon inflammatory insult (De Pinto et al., 2019), we decided to perform an experiment to investigate whether the puncta were localized or not in this organelle. For this we exposed 3rd instar larvae with pan-glial expression of Relish (Repo-G4>UAS-Relish-YFP) to PGN and stained for Cytochrome C, a protein enriched in mitochondria. We saw that some Relish puncta colocalized with Cytochrome C, but others did not (Fig.4.7). This suggests that while some of these Relish puncta might be inside mitochondria, others are not. However, in order to conclude on the identity of these puncta, further experiments are required.

To briefly sum up, we observed that glial cells in m4 ISN respond differently to PGN exposure. While Relish increases in two glial nuclei upon PGN exposure, the same is not true for the third nuclei present in this structure. Additionally, besides nuclear translocation we observed that upon PGN exposure, Relish forms puncta-like structures throughout the nerve that partially co-localize with Cytochrome C.

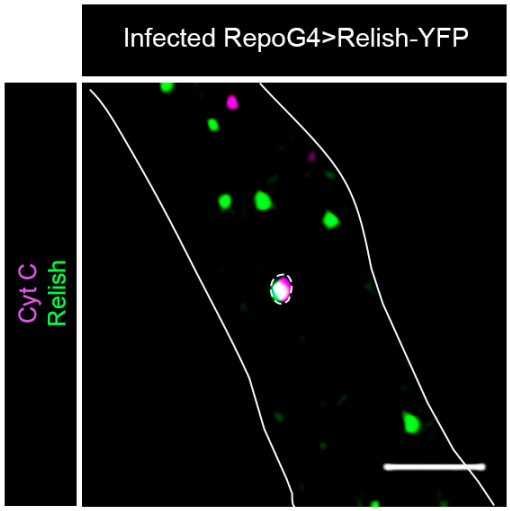

Figure 4.7 **Relish cytosolic puncta partially co-localize with Cytochrome C.** Representative image of Relish-YFP expressed in all glial cells(Repo-G4>UAS-Relish-YFP) and exposed to PGN. Cytochrome C is represented in magenta. White lines represent the limits of the ISN of m4. Scale bar: 10µm.

4.3. Different peripheral glia exhibit different responses to PGN

Knowing that there are three distinct glial subtypes in the ISNs: perineurial, subperineurial and wrapping glia, we hypothesized that the different responses observed could be due to the fact that different glial subtypes respond differently to PGN exposure. To test this, we performed the same inflammatory approach of PGN exposure, previously described, in larvae that specifically expressed Relish-YFP in the different glial subtypes. We expressed UAS-Relish-YFP under the control of: Bsg-G4 (described specific for Perineurial glia); Mdr-G4 (for Subperineurial glial cells); and Nrv2-G4 (For Wrapping glia). Nonetheless, before performing the infection protocol, we confirmed the expression patterns and specificity of these lines by expressing UAS-H2B-YFP (Fig. 4.8). This allowed us to assess and confirm which glial type were present in the ISN that innervates m4 of 3rd instar larvae. It is described that in the m4 ISN there are three glial nuclei, one of each subtype (von Hilchen et al., 2013). By expressing H2B-YFP under the control of each driver we could observe that the Bsg driver is not as specific as previously reported, having expression in Perineurial but also in a subset of Subperineurial glia, since the Bsg driver induces expression in some glia in which the Subperineurial glia driver (Mdr-G4) also induces (Fig.4.8A and B). Therefore, when assessing the individual response of perineurial glia only the nuclei that does not show expression with the Mdr driver was considered. In contrast, Mdr and Nrv2 drivers are

specific, only expressing in one nucleus at the m4 ISN, as previously reported (shown in Fig. 4.8B and 4.8C, respectively).

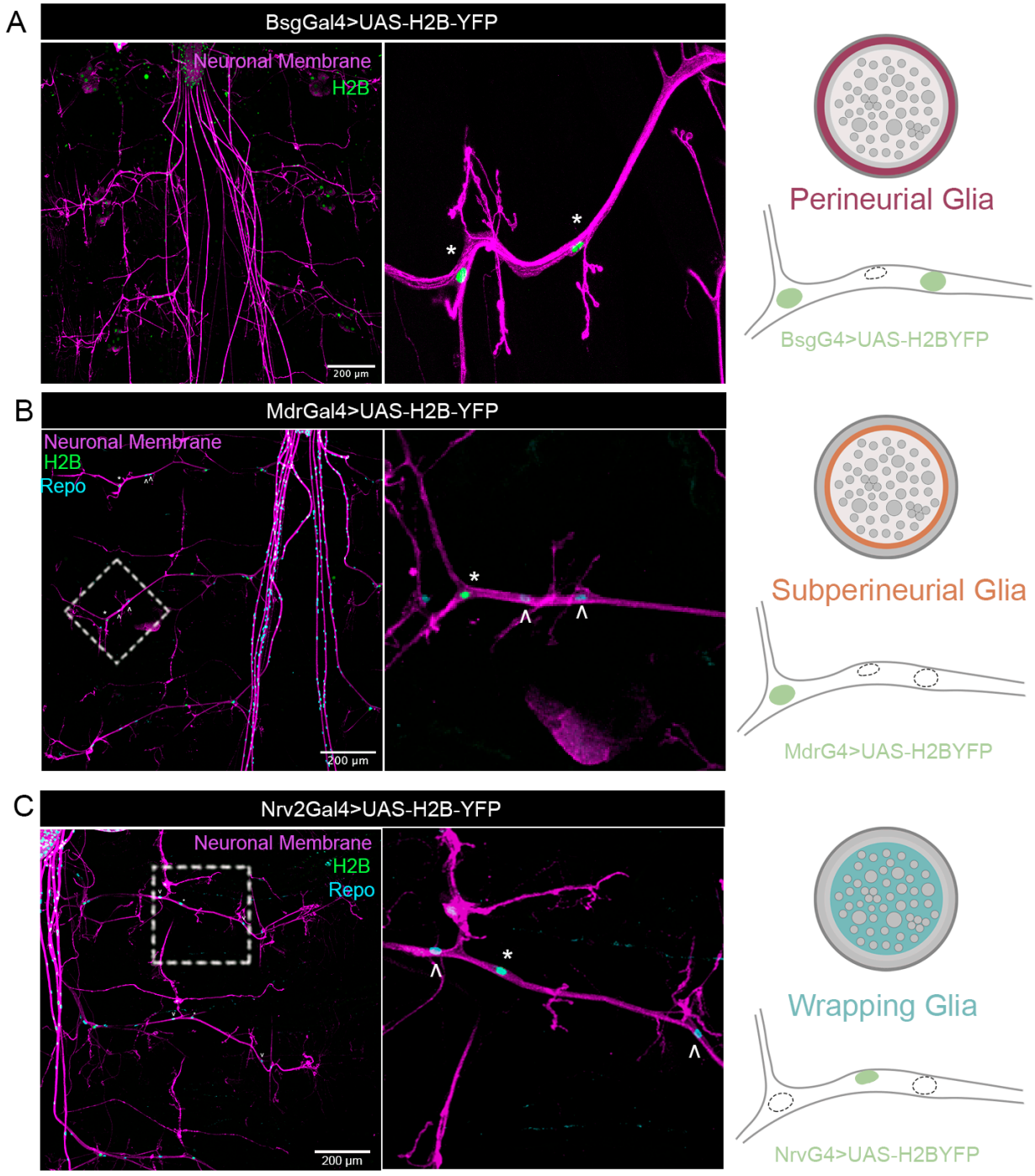

Figure 4.8. **Expression pattern of peripheral glial drivers. (A)** Expression of UAS-H2B-YFP (green) under the control of BsgG4. On the right it is illustrated a scheme of the transversal cut of ISNs with *Perineurial glia* highlighted in dark magenta. The expression pattern of Bsg-G4 driver in the m4 ISN is illustrated, green nuclei represent the nuclei in which Bsg-G4 induces expression **(B)** Expression of UAS-H2B-YFP (green) under the control of MdrG4. On the right it is represented a scheme of Subperineurial glia highlighted in orange, in the bottom is illustrate the expression pattern of Mdr driver in the m4 ISN **(C)** Expression of UAS-H2B-YFP (green) under the control of Nrv2-G4. A scheme of a transversal cut of the ISNs with *Wrapping glia* highlighted in blue

is shown on the right. In the bottom right and a scheme of the expression pattern of Nrv2 driver in the m4 ISN is represented. Glial nuclei is stained with anti-Repo (cyan). Neuronal membrane (magenta) was labelled with anti-HRP antibody. * Represent the glial cells that express H2B-YFP. Glial cells that do not express H2BYFP are identified by a white arrow. Scale bar: 200µm..

Therefore, to individually assess the specific response of each glial subtype we performed infections, as previously described in the methods, and assessed Relish translocation individually in each subtype (schematic of single glial subtype's nuclei positioning is illustrated in Fig. 4.9 A.).

We started by assessing perineurial glia response to PGN. We observed that upon PGN exposure, Relish does not increase in the nuclei of this glial subtype (Fig.4.9B). Our data showed that the ratio between nuclear and cytosolic Relish did not increase in perineurial glia (BsgG4>UAS-Relish-YFP) in infected conditions when compared to uninfected controls (uninfected=1.6±0.2 versus infected =1.4±0.2) (Fig.4.9B'). This means that Perineurial glia are the glial type in which Relish does not translocate to the nucleus upon PGN exposure. Additionally, upon PGN exposure we did not observe the formation of any Relish cytosolic puncta. Since BsgG4 driver expresses in Perineurial and some Subperineurial glia, the absence of Relish puncta in infected conditions suggests that these puncta are not formed neither in perineurial nor subperineurial glia.

As for subperineurial glia response to PGN, we observed that upon infection Relish increased in the nucleus and decreased in the cytosol of these cells when compared to uninfected controls. (Fig.4.9C). In fact, our data showed that, in subperineurial glia (Mdr-G4>UAS-Relish-YFP), the ratio between nuclear and cytosolic Relish was higher in infected larvae (2.5±0.2) when compared to uninfected controls (1.0±0.1) (Fig.4.9C'). This means that Relish was activated in subperineurial glia in response to PGN. In addition, we did not observe any cytosolic puncta being formed in subperineurial glia, reinforcing the idea that Relish puncta are not formed in this glial subtype.

Regarding wrapping glia, we saw that when we specifically express Relish-YFP in this glial subtype (Nrv2G4>UAS-Relish-YFP), Relish increases in the nucleus upon PGN exposure (Fig.4.9D). In this glial subtype, the ratio between nuclear and cytosolic Relish increased in infected larvae (2.3±0.1) when compared to uninfected controls (1.0±0.1) (Fig.4.9D'). Strikingly, whereas in subperineurial glia Relish seems to translocate to the nucleus in a canonical manner (decreasing in the cytosol and increasing in the nucleus) in wrapping glia, in addition to nuclear translocation, Relish forms puncta-like structures in the cytosol (Fig.4.9D). These puncta were observed only when Relish was expressed in all glial subtypes (Repo-G4>UAS-Relish-YFP) or specifically in wrapping glia (Nrv2-G4>UAS-Relish-YFP), suggesting that this type of response is specific to wrapping glia.

In summary, we observed that in the peripheral nervous system of 3rd instar larvae the different glial subtypes respond differently to PGN. While in perineurial glia, Relish does not seem to be activated, in subperineurial and wrapping glia, Relish increased in the nucleus

upon PGN exposure, meaning that it is activated in these subtypes. Additionally, here we attribute the formation of Relish puncta to a specific subtype, the wrapping glia.

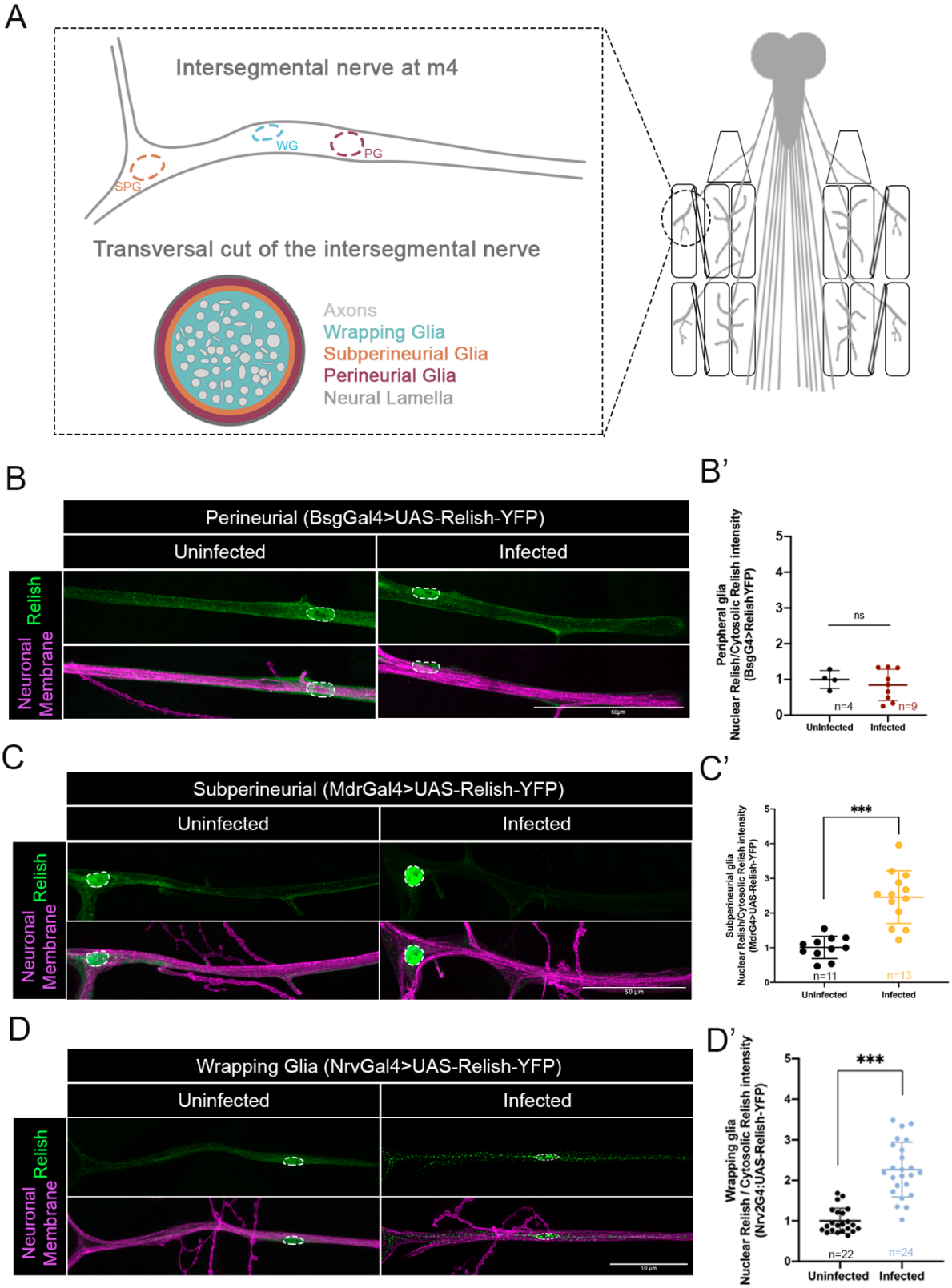

Figure 4.9 Different peripheral glia in ISN respond differently to PGN exposure. *(A) Schematic of peripheral glial subtypes in 3rd instar larvae (B) Perineurial Glia representative images of Relish-YFP (Bsg-G4>UAS-Relish-YFP), in uninfected(left) and infected(right) larvae (C) Subperineurial representative images of Relish (Mdr-G4>UAS-*

RelishYFP) in uninfected (left) and infected (right) conditions. (D) Wrapping glia Relish representative images (Nrv2-G4>UAS-Relish-YFP) in uninfected (left) and infected (right) conditions. ISN is labeled with HRP (magenta). Scale bar: 50 µm. (B' – D') Quantifications of the ratio between nuclear Relish and cytosolic Relish intensity (B') in Perineurial glia(Bsg-G4>UAS-Relish-YFP), (uninfected=1.000±0.125 versus infected=0.847±0.146), Parametric Unpaired t test was used (C') in Subperineurial glia (Mdr-G4>UAS-Relish-YFP), (uninfected=1.009±0.097 versus infected= 2.459±0.210) Parametric Unpaired t test was used. (D') in Wrapping glia (Nrv2-G4>UAS-Relish-YFP) (Uninfected=1.000±0.066; Infected=2.266±0.138) Mann-Whitney test was used. The numbers on x-axis represent the total number of nuclei quantified from the ISN of segments A2-A4. n for each condition is shown in the graph. ****p<0.0001.*

We then hypothesized that these differences in response to PGN, of the different peripheral glia subtypes, could be due to an eventual difference in the expression of PGN receptors. Hence, we started by inquiring where in the nervous system PGRP-LC, one of the main receptors of PGN, was expressed. To achieve this, we expressed UAS-H2B-YFP, under the control of a PGRP-LC gene trap, where a G4 protein is expressed under the regulatory sequences of PGRP-LC. We could not detect any H2B-YFP positive cells in the ISN, which suggests that PGRP-LC does not seem to be expressed in peripheral glia (Fig 4.10. A). In the nervous system, PGRP-LC is described to be present in motor neurons and in glia cells in the CNS (Davie et al., 2018; Harris et al., 2015). Thus, we also assessed if indeed this receptor was expressed in the CNS, using PGRP-LC-G4>UAS-H2B-YFP larvae. We stained the neuronal membrane with HRP and labelled either glial or neuronal nuclei (with Repo and Elav, respectively). We detected the presence of H2B-YFP positive cells in CNS, meaning that PGRP-LC is expressed in those cells. We also observed that H2B-YFP co-localized with Repo in the lobes and in the VNC (Fig4.10 B and C). Additionally, in the VNC we saw that some H2B positive cells did not colocalize with Repo. Moreover, we could not detect any H2B positive cells that co-localized with Elav (neuronal nuclear marker), neither in the VNC nor the lobes (Fig 4.10D and E.). To summarize, PGRP-LC is expressed mainly in glial cells at the CNS but it is not expressed at the periphery.

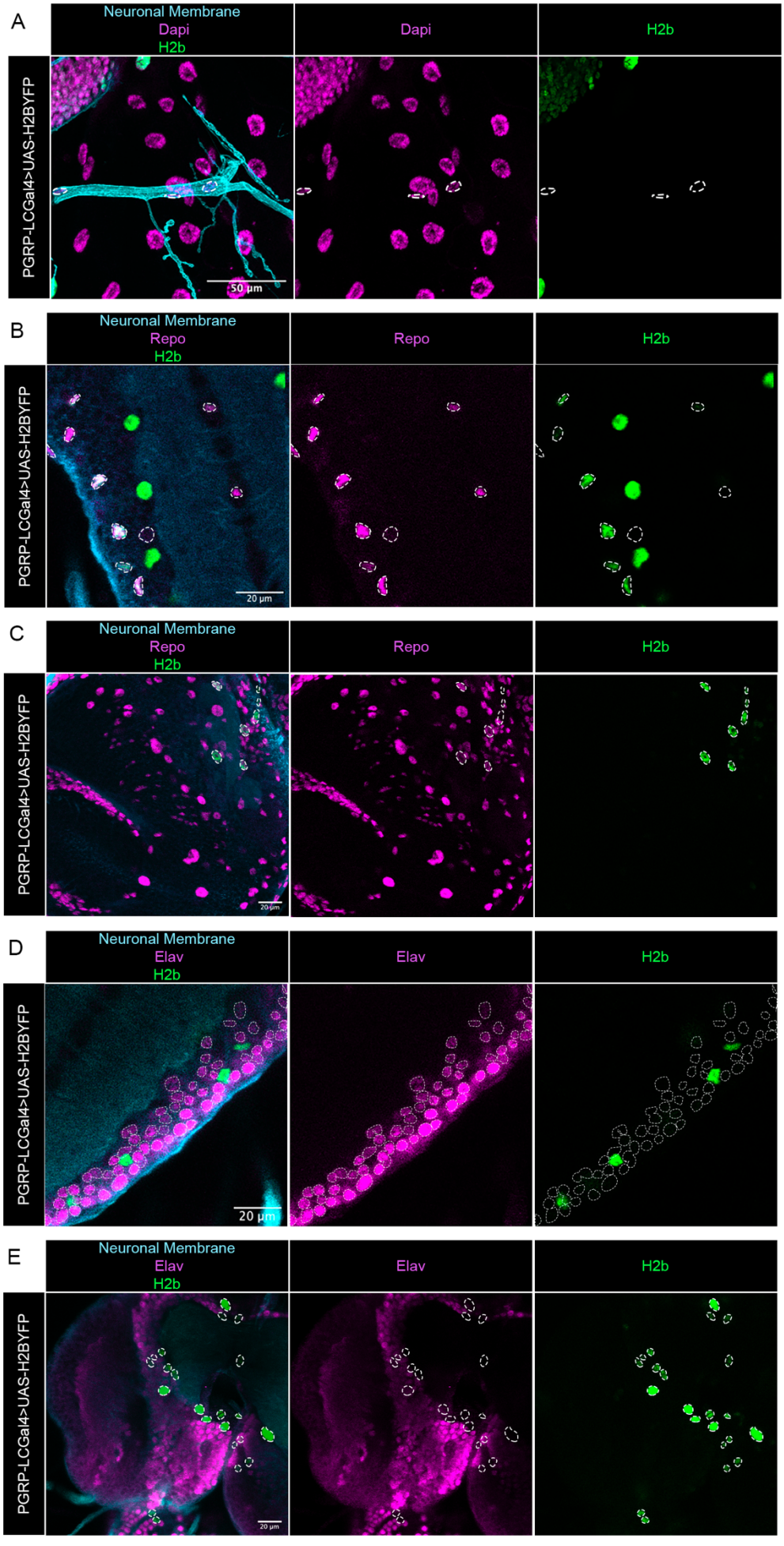
A
Neuronal Membrane
Dapi
H2b
Dapi
H2b
PGRP-LCGal4>UAS-H2BYFP
50 µm
B
Neuronal Membrane
Repo
H2b
Repo
H2b
PGRP-LCGal4>UAS-H2BYFP
20 µm
C
Neuronal Membrane
Repo
H2b
Repo
H2b
PGRP-LCGal4>UAS-H2BYFP
20 µm
D
Neuronal Membrane
Elav
H2b
Elav
H2b
PGRP-LCGal4>UAS-H2BYFP
20 µm
E
Neuronal Membrane
Elav
H2b
Elav
H2b
PGRP-LCGal4>UAS-H2BYFP
20 µm

Figure 4.10 Expression of PGRP-LC in the nervous system. (A) *Representative image of the expression of PGRP-LC in the ISN of m4.* Nuclei (magenta) are labeled with Hoechst. *Scale bar: 50 µm* (B-E) *Representative images of the expression of PGRP-LC in the CNS. In green are represented the nuclei that express PGRP-LC* (B and C) *Representative image of the expression of PGRP-LC in (B)VCN and (C)Lobe. Glial nuclei (magenta) are labelled with Repo.* (D and E) *Representative image of the expression of PGRP-LC in the (D)VCN or (E)Lobe. Neuronal nuclei (magenta) are labelled with Elav. Neuronal membrane (Cyan) is labelled with HRP. Scale bar: 20 µm.*

4.4. Does PGN exposure alter NMJ morphology?

Some infections and the subsequent engaged neuroinflammatory responses have been correlated with many peripheral neuropathies. Thus, we asked whether PGN exposure could have an impact in PNS neurons and glial cell morphology. For this we analyzed the motor neurons and glial cells present at the NMJ of muscles 6/7, of 3rd instar larvae, since this is a highly stereotypical synapse with well-characterized morphology.

Additionally, innate immunity pathways have been correlated not only with homeostatic plasticity and learning and memory (Harris et al., 2015)(Kaltschmidt & Kaltschmidt, 2010), but it has also been demonstrated that inflammatory cues can trigger the enhancement of synaptic connections and activity (Ceasrine & Bilbo, 2021)(P. Cao et al., 2021). Thus, to learn about the possible effects of PGN exposure, an inflammatory cue, we started by assessing whether our protocol of infection induced any alterations in terms of plasticity, namely whether there were morphological changes in the motor neurons, assessed by the appearance of ghost boutons (known to be induced by elevated activity levels). First, we used wild type (W^{1118}) 3rd instar larvae and either exposed them, or not, to PGN (as described in the methods) and fixed the samples. By labelling the neuronal membrane with HRP and the post synapse with DLG we were able to detect that in infected conditions there was an increase (despite modest) in the formation of ghost boutons (Fig4.11 A), pre-synaptic immature structures, when compared to uninfected controls (uninfected = 1,7±0.2 versus infected=2,5±0.3)(Fig. 4.11B).

Additionally, we observed increased levels of synaptic debris around the motor neurons, when larvae were exposed to PGN (Fig. 4.12 A). To quantify the levels of synaptic debris we measured their area and intensity as described in the methods. Additionally, to assess if debris formation was dependent of PGN we used two concentrations: 300ng/ml and 600ng/ml. Specifically, we observed that synaptic debris area increased in larvae exposed to 300 ng/ml (0.052±0.005µm^2) and 600ng/ml of PGN (0.080±0.011µm^2) when compared to uninfected controls (0.019±0.003µm^2) (Fig.4.12 A and B). However, there was no difference between the two infected conditions in terms of synaptic debris area. Moreover, we saw that debris intensity also increased when comparing uninfected to infected conditions. Our data shows that upon PGN exposure debris intensity is higher in both infected conditions (54.50±3.67 for 300ng/ml and for 64.09±7.50 600ng/ml) when compared to uninfected controls (32.04±2.03). However, akin to debris area, debris intensity is not different between the two infected conditions (Fig.4.12 A and B).

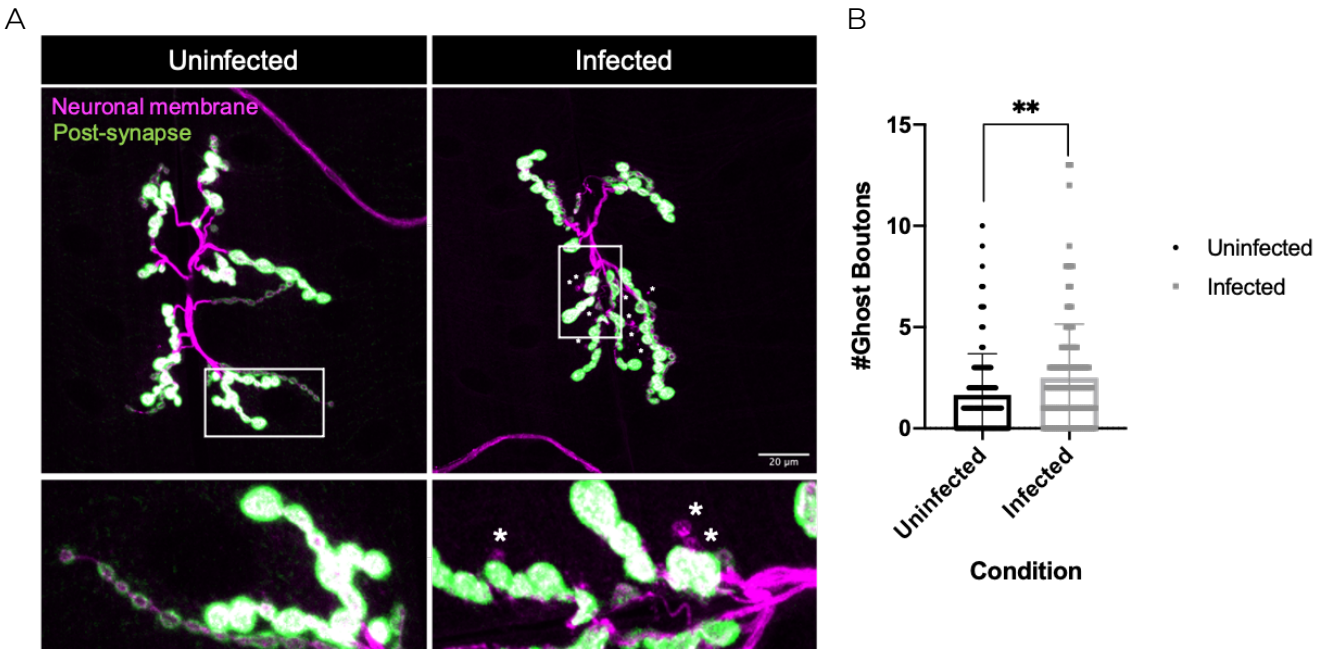

Figure 4.11. Ghost boutons increase in response to PGN insult. *(A) Representative images of W^{1118} uninfected (1h in HL3.1) and infected (30' exposed to 300ng/ml of PGN plus 30' post-infection period - incubated in normal HL3.1) larvae NMJ. Neuronal membrane(magenta) is labelled in magenta. Mature post-synapse is labelled with DLC (green). Ghost boutons, new pre-synaptic structures, are identified by the presence of neuronal membrane and the lack of post-synaptic markers and are identified by asterisks. Scale bar: 20 µm. (B) Quantification of ghost boutons in uninfected(n=111) and infected (n=116), Data points are overlapped to best represent data distribution. WIII8 3rd instar larvae.**p<0.01 Mann-withney t-test was used.*

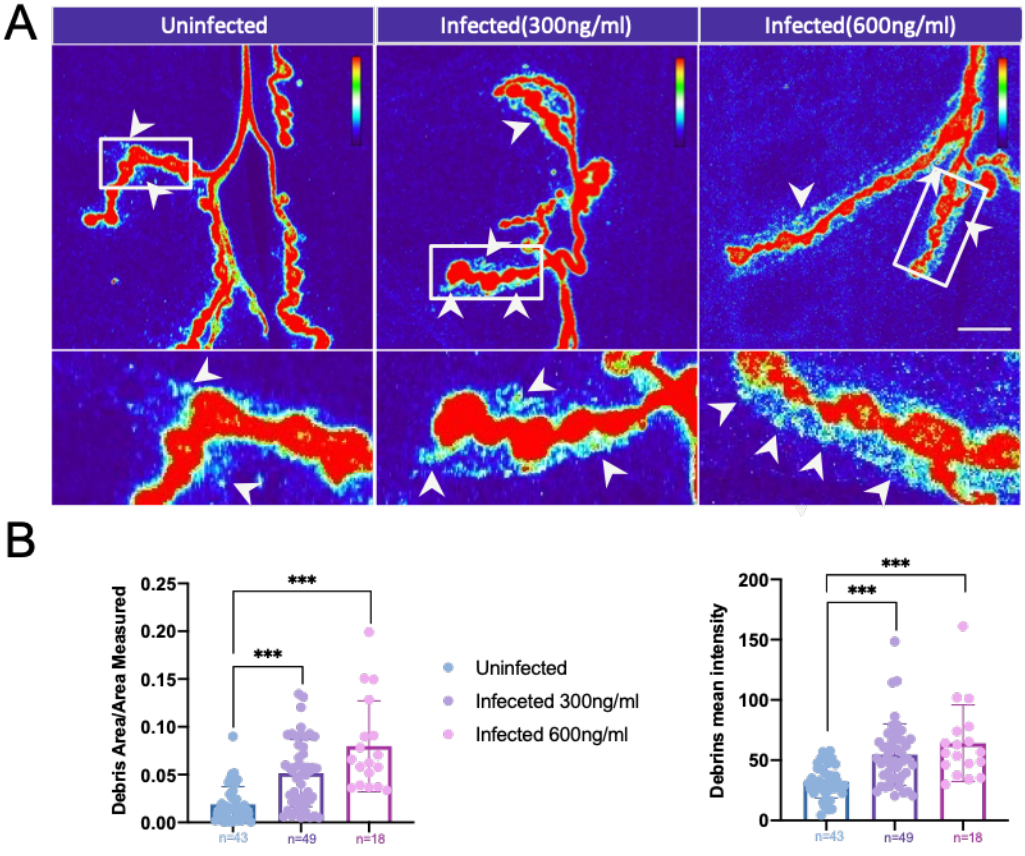

Figure 4.12 Synaptic debris formation in response to PGN exposure in W^{1118}. (A) *Representative images of a region of W^{1118} motor neuron. Uninfected (1h in HL3.1), Infected 300ng/ml (30' infection + 30' post-infection), Infected 600ng/ml (30' infection + 30' post-infection). Neuronal membrane was labelled with HRP which is represented in fire mode. White rectangles identify the area magnified in the bottom. White arrows point to neuronal debris around the motor neuron. Scale bar: 20 µm.* ***(B)*** *Quantification of synaptic debris area(left) Uninfected (0.019±0.003,blue) Infected 300ng/ml (0.052±0.005, purple), Infected 600ng/ml (0.080±0.011,pink). Quantification of Debris intensity (right), Uninfected (32.04±2.03,blue) Infected 300ng/ml (54.50±3.67, purple), Infected 600ng/ml (64.09±7.50,pink). ANOVA- Kruskal-Wallis test was used. ***p<0.0001. n for each condition is shown in the graph.*

In the mammalian nervous system, activation of glial cells after recognition of PAMPs leads to changes in their morphology (Kondo et al., 2011). At the NMJ, subperineurial and perineurial glia extend dynamic processes that can contact and interact with either the muscle, the neuron or both (Brink et al., 2012). These cellular processes are known to change with growth and neuronal activity. Additionally, these glial cells play key roles in the clearance of synaptic debris (Fuentes-medel et al., 2009). However, if they can change their morphology in response to an inflammatory cue such as PGN is unknown. Therefore, to test this, we expressed UAS-CD4-GFP (a membrane protein tagged with a fluorophore) under the control of Repo-G4, and analyzed glial morphology. As expected, we observed that glial processes displayed a wide range of morphologies in both uninfected and infected conditions that ranged from lamellipodia-like extensions, small filopodia-like projections (gliopods) to glial extensions with spherical shape resembling synaptic boutons (gliobulbs). (Fig.4.13 A). However, when comparing glial morphology between uninfected and infected larvae no differences were detected in the overall area, in the area of processes, or its number (Fig.4.13B).

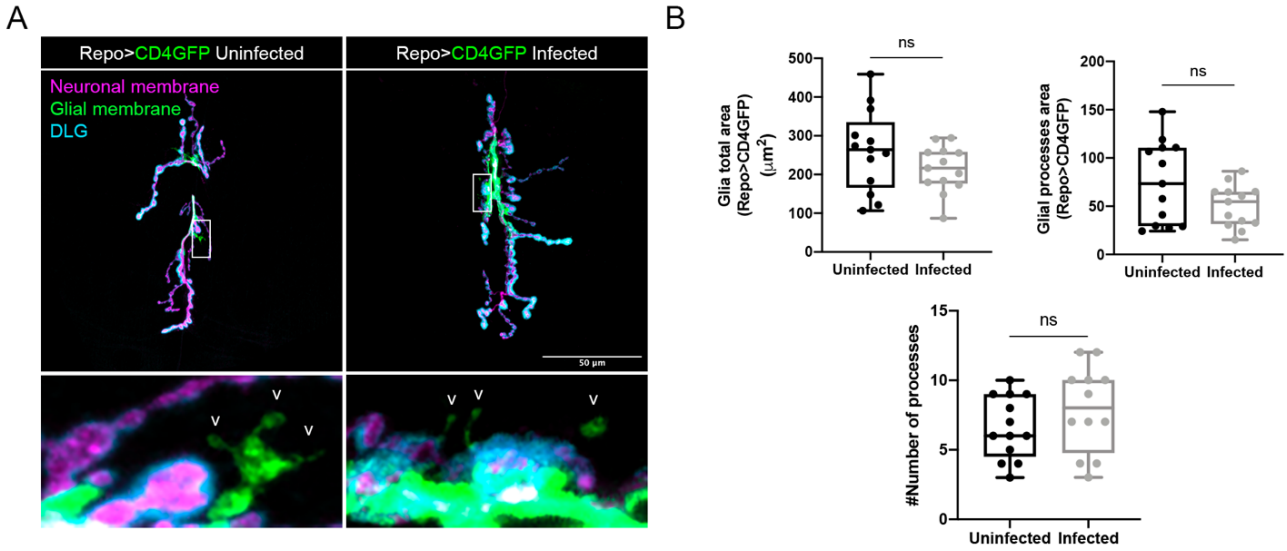

Figure 4.13 NMJ glial morphology is not altered by PGN exposure. (A) *Representative images of glial morphology in Repo-G4>UAS-CD4GFP Uninfected (1h in Hl3.1 left) and Infected (30' exposed to300ng/ml of PGN in HL3.1 plus 30' in normal HL3.1, right) White rectangles identify the region amplified in the bottom. White arrows point to processes that extend beyond the motor neuron. Neuronal membrane (magenta) is labeled with HRP. Post-synapse is labelled with DLG (cyan). Scale bar: 50 µm* ***(B)*** *Quantification of total glia area, of glial processes area and the number of processes of uninfected (n=13) and infected (n=12). Unpaired t-test were used.*

However, at the NMJ both subperineurial and perineurial glia have complex processes that extend from the primary arbor, which we cannot distinguish through expressing CD4-GFP under the control of Repo since it labels both cells. Therefore, and because we previously detected that Relish was only activated in subperineurial glia, we specifically labeled this cell membrane through expressing CD4-GFP under the control of MdrG4 driver. We then assessed Subperineurial glia morphology in response to PGN exposure, as previously described. Similar to what we observed before, subperineurial glia processes have a wide range of morphologies (Fig.4.14A). However, there were no differences in subperineurial glia overall area, processes area or processes number (Fig.4.14B).

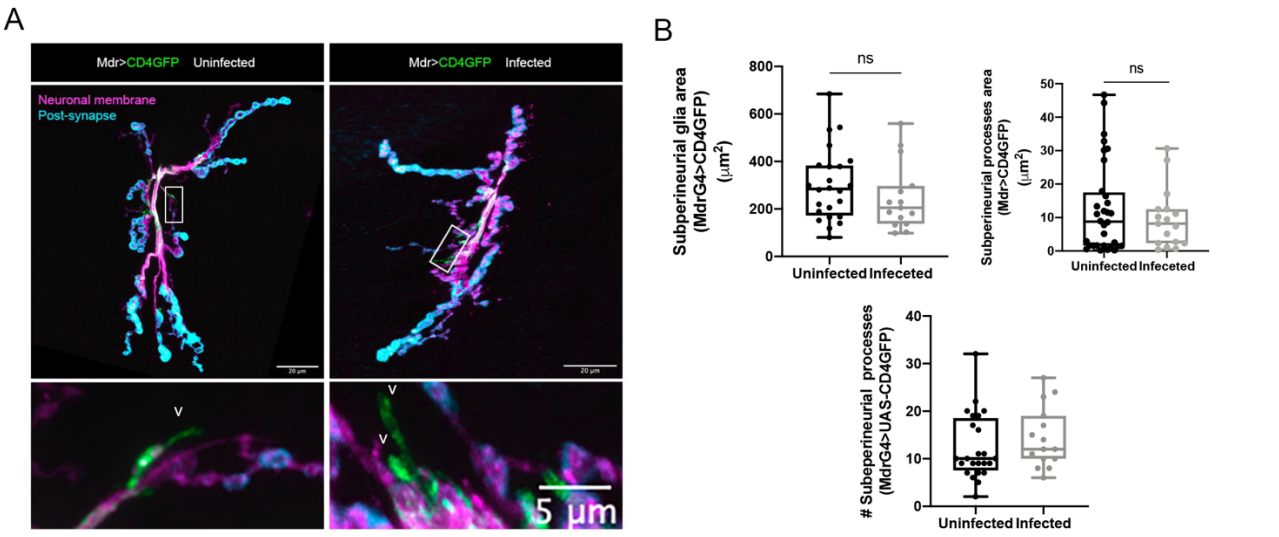

Figure 4.14 NMJ Subperineurial glial morphology does not change in response to PGN exposure. (A) Representative images of Subperineurial glial morphology in MdrG4>UASCD4GFP uninfected (1h in HL3.1) and infected (30' exposed to 300ng/ml of PGN in HL3.1 plus 30' in normal HL3.1) White rectangles identify the region amplified. White arrows point to processes that extend beyond the motor neuron. Neuronal membrane (magenta) is labeled with HRP. Post-synapse is labelled with DLG (cyan). Scale bar: 50 µm ***(B)*** *Quantification of total subperineurial glia area, of glial processes area and the number of processes of uninfected (n=13) and infected (n=12). Unpaired t-test were used.*

Overall, our results show that within the time-frame analyzed there are no alterations in terms of number of processes, overall glial area nor change in glial processes area when comparing uninfected to infected larvae. However, this type of acute exposure might not be sufficient to induce morphologic alterations in glial cells. Therefore, we asked whether consistent genetic activation of Relish could induce any changes in the peripheral nervous system.

4.5. Does persistent activation of Relish induce glial defects?

It is described that hyper activation of Relish in the adult fly induces neurodegeneration. In order to see if the same occurred in Drosophila larvae PNS, we analyzed what happened if we expressed an activated form of Relish (Rel68) in glia (Wiklund et al., 2009). For this we recombined glial drivers with a membrane tagged protein (CD4-GFP or CD8-GFP) and co-stained with HRP to label the neuronal membrane. Normally, perineurial and subperineurial glia wrap around the entire nerve bundle, covering the entire length of ISN. As for wrapping glia, they enwrap axons inside the nerve bundle and provide insulation. When we expressed Rel68 under the control of Repo (Repo-G4>UAS-CD4-GFP:UAS-Rel68), glial morphology was altered at ISN (Fig.4.15A). Specifically, glial membrane appeared fragmented and the ISN nerve was much thicker when compared to controls (Repo-G4>UAS-CD4-GFP) (Fig.4.15A). Furthermore, we also saw that pan-glial expression of Rel-68 induce locomotor defects in 3rd instar larvae (data not shown) and these larvae never reached adult stages, which has been previously described(Winkler et al., 2021). Likewise, when we expressed Rel68 in subperineurial glia (Mdr-G4>UAS-CD4-GFP:UAS-Rel68), the morphology of these glial cells was defective. We observed that, whereas in controls, subperineurial glia wrap the nerve bundle, when we expressed Rel68, subperineurial glia membrane appeared fragmented (Fig.4.15B). Additionally, no glial processes were seen invading the NMJ upon expressing Rel68(data not shown) under the control of Repo nor Mdr. Moreover, when we expressed Rel68 in wrapping glia (Nrv2-G4>UAS-CD8-GFP:UAS-Rel68), severe defects were observed. Whereas in controls Wrapping glia completely surrounded and wrapped the axons, when Rel68 was expressed the membranes of these glia appeared fragmented, failing to enclose and wrap the axons in the bundle (Fig. 4.15 C). These increase in ISN thickness is similar to what have been previously observed when BBB integrity is compromised or in mutants with defective glial developments (Silva-Rodrigues et al., 2020).

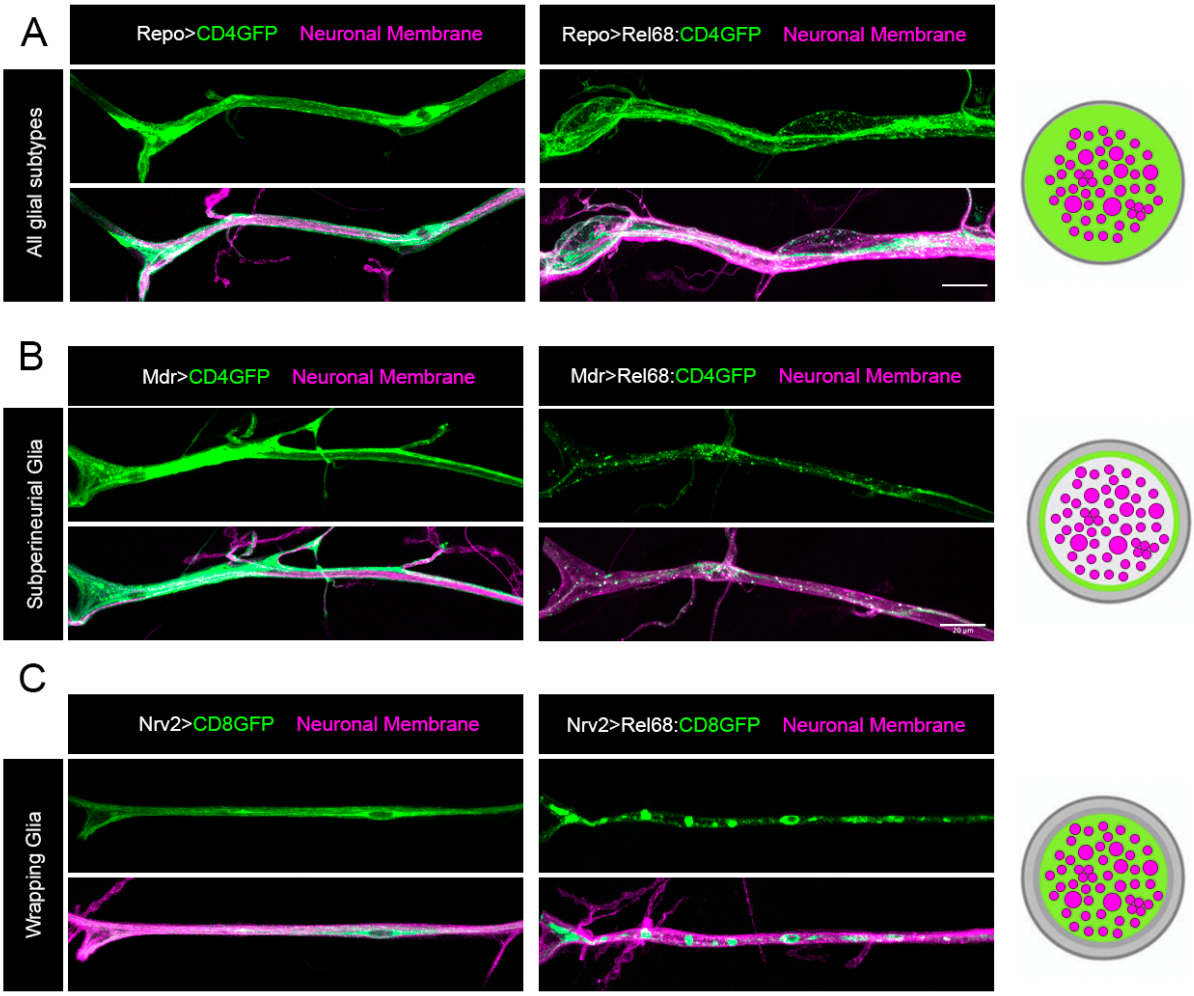

Figure 4.15. Rel 68 induces defects when expressed in peripheral glia. (A) Representative images of control peripheric glial cells (Repo-G4>UAS-CD4-GFP, left) or glial cells overexpressing Rel68 (Repo-G4>UAS-CD4GFP:UAS-Rel68, Right). (B) Representative images of normal Subperineurial glial (MdrG4>UAS-CD8GFP, left) and Subperineurial overexpressing Rel68 (MdrG4>UAS-CD8GFP:UAS-Rel68, Right). Neuronal membrane (magenta) is labelled with HRP. CD4- or CD8-GFP (green) represent glial membrane. (C) Representative images of normal wrapping glial (Nrv2-G4>UAS-CD8-GFP, left) and wrapping glia overexpressing Rel68 (Nrv2>CD8GFP:Rel68, Right). (Scale bar: 20µm. On the left it is represented a schematic of a transversal cut of the ISN with, from top to bottom, all glia, wrapping glial and subperineurial glial represented in green. Axons are represented in magenta.

4.6. Can LMWPM mitigate Relish activation?

Dietary (poly)phenols have neuroprotective and anti-neuroinflammatory potential (Carregosa et al., 2021).. Previously, our group has described Pyr-sulf as a new immune modulator of microglia cells, capable of crossing the BBB and reducing NF-κB *in vitro*, however this has not been verified *in vivo* in a multicellular organism (I. Figueira et al., 2017). Therefore, we questioned whether Pyr-sulf or Aspirin (a known NF-κB inhibitor, already validated in Drosophila (Panettieri et al., 2020; Zhou et al., 2021)) were able to mitigate Relish translocation to the nucleus in normal developmental conditions and in an inflammatory scenario.

To uncover the potential of Pyr-sulf and Aspirin in the inhibition of Relish nuclear translocation, we performed the following: First, we fed larvae, since 1st instar larval stage, that expressed Relish-YFP in all glia (Repo>RelishYFP) with food containing 50μM of Pyr-sulf, or 50μM Aspirin or control food (with no addition of any compound). When larvae reached 3rd instar larval stage we dissected and fixed them as described in the methods. This experiment was conducted without any inflammatory trigger. We imaged and quantified all glial cells present in the ISNs from segments A2-A4, always keeping in mind the presence of different glial subtypes. We quantified Relish nuclear translocation, in all glial cells, through calculating the ratio between nuclear and cytosolic Relish intensity, as previously described. We observed that feeding with Pyr-sulf was able to induce a reduction (although modest) in nuclear Relish in all nuclei as shown in Fig. 4.16. Our data showed that the ratio between nuclear and cytosolic Relish was smaller in larvae fed with Pyr-sulf but not Aspirin when compared to controls (control =1.00±0.05;; Aspirin= 1.07±0.07; Pyr-sulf=0.87±0.04)(Fig.4.16C). Meaning, that Pyr-sulf was able to inhibit Relish nuclear translocation. However, we could observe a large variability within different glial subtypes.

Because we previously saw that the different glia subtypes had different responses to inflammatory insults, observing only Relish activation in subperineurial glia and wrapping glia and because there is a high variability among the different subtypes basal levels, we decided to assess if Aspirin and Pyr-sulf could inhibit basal levels of Relish translocation specifically in subperineurial and wrapping glia. We expressed Relish-YFP specifically in subperineurial glia (MdrG4>UAS-RelishYFP) and fed them with the different food (control food or food containing either Pyr-sulf or Aspirin). We observed that feeding with Aspirin or Pyr-sulf did not alter basal levels of Relish in subperineurial glia when compared to larvae fed in control food (Fig.4.17A and B) (Control food= 1.00±0.06;Aspirin=0.99±0.07;Pyr-sulf=1.00±0.07). By extending this approach to wrapping glia (Nrv2>Relish-YFP) we saw that Aspirin but not Pyr-sulf was able to decrease nuclear and cytosolic Relish ratio when compared to controls (controls = 1.00±0.04, Aspirin= 0.80 ± 0.04; Pyr-sulf= 0.91± 0.04).

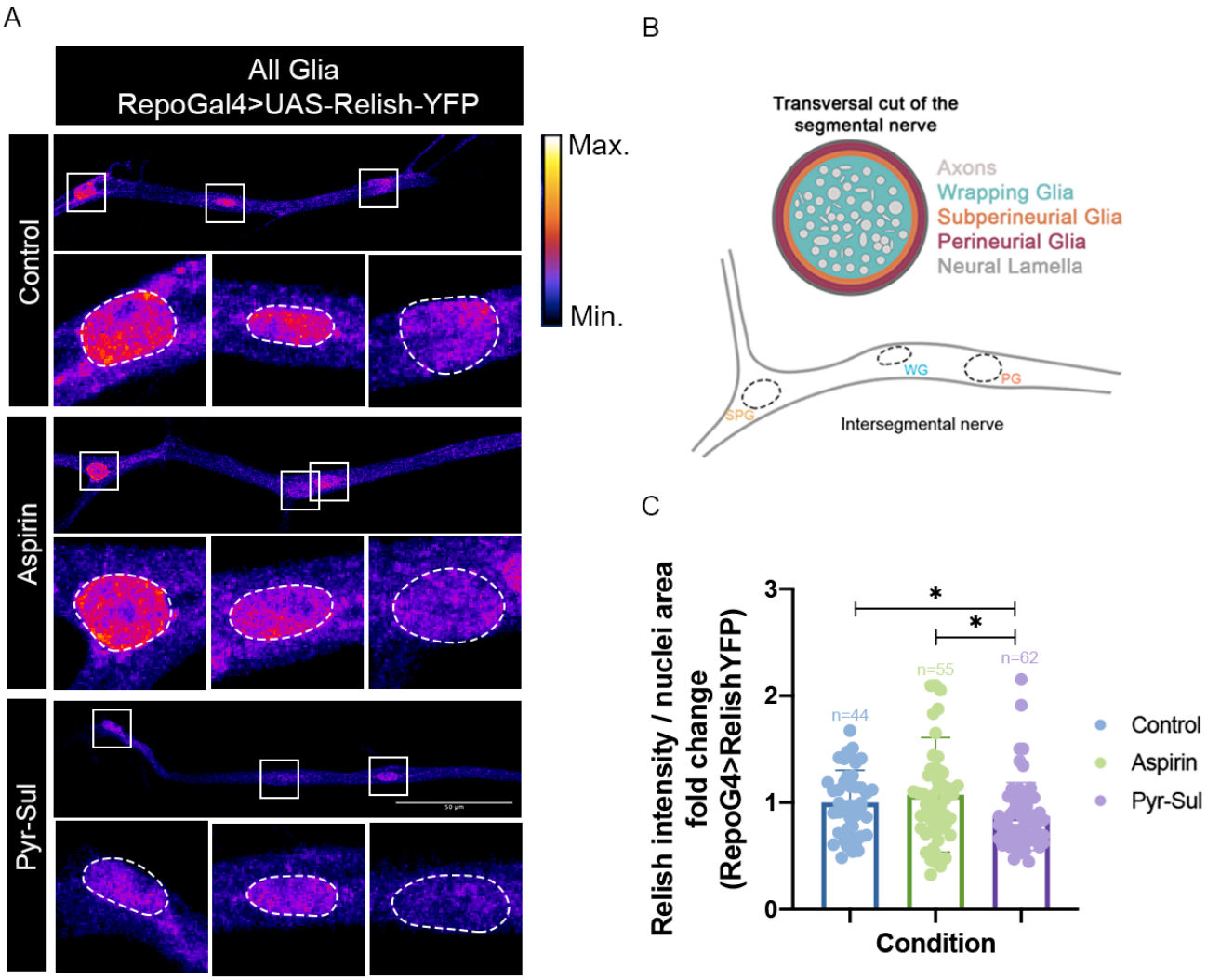

Figure 4.16 Inhibition of Relish in Peripheral glia by Pyr-sulf. *(A) Representative images of Relish intensity in the nuclei and in the cytosol of Repo>Relish-YFP larvae fed with either control food (no compound was added), food containing 50µM of Aspirin or food containing 50µM of Pyr-sulf. White dashed lines represent glial nuclei. White squares represent nuclei magnification on the bottom panels of each condition. Relish is represented in heat map- fire mode. Scale bar: 50 µ m (B) Schematic of the peripheral nerve anatomy with the different glial subtypes cellular positioning. WG- Wrapping glia ; SPG – Subperineurial glia; PG- Perineurial Glia. (C) Quantification of the ratio between nuclear and cytosolic relish fold change between the different feeding conditions: control food (blue): food containing 50µM of Aspirin(green) and food containing 50µM of Pyr-sulf(purple) ;ANOVA- Kruskal-Wallis test was used. n for each condition is shown in the graph. *p<0.05.*

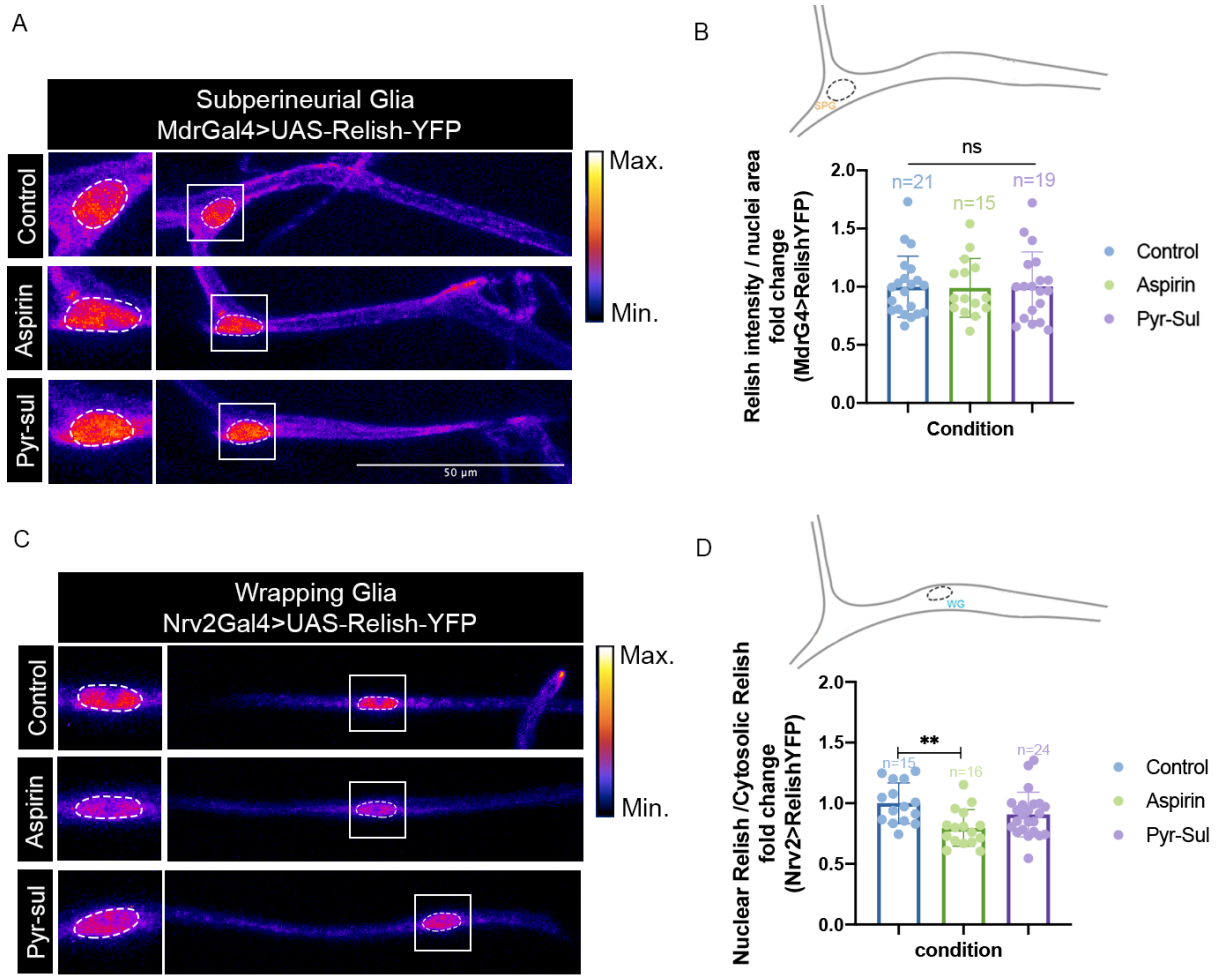

Figure 4.17. Developmental inhibition of Relish activation in Subperineurial and Wrapping glia by Aspirin and Pyr-sulf. *(A) Representative images of Relish intensity in the nuclei and in the cytosol of subperineurial glia (Mdr>Relish-YFP larvae) under different food conditions: fed with either control food (no compound was added), food containing 50µM of Aspirin or food containing 50µM of Pyr-sulf. White dashed lines represent glial nuclei. White squares represent nuclei magnification area. Relish is represented in heat map- fire mode. Scale bar: 50 µm (B)Schematic of the peripheral nerve anatomy with the subperineurial nuclear positioning (Top). Quantification of the ratio between nuclear and cytosolic relish fold change in Subperineurial glia (Mdr>RelishYFP) in the different feeding conditions: control food (blue): food containing 50µM of Aspirin(green) and food containing 50µM of Pyr-sulf(purple) ;ANOVA- Kruskal-Wallis test was used. n for each condition is shown in the graph. (C) Representative images of Relish intensity in the nuclei and in the cytosol of Wrapping glia (Nrv>Relish-YFP larvae) in different food conditions: fed with either control food (no compound was added), food containing 50µM of Aspirin or food containing 50µM of Pyr-sulf. White dashed lines represent glial nuclei. White squares represent nuclei magnification area. Relish is represented in heat map- fire mode. Scale bar: 50 µm (D)Schematic of the peripheral nerve anatomy with the WG nuclear positioning identified (Top). Quantification of the ratio between nuclear and cytosolic relish fold change in Wrapping glia (Mdr>RelishYFP) in the different feeding conditions: control food (blue): food containing 50µM of Aspirin(green) and food containing 50µM of Pyr-sulf(purple) ;; Ordinary one-way ANOVA test was used. n for each condition is shown in the graph. **p<0.01. WG – Wrapping glia; SPG – Subperineurial glia*

The hyperactivation of NF-κB has severe impacts in physiology and it is highly associated with neurodegenerative diseases. Therefore, we assessed whether feeding/pre-conditioning with Pyr-sulf or Aspirin could inhibit PGN induced Relish translocation in peripheral glial cells. First, and similarly to our previous experiments, we expressed Relish-YFP in all glial cells (RepoG4>UAS-Relish-YFP) and either fed them with food containing 50μM of Pyr-sulf, or 50μM Aspirin or control food. After, we either exposed 3rd instar RepoG4>UAS-Relish-YFP larvae to PGN (infected condition) or left them unexposed (uninfected condition) and assessed Relish translocation to the nucleus as described before.

As expected, upon PGN exposure Relish is activated in glial cells of larvae kept on control food when compared to uninfected larvae also kept on control food (Fig.4.18 A and B). Our results showed that the ratio between nuclear and cytosolic Relish increased upon PGN exposure when compared to uninfected condition (uninfected Control food=1.11± 0.11; infected Control food= 2.23±0.23). Interestingly, we observed that the larvae kept in food either containing Aspirin or Pyr-sulf significantly reduced the PGN-induced Relish nuclear translocation, decreasing Relish nuclear/cytosolic ratio to uninfected levels, supporting the notion that these compounds can work as protective factors in the presence of an inflammatory insult.

Specifically, the ratio between nuclear and cytosolic Relish is similar between infected and uninfected larvae fed with Aspirin (Uninfected Aspirin food = 1.11± 0.07; Infected Aspirin= 1.24± 0.14). Similar, the ratio between nuclear and cytosolic Relish in larvae fed with food containing Pyr-sulf were identical between uninfected and infected (uninfected Pyr-sulf= 1.118± 0.07178; Infected Pyr-sulf food= 1.26± 0.05) (Fig.4.18 A and B). Once more, we also observed a high variability within each condition due to the different responses of the peripheric glial subtypes. However, we could notice that the intensity of nuclear Relish in both subperineurial and wrapping glia was decreased in infected conditions fed with Pyr-sulf and Aspirin when comparing to the infected condition fed with normal food, which is also demonstrated by the nuclear and cytosolic ratios (Infected Control food= 2.26±0.23; Infected Aspirin= 1.24± 0.14; Infected Pyr-sulf food= 1.26± 0.05).

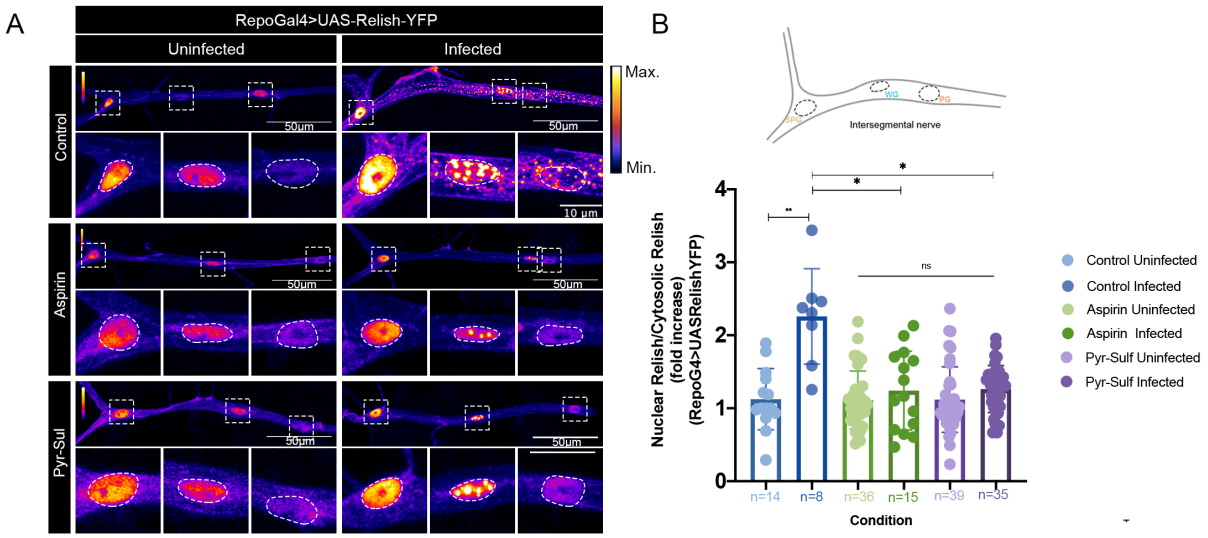

Figure 4.18. Inhibition of PGN dependent Relish nuclear translocation by Pyr-sulf and Aspirin. *(A) Representative images of Relish intensity in the nuclei and in the cytosol of Peripheral glia (Repo>Relish-YFP larvae) in different food conditions: control food (no compound was added), food containing 50µM of Aspirin or food containing 50µM of Pyr-sulf. Uninfected conditions (non-exposed to PGN) (left). Infected conditions (Right). White dashed lines represent glial nuclei. White squares represent nuclei magnification area. Relish is represented in heat map- fire mode. Scale bar: 50 µ m (D)Schematic of the peripheral nerve anatomy with SPG, WG and Perineurial glia nuclear positioning identified (Top). Quantification of the ratio between nuclear and cytosolic Relish fold change in all peripheral glia (Repo>RelishYFP) in the different feeding conditions: control food (blue): food containing 50µM of Aspirin(green) and food containing 50µM of Pyr-sulf(purple). Uninfected conditions are identified by lighter colors and infected conditions by darker colors ; test was used. n for each condition is shown in the graph. Kruskal-Wallis test was used *p<0.05, **p<0.01 ***p<0.001, SPG – Subperineurial glia; PG – Perineurial glia; WG – Wrapping glia*

Since we already know that peripheral glia respond differently to PGN, we tested if pre-conditioning with Aspirin or Pyr-sulf could inhibit Relish activation in a cell specific manner, only in subperineurial glia. For this we fed larvae that only expressed Relish in Subperineurial glia (MdrG4>UAS-RelishYFP) and assessed the ability of these compounds to prevent Relish activation after PGN exposure. As expected, in larvae fed with control food, the ratio between nuclear and cytosolic Relish increased in subperineurial glia upon PGN exposure (uninfected control food=1.00±0.08; Infected control food= 1.78±0.14) (Fig.4.19A and B). In contrast, the same does not happen in larvae fed with 50µM of Aspirin or 50µM Pyr-sulf. In fact, when larvae are fed with Aspirin and exposed to PGN, Relish does not translocate to the nucleus as much when comparing to larvae fed with control food. Our data demonstrates that the ratio between nuclear and cytosolic Relish does not change significantly between uninfected and infected larvae fed with Aspirin (uninfected Aspirin food=1.48±0.11; infected Aspirin food=1.33±0.10) (Fig.4.19B). However, uninfected larvae fed with Aspirin have a higher ratio between nuclear and cytosolic Relish when compared to uninfected larvae fed with control food (uninfected control food= 1.00±0.08; uninfected Aspirin food=1.48± 0.11) (Fig.4.19B). Regarding Pyr-sulf, inhibition of Relish translocation was also observed. Our results showed that pre-conduiting larvae with 50µM of Pyr-sulf decreased the PGN induced Relish activation in subperineurial glia, since the

ratio between nuclear and cytosolic relish does not change between uninfected and infected larvae (uninfected Pyr-sulf food = 1.15± 0.10; infected Pyr-sulf food= 1.41 ± 0.17) (Fig. 4.19B).

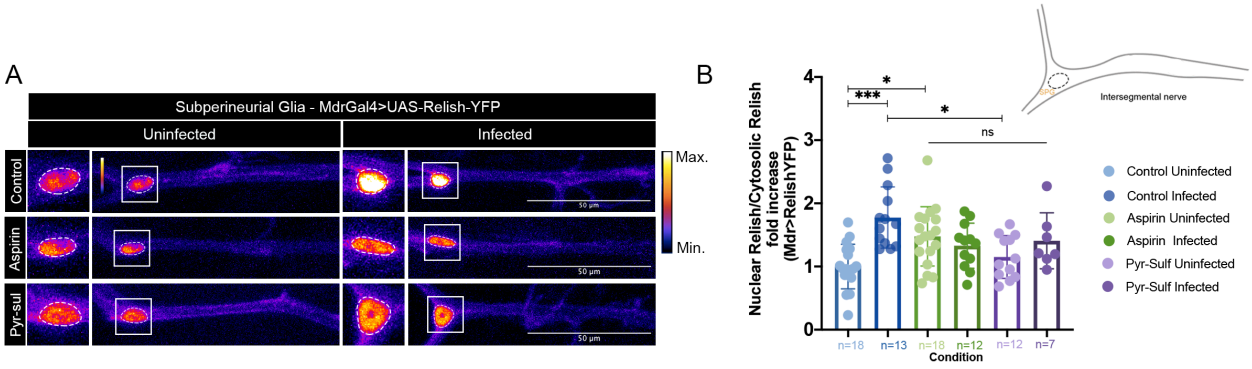

Figure 4.19. Subperineurial Relish dependent nuclear translocation inhibition by Pyr-sulf and Aspirin. *(A) Representative images of Relish intensity in the nuclei and in the cytosol of Subperineurial (MdrG4>UAS-Relish-YFP larvae) in different food conditions: control food (no compound was added), food containing 50µM of Aspirin or food containing 50µM of Pyr-sulf. Uninfected conditions (non-exposed to PGN) (left). Infected conditions (Right). White dashed lines represent glial nuclei. White squares represent nuclei magnification area. Relish is represented in heat map- fire mode. Scale bar: 50 µ m (B)Schematic of the peripheral nerve anatomy with SPG, nuclear positioning identified (Top). Quantification of the ratio between nuclear and cytosolic Relish fold change in SPG (MdrG4>UAS-RelishYFP) in the different feeding conditions: control food (blue): food containing 50µM of Aspirin(green) and food containing 50µM of Pyr-sulf(purple). Uninfected conditions are identified by lighter colors and infected conditions by darker colors; Ordinary one-way ANOVA test was used. n for each condition is shown in the graph. *p<0.05, **p<0.01, ***p<0.0001*

5. DISCUSSION

In this thesis, I developed a novel *in vivo* paradigm to study NF-κB activation in a neuroinflammatory context in Drosophila. This model identified peripheral glia, namely subperineurial glia and wrapping glia, as glial types able to sense PGN exposure and induce Relish activation and translocation to the nucleus. Additionally, this model allows the use of peripheral glia as an *in vivo* system in which to test new drugs in the context of neuroinflammation, by easily assessing the degree of Relish nuclear translocation. In fact, we showed that Aspirin (a known NF-κB inhibitor in both mammals and invertebrates) and pyrogallol-sulfate (a LMWPM shown to have anti-inflammatory abilities *in vitro*) were able to decrease Relish hyperactivation in this PGN-dependent paradigm, showing anti-neuroinflammatory abilities. Furthermore, our approach also allows the assessment of the impact that an inflammatory cue has on other cell types, such as motor neurons.

PGN *ex-vivo* exposure as a new method to study immune response and inflammation

In this project, our main goal was to develop a new method that allowed both the study of the effects of NF-κB activation in the nervous system, and the development of an accessible system in which to uncover the anti-neuroinflammatory potential of nutrition-based compounds.

For the development of this method, we took advantage of the fact that Drosophila NF-κB pathways (such as Imd) are activated upon the recognition of PGN and secondly, of the outstanding genetic tools available, which allowed us to easily track Imd activation. Our inflammatory method consisted in the dissection of 3rd instar larvae of the desired genotype and its exposure to 300ng/ml of PGN from *E. coli* in HL3.1 (a hemolymph mimetic that sustains larval viability). Additionally, to track Imd activation we used a Relish-YFP transgene expressed in glia or other tissues. With this approach we were able to observe the acute consequences of PGN exposure in both live and fixed tissues.

To developed a new inflammatory method, we started by optimizing the exposure to PGN method. We assessed the effect of different PGN concentrations (300ng/ml, 600ng/ml and 1μg/ml) as well as exposure times, on larval tissue viability. We observed that higher PGN concentrations (600ng/ml and 1μg/ml) induced a high degree of tissue damage when compared to the lowest concentration (300ng/ml). Therefore, we decided to proceed with the lowest concentration tested, which did not cause visible tissue damage. Similarly, we observed that longer exposure times to PGN, even with the lowest concentration, also led to tissue damage. For this reason, we chose to expose larvae to PGN for 30' and then change the solution to HL3.1, without bacterial PGN.

After optimization, we began by confirming that our method induced an immune activation in already immune-described tissues. Our results showed that Drosophila larval fat bodies and muscles can detect PGN, since Relish became activated (Fig.4.1 and Fig.4.2). These results are in accordance to the current state of the art, and showed that our method is able to trigger an immune activation. However, we observed some variability, within the same animal, in these tissues' response. This variability might be explained by the fact that the concentration of PGN suspension used throughout our experiments is much lower (300ng/ml) when compared to other studies. In fact, studies that also use Relish as a reporter protein to assess its nuclear translocation in the fat body, use much higher concentrations of PGN (10μg/ml) (Bettencourt et al., 2004). Additionally, in Drosophila it is well establish that Imd activation and the subsequent AMPs expression is highly dependent on PGN amount, for instance *E .coli* PGN concentrations in the range of 600ng/ml induce milder expression of AMPs when compared to 6ug/ml of PGN (Leulier et al., 2003). Thus, increasing the concentration of PGN upon the moment of exposure would be a plausible strategy to test if the variability in Relish activation within these tissues is due to PGN concentration. However, when optimizing this method, we observed that higher PGN induced severe tissue damage. Therefore, we chose to continue with the lowest concentration(300ng/ml). Moreover, another limiting factor of our approach is the availability of PGN, since PGN is an insoluble molecule, it might not reach the tissues in a uniform manner. this also represents a plausible justification for the variability observed in these already described immune tissues.

In addition, we have to consider that our experiments are not performed in germ-free animals, meaning that the animals used in this study have been in contact with microorganisms. Therefore, another hypothesis is that the variability that we observed in some cases in our experiments, might be due to a possible encounter or challenge with a pathogen throughout animal development.

Another limitation of our method is the time constrain of ex vivo larvae viability. Here, we used dissected 3rd instar larvae with intact organs and exposed them to PGN in a solution that mimics the hemolymph of the larvae. However, the preparation viability is not maintained for more than 3h. Consequently, our method only allows the assessment of acute effects of exposure and the responses that can be trigger within that time-frame. In the future, it would be interesting to address how PGN can impact tissues in a longer time frame. To achieve this, small changes in our current method would need to be performed. For example, change the medium of incubation to Schneider's Insect Medium, which is described to maintain larvae viability for much longer periods (up to 72h). However, some optimizations would be required. Additionally, another way to overcome this problem would be to change the exposure method and directly inject PGN in the hemolymph of intact larvae. This last approach would not only allow to keep larvae for longer periods but also to enable the assessment of more chronic long-lasting impacts of PGN exposure. In spite of the advantages that direct PGN injection would provide this method faces some challenges. During the development of this project, we also tested an injection approach (not shown), facing many step-backs: First, this method induced a high larval death rate perhaps due to puncture, since high death rates occurred even upon injection with a non-inflammatory solution. Second, to administer a precise amount of solution we would need to use a microinjector which would further require several other optimizations.

Nevertheless, despite some limitations, our method provides a simple, reproducible and fast way to assess inflammatory responses in several tissues and cells, both individually or at the same time also allowing the observation of PGN impact in live and fixed samples.

PERIPHERAL GLIA: A NOVEL PLAYER IN INNATE IMMUNITY?

Our work demonstrated that subperineurial and wrapping glia in the peripheral nervous system are able to perceive a PGN inflammatory insult and engage an immune response that culminates in the activation of Relish. Additionally, we observed that Relish activation differs in these glial subtypes (Fig. 4.9.). In subperineurial glia, PGN induces Relish nuclear translocation in a canonical manner, while in wrapping glia, in addition to increasing in the nucleus, Relish also accumulates in the cytosol forming puncta-like structures. The different responses of subperineurial and wrapping glia suggests that the immune response that these glial cells engage upon PGN perception might be different. In fact, we tried to unveil the localization of these cell-specific Relish puncta by assessing if these puncta were localized to a particular organelle, specifically mitochondria. Our results showed that some of the Relish puncta that were formed in response to PGN co-localize with Cytochrome-C, a protein very abundant in the mitochondria. However, to further verify Relish presence in the mitochondria upon PGN exposure, additional experiments are

required. One interesting experiment would be to do dual live-imaging of mitochondria and Relish upon PGN exposure. This would not only allow us to assess Relish accumulation in mitochondria over time, but also allow to assess the impact that PGN exposure might have in mitochondrial dynamics. Our discovery of Relish in the mitochondria is supported by previous findings, since we are not the first to detect NF-κB inside this organelle after an inflammatory stimulus (Cogswell et al., 2003; De Pinto et al., 2019) Despite the existence of several studies showing that NF-κB is present in mitochondria, little progress has been made in uncovering the specific roles for mitochondrial NF-κB, and its function in the cell's powerhouse. The evidence gathered seems to be controversial and complex, suggesting that mitochondrial NF-κB have functions in several processes that range from mitochondrial dynamics, apoptosis to gene expression. Therefore, further studies are needed to disclose its precise function and assess if it regulates more than one aspect of mitochondrial function.

In contrast to subperineurial and wrapping glia, perineurial glia in the PNS either fail to sense PGN or to induce Relish activation. We conducted an experiment to exclude the possibility that this lack of response was due to absence of expression of Relish in perineurial glia, due to the G4 drivers used. We expressed H2BYFP under the control of each driver used and our data demonstrated that H2BYFP was present in perineurial glia. Thus, the absent activation of Relish observed in perineurial glia was not due to lack or weak expression by the Gal4 drivers used. However, the absent observation of Relish activation does not mean that perineurial glia are unresponsive. In fact, these cells may have a later onset response to PGN. This hypothesis could be tested if we were able to change our method and increase the periods of observation after PGN exposure. Another possibility was through the induction of a more chronic type of insult, such as the early onset injection of PGN directly in the larvae hemolymph and the assessment of perineurial glial responses at different timepoints. Yet another possibility, is that PGN administration to the dissected larvae does not reach perineurial glia. For example, if perineurial and subperineurial glia form a diffusion barrier (possibly the BNB) that prevents PGNs from accessing one glial subtype but not the other. To test this hypothesis, we could repeat the experiments performed using a mutant with a disrupted BNB.

Additionally, a question that still remains unanswered is the ability of these peripheric glial, namely subperineurial and wrapping glia, to further trigger an inflammatory reaction such as the induction of AMP expression or the expression of other Relish targets.

Recently, Winkler *et al.*, showed that, upon infection with a neurotrophic pathogen, Imd-Relish is activated, which induces AMP's increase in the brain and the expression of Pfv2 which triggers macrophages recruitment (Winkler et al., 2021). This macrophage recruitment by glial cells is highly dependent on Imd activation in perineurial and subperineurial glia. Nonetheless, the authors state that additional glial types are likely to be involved since individually perineurial and subperineurial Imd activation failed to induce any macrophage invasion into the CNS. This study points towards an immune responsive ability of glial cells. While Winkler *et al.,* reported an immune function for glial cells in the CNS, the individual relevance and contribution of each subtype, as well as the cue that activates this response upon pathogen infection remains largely a mystery. Our

observations, in addition to support an innate immune function for Drosophila glial cells, specifically differentiate between responsive and non-responsive glial subtypes in the PNS in 3rd instar larvae. Furthermore, our results identified PGN as the possible inflammatory molecule responsible for activating Imd-Relish in glial cells (Winkler et al., 2021).

Additionally, to dive into the possible molecular mechanisms that drive the different responses between glia, we have tested if PGRP-LC, the main PGRP receptor was expressed in peripheral glia. This experiment was based in labelling the cells that expressed these receptors, through the use of a Gal4 trap inserted in the receptor promoter, and expressing a nuclear florescent marker. In our data we were not able to detect PGRP-LC in any peripheral glia, suggesting that PGRP-LC is not expressed in these cells. However, it has been observed that many Gal4 traps do not mimic faithfully the expression of their targets, which is thought to depend on the exact location of the insertion site on the promoter of the gene. Therefore, additional experiments should be conducted to assess the presence of this receptor in peripheral glia. It is also possible that PGN fragments might be sensed by other PGRPs such as PGRP-LE or PGRP-SA, which are also known to activate Imd pathway culminating in Relish nuclear translocation and thus should be investigated.

To briefly recapitulate, our experiments showed that in the PNS, glial cells respond differently to PGN exposure. While subperineurial and wrapping glia are responsive and can trigger Relish activation, perineurial glia do not seem to be able to perceive and induce Relish activation, at least in the time points analyzed. Our results additionally showed that Relish is activated differently in subperineurial and wrapping glia suggesting that these glial subtypes engage in different responses (Fig 4.9). Still, further experiments need to be performed in order to address which are the Relish targets in wrapping and subperineurial glia and what governs the basis of their different responses.

New immature pre-synaptic structures and synaptic debris are formed in response to PGN exposure

Neuroinflammation has been correlated with many peripheral neuropathies. Thus, we asked whether PGN exposure could have an impact in motor neurons. Our results showed that upon PGN exposure, motor neurons shed neuronal debris and form new immature pre-synaptic structures. Normally, new immature synaptic boutons and the shedding of neuronal debris occurs when there is an increase in neuronal activity. After formation, new immature synaptic boutons can either mature and become functional or, just like synaptic debris, be engulfed by glia and muscles (Fuentes-medel et al., 2009). Unfortunately, we did not have time to assess the future of this newly formed structures. Nonetheless, in the future it would be interesting to perform long term imaging of these newly formed structures and assess if they could mature, through analyzing the recruitment of mature and functional synapse markers (such as DLG). Additionally, if PGN exposure induces the formation of new ghost boutons directly, is not clear. One possibility would be that PGN would directly bind to PGRP-LC, which has been previously shown to function locally at the pre-synaptic terminal of the motor neuron to regulate homeostatic plasticity (Harris et al., 2015). Therefore, one hypothesis is that the direct binding of PGN to PGRP could trigger the

direct action of the canonical Imd-kinase signaling pathway, activating the transcription factor Relish, which would then govern the rapid or long-term, transcription-dependent synaptic alterations. This would not be surprising since in live neurons NF-kB was reported to be retrogradely transported from the synapse to the nucleus and which elimination negatively impacted cognition in mice (Meffert et al., 2003; Wellmann et al., 2001).

Additionally, infections and the recognition of PAMPs are known to trigger the formation of ROS in several tissues with the primer goal to eliminate pathogens. Plus, some studies in Drosophila have also highlighted the role of ROS as a second messenger in synaptic plasticity, more specifically in bouton formation (Oswald et al., 2018). Therefore, another possibility is that the formation of these immature boutons is triggered in response to increase ROS levels.

Altogether, whether or not these hypotheses are correct, our data opens the door towards the understanding of how inflammatory cues and immune signaling come together to influence neuronal structure and function at a cellular level.

PGN effects at NMJ: Glial morphology is not altered

In mammals, glial cells play pivotal immune roles. For instance, microglia cells are immune responsive and upon the recognition of PAMPs are able to change their morphology and change into activated states, engaging in inflammatory responses to cope with the hazard previously detected, and to effectively clear neuronal debris. In Drosophila the role of glial cells in clearing neuronal debris has been studied (Fuentes-medel et al., 2009). However, to our knowledge, the ability of Drosophila glial cells to change morphology in response to PAMPs has not been reported. Thus, we used 3rd instar Drosophila larvae to inquire about peripheral glial morphology in response to PAMPs, specifically, PGN from *E. coli*. Our data suggested that within the time frame analyzed, the overall area, number of processes and area of processes is not altered. Even though we were unable to detect any morphologic alterations, it is still possible that these cells change in response to PGN. One possibility is that PGN takes longer to induce morphologic alterations in glial cells which, with our approach, we were not able to detect. Additionally, glial cellular extensions at the NMJ are highly dynamic and thought to continuously survey the environment, thus another possibility is that PGN induces alterations in these dynamics, which in fixed samples are impossible to observe. Thus, in the future, it would be interesting to assess if PGN induces changes in glial processes dynamics overtime or in response to longer exposure periods of PGN through live imaging. In the absence of visible morphological alterations, it is possible that there are signaling pathways that are activated upon PGN exposure, which should also be tested in the future.

Inhibition of Relish by Pyr-sulf and Aspirin

There are several studies that started to disclose the impact of (poly)phenol properties in health and disease generating accumulating evidence that indicates that (poly)phenols

are beneficial against human diseases and in controlling neuroinflammation. *Drosophila melanogaster* is progressively emerging as a model organism to study the role of (poly)phenol metabolites with the majority of studies focusing in their abilities to extend lifespan or their protective abilities in neurodegenerative models. In fact, several studies have shown that Gallic acid, a LMWPM of the class of benzoic acids, is protective in Parkinson disease models, as well as protective against genotoxic agents (Carregosa et al., 2021). Several LMWPM of the cinnamic acids class such as ferulic acid and caffeic acid have also been shown to be able to ameliorate PD-like phenotypes in chemical induced Parkinson's disease models (Carregosa et al., 2021). Additionally, there are several other studies in Drosophila that point towards a positive impact of a Mediterranean diet, as well as a beneficial role of (poly)phenols. These studies showed that supplementation with food extracts rich in (poly)phenols were able to increase lifespan in normal WT flies as well as to improve neurodegenerative-like phenotypes in several neurodegenerative models (Carregosa et al., 2021). Although informative, the use of food extracts rich in (poly)phenols, makes it difficult to precise the potential bioactivity of each individual compound. Furthermore, the research in Drosophila (poly)phenol's ability has extensively been focused on (poly)phenol overall ability to improve or ameliorate neurodegenerative phenotypes with the precise activity of this compounds being highly overlooked. However, age-related neurodegenerative diseases are considered multifactorial diseases with several mechanisms such as neuroinflammation and oxidative stress highly associated with its development and progression. Therefore, understanding how specific LMWPM influence specific molecular pathways involved in neurodegeneration is essential for the future design of therapeutic strategies. As previously mentioned, chronic immune activation such as prolonged glial NF-κB activation has been implicated as a factor underlying neurodegeneration, leading to the development and acceleration of disease progression.

Pyr-sulf, a LMWPM, was first identified in human plasma from volunteers after ingestion of a fruit puree in concentrations up to 20 μM (Pimpão et al., 2015). This compound has also been shown to be able to cross an in vitro model of the blood-brain barrier and to be neuroprotective, by modulate and attenuating neuroinflammatory markers in microglial cells in vitro, through the reduction of LPS-induced NF-κB activation (I. Figueira et al., 2017). However, the ability for this metabolite to decrease NF-κB activation after an inflammatory insult in a multicellular organism has not yet been tested before.

Here we aimed to address the ability of Pyr-sulf in decreasing NF-κB activation in an overexpression and neuroinflammatory context. For this we took advantage of our new paradigm which allows the tracking of Relish activation after in basal levels or after PGN inflammatory insult. To assess Pyr-sulf ability to decrease Relish activation we fed the larvae with food containing 50μM of Pyr-sulf or food not containing any additional compound. As a positive control we also fed larvae with food containing 50μM of Aspirin, a known NF-κB inhibitor.

Regarding Relish basal levels, when analyzing all glial cells simultaneously, our results suggested that Pyr-sulf was able to inhibit Relish nuclear translocation throughout development (Fig.4.16). However, the effects of Pyr-sulf on nuclear translocation were not observed in subperineurial and wrapping glia when we specifically expressed Relish in

these subtypes (Fig.4.17), suggesting that the Pyr-sulf exerted most of its effects in perineurial glia or that more complex effects are at play. On the other side, we observed that Aspirin exerted most of its effects in wrapping glia (Fig.4.17). One possibility would be that these different molecules affected different molecular mechanisms or glial subtypes, thus explaining the differences observed. Nonetheless, the mechanism of action of Pyr-sulf is not yet known and further studies are required to infer if this hypothesis is true. Nonetheless, these experiments should be repeated in order to re-confirm the observed results.

Our results demonstrated that PGN-induced Relish activation in peripheral glia can be inhibited by a validated anti-inflammatory compound, Aspirin. Interestingly, we here showed that Pyr-sulf pre-conditioning was also able to decrease Relish-PGN induced activation. These results highlight the potential Pyr-sulf metabolite as preventive approach to control neuroinflammation, further supporting previous results about the ability of these compound to control neuroinflammation and decrease NF-κB in microglia (I. Figueira et al., 2017). Studies specifically related to the effect of (poly)phenols in decreasing neuroinflammation in animal models are scarce and, to the best of our knowledge, we are the first to use a LMWPM in the context of neuroinflammation in *Drosophila melanogaster*. In the future it would be interesting to address whether other LMWPM could also decrease Relish activation in this new paradigm. Additionally, through taking advantage of the genetic tools available in Drosophila one could assess the mechanism through which these compounds would act upon to regulate and inhibit Relish activation.

Additionally, we developed a powerful method that could be used in the future to promote the discovery of new possible therapeutic targets to decrease neuroinflammation. The use of this method would allow for the fast and efficient screening of anti-inflammatory molecules potentiating the discovery of novel therapeutic compounds to control neuroinflammation, which could posteriorly be extended to vertebrates and help control and tame neuroinflammation and its deleterious effects.

6. CONCLUSION

In this thesis, we developed a new method to induce inflammation, using the Drosophila 3rd instar larvae. Our method combines the use of a larval preparation that preserves tissue integrity, with the addition of peptidoglycans as an inflammatory cue, which makes possible the assessment of the impact that inflammation has on several tissues. Here, by taking advantage of a Relish (NF-κB) construct fused with YFP, we show that larval peripheral glial cells, namely subperineurial glia and wrapping glia are able to sense PGN exposure and activate an innate immune-related pathway, specifically Imd-Relish. Additionally, we report different responses regarding Relish activation in subperineurial and wrapping glia, suggesting that they engage in different immune responses upon PGN exposure. In contrast, we see that perineurial glial are not able to engage in Relish activation after PGN exposure, suggesting that this glial subtype is not immune responsive or that the PGN does not reach this glial subtype in the larval preparation used.

Furthermore, we took advantage of the fact that our model allows the tracking of Relish activation to study the potential of Pyr-sulf and Aspirin in controlling Relish activation. We show that both Pyr-sulf and Aspirin are able to decrease PGN-induced Relish activation in peripheral glia. Thus, our new method allows a straightforward, versatile and scalable method for the screening of putative anti-neuroinflammatory compounds. Additionally, due to the vast genetic toolkits available in Drosophila, in the future it is possible to study the molecular mechanism through which these compounds act upon to control NF-κB activation, namely by expressing RNAi of genes of interest in specific cell types, and assessing the effect (or lack of it) in NF-κB activation.

Overall, the development of this new paradigm provides new insights about the cellular players that mediate neuroinflammation in Drosophila, helping to understand how the nervous system responds to inflammatory molecules. This new method also opens the door to the fast screening of potential compounds for controlling neuroinflammation, which can then be further tested in vertebrates.

7. FUNDING

This work has received funding from the European Research Council (ERC) under the European Union's Horizon 2020 research and innovation programme under grant agreement No 804229. iNOVA4Health Research Unit (LISBOA—01–0145—FEDER—007344), which is co- funded by Fundação para a Ciência e Tecnologia (FCT)/Ministério da Ciência e do Ensino Superior, through national funds, and by FEDER under the PT2020 Partnership Agreement, is acknowl- edged. Authors would like to acknowledge FCT for financial support of D.C (2020.04630.BD), R.M (CEEC/04567/CBIOS/2020) and S.F (UIDP/BD4/04567/2020).

8. REFERENCES

Alcamí, P., & Pereda, A. E. (2019). Beyond plasticity: the dynamic impact of electrical synapses on neural circuits. *Nature Reviews Neuroscience*, *20*(5), 253–271. https://doi.org/10.1038/s41583-019-0133-5

Allocca, M., Zola, S., & Bellosta, P. (2016). *The Fruit Fly, Drosophila melanogaster: The Making of a Model (Part I) Provisional chapter The Fruit Fly, Drosophila melanogaster: The Making of a Model (Part I)*. https://doi.org/10.5772/intechopen.72832

Arora, S., & Ligoxygakis, P. (2020). Beyond Host Defense: Deregulation of Drosophila Immunity and Age-Dependent Neurodegeneration. *Frontiers in Immunology*, *11*(July), 1–13. https://doi.org/10.3389/fimmu.2020.01574

Badinloo, M., Nguyen, E., Suh, W., Alzahrani, F., Castellanos, J., Klichko, V. I., Orr, W. C., & Radyuk, S. N. (2018). Overexpression of antimicrobial peptides contributes to aging through cytotoxic effects in Drosophila tissues. *Archives of Insect Biochemistry and Physiology*, *98*(4), 1–22. https://doi.org/10.1002/arch.21464

Barajas-azpeleta, R., Wu, J., Gill, J., & Welte, R. (2018). *Antimicrobial peptides modulate long-term memory*. 1–26.

Bauke, A. C., Sasse, S., Matzat, T., & Klämbt, C. (2015). A transcriptional network controlling glial development in the drosophila visual system. *Development (Cambridge)*, *142*(12), 2184–2193. https://doi.org/10.1242/dev.119750

Baumgartner, S., Littleton, J. T., Broadie, K., Bhat, M. A., Harbecke, R., Lengyel, J. A., Chiquet-Ehrismann, R., Prokop, A., & Bellen, H. J. (1996). A Drosophila neurexin is required for septate junction and blood-nerve barrier formation and function. *Cell*, *87*(6), 1059–1068. https://doi.org/10.1016/S0092-8674(00)81800-0

Bettencourt, R., Asha, H., Dearolf, C., & Ip, Y. T. (2004). Hemolymph-dependent and -independent responses in Drosophila immune tissue. *Journal of Cellular Biochemistry*, *92*(4), 849–863. https://doi.org/10.1002/jcb.20123

Blanchette, M., & Daneman, R. (2015). Formation and maintenance of the BBB. *Mechanisms of Development*, *138*, 8–16. https://doi.org/10.1016/j.mod.2015.07.007

Bonetto, G., Kamen, Y., Evans, K. A., & Káradóttir, R. T. (2020). Unraveling Myelin Plasticity. *Frontiers in Cellular Neuroscience*, *14*, 156. https://doi.org/10.3389/FNCEL.2020.00156/BIBTEX

Brand, a H., & Perrimon, N. (1993). Targeted gene expression as a means of altering cell fates and generating dominant phenotypes. *Development (Cambridge, England)*, *118*(2), 401–415.

Brink, D. L., Gilbert, M., Xie, X., Petley-Ragan, L., & Auld, V. J. (2012). Glial Processes at the Drosophila Larval Neuromuscular Junction Match Synaptic Growth. *PLoS ONE*, *7*(5), 37876. https://doi.org/10.1371/journal.pone.0037876

Brunger, A. T., Choi, U. B., Lai, Y., Leitz, J., White, K. I., & Zhou, Q. (2019). The pre-synaptic fusion machinery. *Current Opinion in Structural Biology*, *54*, 179–188. https://doi.org/10.1016/j.sbi.2019.03.007

Buchon, N., Silverman, N., & Cherry, S. (2014). Immunity in Drosophila melanogaster-from microbial recognition to whole-organism physiology. *Nature Reviews Immunology*, *14*(12), 796–810. https://doi.org/10.1038/nri3763

Cao, P., Chen, C., Liu, A., Shan, Q., Zhu, X., Jia, C., Peng, X., Zhang, M., Farzinpour, Z., Zhou, W., Wang, H., Zhou, J. N., Song, X., Wang, L., Tao, W., Zheng, C., Zhang, Y., Ding, Y. Q., Jin, Y., … Zhang, Z. (2021). Early-life inflammation promotes depressive symptoms in adolescence via microglial engulfment of dendritic spines. *Neuron*, *109*(16), 2573-2589.e9. https://doi.org/10.1016/j.neuron.2021.06.012

Cao, Y., Chtarbanova, S., Petersen, A. J., & Ganetzky, B. (2013). *Dnr1 mutations cause neurodegeneration in Drosophila by activating the innate immune response in the brain*. https://doi.org/10.1073/pnas.1306220110

Carr, M. J., & Johnston, A. P. (2017). Schwann cells as drivers of tissue repair and regeneration. *Current Opinion in Neurobiology*, *47*, 52–57. https://doi.org/10.1016/j.conb.2017.09.003

Carregosa, D., Carecho, R., & Santos, C. N. (2019). *Low-Molecular Weight Metabolites from Polyphenols as Effectors for Attenuating Neuroinflammation*. https://doi.org/10.1021/acs.jafc.9b02155

Carregosa, D., Mota, S., Ferreira, S., Alves-Dias, B., Loncarevic-Vasiljkovic, N., Crespo, C. L., Menezes, R., Teodoro, R., Nunes, C., & Santos, D. (2021). *Overview of Beneficial Effects of (Poly)phenol Metabolites in the Context of Neurodegenerative Diseases on Model Organisms*. https://doi.org/10.3390/nu13092940

Ceasrine, A. M., & Bilbo, S. D. (2021). Primetime for microglia: When stress and infection collide. *Neuron*, *109*(16), 2503–2505. https://doi.org/10.1016/j.neuron.2021.07.023

Chatterjee, A., Roy, D., Patnaik, E., & Nongthomba, U. (2016). Muscles provide protection during microbial infection by activating innate immune response pathways in Drosophila and zebrafish. *DMM Disease Models and Mechanisms*, *9*(6), 697–705. https://doi.org/10.1242/dmm.022665

Chung, W. S., Allen, N. J., & Eroglu, C. (2015). Astrocytes control synapse formation, function, and elimination. *Cold Spring Harbor Perspectives in Biology*, *7*(9). https://doi.org/10.1101/cshperspect.a020370

Cogswell, P. C., Kashatus, D. F., Keifer, J. A., Guttridge, D. C., Reuther, J. Y., Bristow, C., Roy, S., Nicholson, D. W., & Baldwin, A. S. (2003). NF-κB and IκBα Are Found in the Mitochondria: EVIDENCE FOR REGULATION OF MITOCHONDRIAL GENE EXPRESSION BY NF-κB *. *Journal of Biological Chemistry*, *278*(5), 2963–2968. https://doi.org/10.1074/JBC.M209995200

Daneman, R, Zhou, L., Agalliu, D., Cahoy, J. D., & Kaushal, A. (2010). The Mouse Blood-Brain Barrier Transcriptome: A New Resource for Understanding the Development and Function of Brain Endothelial Cells. *PLoS ONE*, *5*(10), 13741. https://doi.org/10.1371/journal.pone.0013741

Daneman, Richard, & Prat, A. (2015). *The Blood-Brain Barrier*. https://doi.org/10.1101/cshperspect.a020412

Daneman, Richard, Zhou, L., Kebede, A. A., & Barres, B. A. (2010). *Pericytes are required for blood-brain barrier integrity during embryogenesis*. https://doi.org/10.1038/nature09513

Das, M., Matzat, T., Xie, X., & Auld, V. J. (2018). *Understanding the molecular mechanisms underlying Glia-Glia communication in the drosophila peripheral nerve* (Issue March) [THE UNIVERSITY OF BRITISH COLUMBIA]. http://ieeeauthorcenter.ieee.org/wp-content/uploads/IEEE-Reference-Guide.pdf%0Ahttp://wwwlib.murdoch.edu.au/find/citation/ieee.html%0Ahttps://doi.org/10.1016/j.cie.2019.07.022%0Ahttps://github.com/ethereum/wiki/wiki/White-Paper%0Ahttps://tore.tuhh.de/hand

Davie, K., Janssens, J., Koldere, D., De Waegeneer, M., Pech, U., Kreft, Ł., Aibar, S., Makhzami, S., Christiaens, V., Bravo González-Blas, C., Poovathingal, S., Hulselmans, G., Spanier, K. I., Moerman, T., Vanspauwen, B., Geurs, S., Voet, T., Lammertyn, J., Thienpont, B., … Aerts, S. (2018). A Single-Cell Transcriptome Atlas of the Aging Drosophila Brain. *Cell*, *174*(4), 982-998.e20. https://doi.org/10.1016/j.cell.2018.05.057

De Pinto, V., Mishmar, D., & Albensi, B. C. (2019). *What Is Nuclear Factor Kappa B (NF-κB) Doing in and to the Mitochondrion?* https://doi.org/10.3389/fcell.2019.00154

DiSabato, D. J., Quan, N., & Godbout, J. P. (2016). *Neuroinflammation: the devil is in the details*. https://doi.org/10.1111/jnc.13607

Fernandes, A. R., Mendes, C. S., Gomes, E. R., & Teodoro, R. O. (2021). Motor neuron boutons remodel through membrane blebbing. *BioRxiv*, 2021.03.07.434250. https://doi.org/10.1101/2021.03.07.434250

Figueira, I., Garcia, G., Pimpão, R. C., Terrasso, A. P., Costa, I., Almeida, A. F., Tavares, L., Pais, T. F., Pinto, P., Ventura, M. R., Filipe, A., McDougall, G. J., Stewart, D., Kim, K. S., Palmela, I., Brites, D., Brito, M. A., Brito, C., & Santos, C. N. (2017). Polyphenols journey through blood-brain barrier towards neuronal protection. *Scientific Reports*, *7*(1), 1–16. https://doi.org/10.1038/s41598-017-11512-6

Figueira, Ines ;, Garcia, G., Pimpão, R. C., Terrasso, A. P., Costa, I., Almeida, A. F., Tavares, L., Pais, T. F., Pinto, P., Ventura, M. R., Filipe, A., Mcdougall, G. J., Stewart, D., Kim, K. S., Palmela, I., Brites, D., Brito, M. A., Brito, C., & Santos, C. N. (2017). *Polyphenols journey through blood-brain barrier towards neuronal protection*. https://doi.org/10.1038/s41598-017-11512-6

Fuentes-medel, Y., Logan, M. A., Ashley, J., Ataman, B., Budnik, V., & Freeman, M. R. (2009). *Glia and Muscle Sculpt Neuromuscular Arbors by Engulfing Destabilized Synaptic Boutons and Shed Presynaptic Debris*. *7*(8). https://doi.org/10.1371/journal.pbio.1000184

Glass, C. K., Saijo, K., Winner, B., Marchetto, M. C., & Gage, F. H. (2010). *Mechanisms Underlying Inflammation in Neurodegeneration*. https://doi.org/10.1016/j.cell.2010.02.016

Hammond, T. R., Robinton, D., & Stevens, B. (2018). Microglia and the Brain: Complementary Partners in Development and Disease. *Annual Review of Cell and Developmental Biology*, *34*, 523–544. https://doi.org/10.1146/annurev-cellbio-100616-060509

Han, M. H., Kwon, M. J., Ko, B. S., Hyeon, D. Y., Lee, D., Kim, H. J., Hwang, D., & Lee, S. B. (2020). NF-κB disinhibition contributes to dendrite defects in fly models of neurodegenerative diseases. *The Journal of Cell Biology*, *219*(12). https://doi.org/10.1083/jcb.202004107

Hanson, M. A., & Lemaitre, B. (2020). New insights on Drosophila antimicrobial peptide function in host defense and beyond. *Current Opinion in Immunology*, *62*, 22–30. https://doi.org/10.1016/j.coi.2019.11.008

Harris, N., Braiser, D. J., Dickman, D. K., Fetter, R. D., Tong, A., & Davis, G. W. (2015). The Innate Immune Receptor PGRP-LC Controls Presynaptic Homeostatic Plasticity. *Neuron*, *88*(6), 1157–1164. https://doi.org/10.1016/j.neuron.2015.10.049

Harris, N., Fetter, R. D., Brasier, D. J., Tong, A., & Davis, G. W. (2018). Molecular Interface of Neuronal Innate Immunity, Synaptic Vesicle Stabilization, and Presynaptic Homeostatic Plasticity. *Neuron*, *100*(5), 1163-1179.e4. https://doi.org/10.1016/j.neuron.2018.09.048

Kaltschmidt, B., & Kaltschmidt, C. (2010). NF- B in the Nervous System. *Cold Spring Harbor Perspectives in Biology*, *2*(1), a001271_erratum-a001271_erratum. https://doi.org/10.1101/cshperspect.a001271_erratum

Kierdorf, K., Hersperger, F., Sharrock, J., Vincent, C. M., Ustaoglu, P., Dou, J., Gyoergy, A., Groß, O., Siekhaus, D. E., & Dionne, M. S. (2020). Muscle function and homeostasis require cytokine inhibition of AKT activity in drosophila. *ELife*, *9*, 1–24. https://doi.org/10.7554/eLife.51595

Kobler, J. M., Rodriguez Jimenez, F. J., Petcu, I., & Grunwald Kadow, I. C. (2020). Immune Receptor Signaling and the Mushroom Body Mediate Post-ingestion Pathogen

Avoidance. *Current Biology : CB*, *30*(23), 4693-4709.e3. https://doi.org/10.1016/J.CUB.2020.09.022

Kohsaka, H., Okusawa, S., Itakura, Y., Fushiki, A., & Nose, A. (2012). Development of larval motor circuits in Drosophila. *Development Growth and Differentiation*, *54*(3), 408–419. https://doi.org/10.1111/J.1440-169X.2012.01347.X

Kondo, S., Kohsaka, S., & Okabe, S. (2011). Long-term changes of spine dynamics and microglia after transient peripheral immune response triggered by LPS in vivo. *Molecular Brain*, *4*(1), 1–16. https://doi.org/10.1186/1756-6606-4-27/FIGURES/8

Kottmeier, R., Bittern, J., Schoofs, A., Scheiwe, F., Matzat, T., Pankratz, M., & Klämbt, C. (2020). *Wrapping glia regulates neuronal signaling speed and precision in the peripheral nervous system of Drosophila*. https://doi.org/10.1038/s41467-020-18291-1

Kounatidis, I., Chtarbanova, S., Cao, Y., Hayne, M., Jayanth, D., Ganetzky, B., & Neurodegeneration, A. (2017). NF- k B Immunity in the Brain Determines Fly Lifespan in Healthy Aging and Age-Related Article NF- k B Immunity in the Brain Determines Fly Lifespan in Healthy Aging. *CellReports*, *19*(4), 836–848. https://doi.org/10.1016/j.celrep.2017.04.007

Kucukdereli, H., Allen, N. J., Lee, A. T., Feng, A., Ilcim Ozlu, M., Conatser, L. M., Chakraborty, C., Workman, G., Weaver, M., Sage, E. H., Barres, B. A., & Eroglu, C. (n.d.). *Control of excitatory CNS synaptogenesis by astrocyte-secreted proteins Hevin and SPARC*. https://doi.org/10.1073/pnas.1104977108

Kuo, T. H., Pike, D. H., Beizaeipour, Z., & Williams, J. A. (2010). Sleep triggered by an immune response in Drosophila is regulated by the circadian clock and requires the NFκB Relish. *BMC Neuroscience*, *11*(1), 1–12. https://doi.org/10.1186/1471-2202-11-17/FIGURES/5

Landgraf, M., Bossing, T., Technau, G. M., & Bate, M. (1997). The Origin, Location, and Projections of the Embryonic Abdominal Motorneurons of Drosophila. *Journal of Neuroscience*, *17*(24), 9642–9655. https://doi.org/10.1523/JNEUROSCI.17-24-09642.1997

Lemaitre, B., & Hoffmann, A. H. (1997). *Drosophila host defense : Differential induction of antimicrobial peptide genes after infection by various classes of microorganisms*. *94*(December), 14614–14619. https://doi.org/10.1073/pnas.94.26.14614

Lemaitre, B., & Hoffmann, J. (2007). The Host Defense of Drosophila melanogaster. *Annual Review of Immunology*. https://doi.org/10.1146/annurev.immunol.25.022106.141615

Lemaitre, B., Nicolas, E., Michaut, L., Reichhart, J. M., & Hoffmann, J. A. (1996). The Dorsoventral Regulatory Gene Cassette spätzle/Toll/cactus Controls the Potent Antifungal Response in Drosophila Adults. *Cell*, *86*(6), 973–983. https://doi.org/10.1016/S0092-8674(00)80172-5

Leulier, F., Parquet, C., Pili-Floury, S., Ryu, J. H., Caroff, M., Lee, W. J., Mengin-Lecreulx, D., & Lemaitre, B. (2003). The Drosophila immune system detects bacteria through specific peptidoglycan recognition. *Nature Immunology*, *4*(5), 478–484. https://doi.org/10.1038/ni922

Li, G., Forero, M. G., Wentzell, J., Durmus, I., Wolf, R., Anthoney, N., Parker, M., Jiang, R., Hasenauer, J., Strausfeld, N., Heisenberg, M., & Hidalgo, A. (2020). A toll-receptor map underlies structural brain plasticity. *ELife*, *9*, 1–32. https://doi.org/10.7554/eLife.52743

Li, Y. X., Sibon, O. C. M., & Dijkers, P. F. (2018). *Inhibition of NF-κB in astrocytes is sufficient to delay neurodegeneration induced by proteotoxicity in neurons*. 1–17.

Liauw, J., Hoang, S., Choi, M., Eroglu, C., Choi, M., Sun, G.-H., Percy, M., Wildman-Tobriner, B., Bliss, T., Guzman, R. G., Barres, B. A., & Steinberg, G. K. (2008). Thrombospondins 1 and 2 are necessary for synaptic plasticity and functional recovery after stroke. *Journal of Cerebral Blood Flow & Metabolism*, *28*, 1722–1732. https://doi.org/10.1038/jcbfm.2008.65

Limmer, S., Weiler, A., Volkenhoff, A., Babatz, F., Klämbt, C., Saunders, N. R., Brankatschk, M., & Planck, M. (2014). *The Drosophila blood-brain barrier: development and function of a glial endothelium*. https://doi.org/10.3389/fnins.2014.00365

Lu, Y., Su, F., Li, Q., Zhang, J., Li, Y., Tang, T., Hu, Q., & Yu, X. Q. (2020). Pattern recognition receptors in Drosophila immune responses. In *Developmental and Comparative Immunology* (Vol. 102). Elsevier Ltd. https://doi.org/10.1016/j.dci.2019.103468

Luo, L. (2016). *Principles of neurobiology*.

Maillet, F., Bischoff, V., Vignal, C., Hoffmann, J., & Royet, J. (2008). The Drosophila Peptidoglycan Recognition Protein PGRP-LF Blocks PGRP-LC and IMD/JNK Pathway Activation. *Cell Host and Microbe*, *3*(5), 293–303. https://doi.org/10.1016/j.chom.2008.04.002

Maitra, U., Scaglione, M. N., Chtarbanova, S., & O'donnell, J. M. (2019). innate immune responses to paraquat exposure in a Drosophila model of parkinson's disease. *Scientific Reports*, *9*(1). https://doi.org/10.1038/s41598-019-48977-6

Masuzzo, A., Montanari, M., Kurz, L., & Royet, J. (2020). How Bacteria Impact Host Nervous System and Behaviors: Lessons from Flies and Worms. In *Trends in Neurosciences* (Vol. 43, Issue 12, pp. 998–1010). https://doi.org/10.1016/j.tins.2020.09.007

Matias-Guiu, J., Ballerini, C., Sarkar, S., Wang, G., Liu, L., Liu, J., Bao, J., & Bai, Q. (2020). Interaction of Microglia and Astrocytes in the Neurovascular Unit. *Front. Immunol*, *11*, 1024. https://doi.org/10.3389/fimmu.2020.01024

McIlroy, G., Foldi, I., Aurikko, J., Wentzell, J. S., Lim, M. A., Fenton, J. C., Gay, N. J., & Hidalgo, A. (2013). Toll-6 and Toll-7 function as neurotrophin receptors in the Drosophila melanogaster CNS. *Nature Neuroscience 2013 16:9*, *16*(9), 1248–1256. https://doi.org/10.1038/nn.3474

McLaughlin, C. N., Perry-Richardson, J. J., Coutinho-Budd, J. C., & Broihier, H. T. (2019). Dying Neurons Utilize Innate Immune Signaling to Prime Glia for Phagocytosis during Development. In *Developmental Cell* (Vol. 48, Issue 4, pp. 506-522.e6). https://doi.org/10.1016/j.devcel.2018.12.019

Meffert, M. K., Chang, J. M., Wiltgen, B. J., Fanselow, M. S., & Baltimore, D. (2003). NF-κB functions in synaptic signaling and behavior. *Nature Neuroscience*, *6*(10), 1072–1078. https://doi.org/10.1038/nn1110

Michelucci, A., Syed, M. H., Adzemovic, M. Z., Kounatidis, I., & Chtarbanova, S. (2018). *Role of Glial immunity in Lifespan Determination: A Drosophila Perspective*. *9*, 1362. https://doi.org/10.3389/fimmu.2018.01362

Miller, M. G., Hamilton, D. A., Joseph, J. A., & Shukitt-Hale, B. (2018). Dietary blueberry

improves cognition among older adults in a randomized, double-blind, placebo-controlled trial. *European Journal of Nutrition*, *57*(3), 1169–1180. https://doi.org/10.1007/S00394-017-1400-8

Montanari, M., & Royet, J. (2021). Impact of microorganisms and parasites on neuronally controlled drosophila behaviours. *Cells*, *10*(9). https://doi.org/10.3390/CELLS10092350

Morgan, T. H. (1915). *LOCALIZATION OF THE HEREDITARY MATERIAL IN THE GERM CELLS*. *1*.

Muller, H. J. (1928). THE PRODUCTION OF MUTATIONS BY X-RAYS. *Amer. J. Physiol*, *13*(2).

Myllymäki, H., Valanne, S., & Rämet, M. (2014). The Drosophila Imd Signaling Pathway . *The Journal of Immunology*, *192*(8), 3455–3462. https://doi.org/10.4049/jimmunol.1303309

Nguyen, M. D., Julien, J., & Rivest, S. (2016). *Innate Immunity : The missing link in neuroprotection and neurodegeneration? April 2002*. https://doi.org/10.1038/nrn752

Nocera, G., & Jacob, C. (2020). Mechanisms of Schwann cell plasticity involved in peripheral nerve repair after injury. *Cellular and Molecular Life Sciences*, *77*, 3977–3989. https://doi.org/10.1007/s00018-020-03516-9

Nooyens, A. C. J., Bueno-De-Mesquita, H. B., Van Boxtel, M. P. J., Van Gelder, B. M., Verhagen, H., & Verschuren, W. M. M. (2011). Fruit and vegetable intake and cognitive decline in middle-aged men and women: the Doetinchem Cohort Study. *The British Journal of Nutrition*, *106*(5), 752–761. https://doi.org/10.1017/S0007114511001024

Oswald, M. C. W., Brooks, P. S., Zwart, M. F., Mukherjee, A., West, R. J. H., Giachello, C. N. G., Morarach, K., Baines, R. A., Sweeney, S. T., & Landgraf, M. (2018). Reactive oxygen species regulate activity- dependent neuronal plasticity in Drosophila. *ELife*, *7*. https://doi.org/10.7554/eLife.39393

Ovsepian, S. V. (2017). The birth of the synapse. *Brain Structure and Function*, *222*(8), 3369–3374. https://doi.org/10.1007/s00429-017-1459-2

Pan, S., Mayoral, S. R., Choi, H. S., Chan, J. R., & Kheirbek, M. A. (2020). Preservation of a remote fear memory requires new myelin formation. *NAtuRe NeuRoSCieNCe |*, *23*. https://doi.org/10.1038/s41593-019-0582-1

Panettieri, S., Paddibhatla, I., Chou, J., Rajwani, R., Moore, R. S., Goncharuk, T., John, G., & Govind, S. (2020). Discovery of Aspirin-triggered eicosanoid-like mediators in a Drosophila metainflammation blood tumor model. *Journal of Cell Science*, *133*(5). https://doi.org/10.1242/JCS.236141/266051/AM/DISCOVERY-OF-ASPIRIN-TRIGGERED-EICOSANOID-LIKE

Paolicelli, R. C., Bolasco, G., Pagani, F., Maggi, L., Scianni, M., Panzanelli, P., Giustetto, M., Ferreira, T. A., Guiducci, E., Dumas, L., Ragozzino, D., & Gross, C. T. (2011). Synaptic pruning by microglia is necessary for normal brain development. *Science*, *333*(6048), 1456–1458. https://doi.org/10.1126/science.1202529

Petersen, A. J., Katzenberger, R. J., & Wassarman, D. A. (2013). *The Innate Immune Response Transcription Factor Relish Is Necessary for Neurodegeneration in a Drosophila Model of Ataxia-Telangiectasia*. https://doi.org/10.1534/genetics.113.150854

Pimpão, R. C., Ventura, M. R., Ferreira, R. B., Williamson, G., & Santos, C. N. (2015). Phenolic

sulfates as new and highly abundant metabolites in human plasma after ingestion of a mixed berry fruit purée. *The British Journal of Nutrition*, *113*(3), 454–463. https://doi.org/10.1017/S0007114514003511

Pitman, J. L., Mcgill, J. J., Keegan, K. P., & Allada, R. (2006). *A dynamic role for the mushroom bodies in promoting sleep in Drosophila*. https://doi.org/10.1038/nature04739

Psaltopoulou, T., Sergentanis, T. N., Panagiotakos, D. B., Sergentanis, I. N., Kosti, R., & Scarmeas, N. (2013). Mediterranean diet, stroke, cognitive impairment, and depression: A meta-analysis. *Annals of Neurology*, *74*(4), 580–591. https://doi.org/10.1002/ANA.23944

Rodrigues, F., Schmidt, I., & Kla, C. (2011). *Comparing peripheral glial cell differentiation in Drosophila and vertebrates*. 55–69. https://doi.org/10.1007/s00018-010-0512-6

Rut Franzdóttir, S., Engelen, D., Yuva-Aydemir, Y., Schmidt, I., Aho, A., & Klämbt, C. (2009). *Switch in FGF signalling initiates glial differentiation in the Drosophila eye*. https://doi.org/10.1038/nature08167

Saijo, K., & Glass, C. K. (2011). Microglial cell origin and phenotypes in health and disease. *Nature Reviews Immunology*, *11*(11), 775–787. https://doi.org/10.1038/nri3086

Silva-Rodrigues, J. F., Patrício-Rodrigues, C. F., De Sousa-Xavier, V., Augusto, P. M., Fernandes, A. C., Farinho, A. R., Martins, J. P., & Teodoro, R. O. (2020). Peripheral axonal ensheathment is regulated by RalA GTPase and the exocyst complex. In *Development (Cambridge)* (Vol. 147, Issue 3). https://doi.org/10.1242/dev.174540

Snow, P. M., Patel, N. H., Harrelson, A. L., & Goodman, C. S. (1987). Neural-Specific Carbohydrate Moiety Shared by Many Surface Glycoproteins in Drosophila and Grasshopper Embryos. *The Journal of Neuroscience*, *7*(12), 4137–4144.

Sonnenfeld, M. J., & Jacobs, J. R. (1995). Macrophages and Glia Participate in the Removal of Apoptotic Neurons From the Drosophila Embryonic Nervous System. *THE JOURNAL OF COMPARATIVE NEUROLOGY*, *359*(644), 652.

Spencer, J. P. E. (2022). Symposium on “Diet and mental health” Food for thought: the role of dietary flavonoids in enhancing human memory, learning and neuro-cognitive performance. *Proceedings of the Nutrition Society*, *67*, 36. https://doi.org/10.1017/S0029665108007088

Stankovic, N. D., Teodorczyk, M., Ploen, R., Zipp, F., Mirko, ·, & Schmidt, H. H. (2016). Microglia-blood vessel interactions: a double-edged sword in brain pathologies. *Acta Neuropathol*, *3*, 347–363. https://doi.org/10.1007/s00401-015-1524-y

Stevens, B. (2003). Glia: much more than the neuron’s side-kick. *Current Biology : CB*, *13*(12), 469–472. https://doi.org/10.1016/s0960-9822(03)00404-4

Stevens, B., Allen, N. J., Vazquez, L. E., Howell, G. R., Christopherson, K. S., Nouri, N., Micheva, K. D., Mehalow, A. K., Huberman, A. D., Stafford, B., Sher, A., Litke, A. M., Lambris, J. D., Smith, S. J., John, S. W. M., & Barres, B. A. (2007). The Classical Complement Cascade Mediates CNS Synapse Elimination. *Cell*. https://doi.org/10.1016/j.cell.2007.10.036

Steward, R. (1989). Relocalization of the dorsal protein from the cytoplasm to the nucleus correlates with its function. *Cell*, *59*(6), 1179–1188. https://doi.org/10.1016/0092-8674(89)90773-3

Stork, T., Engelen, D., Krudewig, A., Silies, M., Bainton, R. J., & Klämbt, C. (2008). Organization and function of the blood-brain barrier in Drosophila. *Journal of Neuroscience*, *28*(3), 587–597. https://doi.org/10.1523/JNEUROSCI.4367-07.2008

Subramanian, J., Cunha, R. A., Fuenzalida, M., Paolicelli, R. C., Henstridge, C. M., & Tzioras, M. (2019). *Glial Contribution to Excitatory and Inhibitory Synapse Loss in Neurodegeneration*. https://doi.org/10.3389/fncel.2019.00063

Tasdemir-Yilmaz, O. E., & Freeman, M. R. (2014). Astrocytes engage unique molecular programs to engulf pruned neuronal debris from distinct subsets of neurons. *Genes & Development*, *28*(1), 20–33. https://doi.org/10.1101/GAD.229518.113

Tzou, P., Meister, M., & Lemaitre, B. (2002). 27 Methods for studying infection and immunity in Drosophila. In *Infection and immunity in Drosophila* (Vol. 9517, Issue November 2017). https://doi.org/10.1016/S0580-9517(02)31028-6

Tzou, P., Ohresser, S., Ferrandon, D., Capovilla, M., Reichhart, J. M., Lemaitre, B., Hoffmann, J. A., & Imler, J. L. (2000). Tissue-specific inducible expression of antimicrobial peptide genes in Drosophila surface epithelia. *Immunity*, *13*(5), 737–748. https://doi.org/10.1016/S1074-7613(00)00072-8

Vanha-aho, L. M., Valanne, S., & Rämet, M. (2016). Cytokines in Drosophila immunity. *Immunology Letters*, *170*, 42–51. https://doi.org/10.1016/j.imlet.2015.12.005

Vaz, F., Kounatidis, I., Covas, G., Parton, R. M., Harkiolaki, M., Davis, I., Filipe, S. R., & Ligoxygakis, P. (2019). Accessibility to Peptidoglycan Is Important for the Recognition of Gram-Positive Bacteria in Drosophila. *Cell Reports*, *27*(8), 2480-2492.e6. https://doi.org/10.1016/j.celrep.2019.04.103

Venken, K. J. T., Simpson, J. H., & Bellen, H. J. (2011). Genetic manipulation of genes and cells in the nervous system of the fruit fly. *Neuron*, *72*(2), 202–230. https://doi.org/10.1016/j.neuron.2011.09.021

von Hilchen, C. M., Bustos, Á. E., Giangrande, A., Technau, G. M., & Altenhein, B. (2013). Predetermined embryonic glial cells form the distinct glial sheaths of the Drosophila peripheral nervous system. *Development (Cambridge)*, *140*(17), 3657–3668. https://doi.org/10.1242/dev.093245

von Philipsborn, A. C., Liu, T., Yu, J. Y., Masser, C., Bidaye, S. S., & Dickson, B. J. (2011). Neuronal Control of Drosophila Courtship Song. *Neuron*, *69*(3), 509–522. https://doi.org/10.1016/J.NEURON.2011.01.011/ATTACHMENT/900CDA4B-6852-4CA6-8AE8-2407D77B7B8E/MMC10.MOV

Wellmann, H., Kaltschmidt, B., & Kaltschmidt, C. (2001). Retrograde Transport of Transcription Factor NF-κB in Living Neurons. *Journal of Biological Chemistry*, *276*(15), 11821–11829. https://doi.org/10.1074/JBC.M009253200

Wiklund, M. L., Steinert, S., Junell, A., Hultmark, D., & Stöven, S. (2009). The N-terminal half of the Drosophila Rel/NF-κB factor Relish, REL-68, constitutively activates transcription of specific Relish target genes. *Developmental and Comparative Immunology*, *33*(5), 690–696. https://doi.org/10.1016/j.dci.2008.12.002

Williams, J. A., Sathyanarayanan, S., Hendricks, J. C., & Sehgal, A. (2007). Interaction Between Sleep and the Immune Response in Drosophila: A Role for the NFκB Relish. *Sleep*, *30*(4), 389–400. https://doi.org/10.1093/SLEEP/30.4.389

Williams, M. J. (2007). Drosophila Hemopoiesis and Cellular Immunity . *The Journal of Immunology*, *178*(8), 4711–4716. https://doi.org/10.4049/jimmunol.178.8.4711

Wilton, D. K., Dissing-Olesen, L., & Stevens, B. (2019). Neuron-Glia Signaling in Synapse Elimination. *Annual Review of Neuroscience*, *42*, 107–127. https://doi.org/10.1146/annurev-neuro-070918-050306

Winkler, B., Funke, D., Benmimoun, B., Spéder, P., Rey, S., Logan, M. A., & Klämbt, C. (2021). *Brain inflammation triggers macrophage invasion across the blood-brain barrier in Drosophila*. *October*, 1–16.

Yang, Q. qiao, & Zhou, J. wei. (2019). Neuroinflammation in the central nervous system: Symphony of glial cells. *Glia*, *67*(6), 1017–1035. https://doi.org/10.1002/glia.23571

Yeh Jan, L., & Nung Jan, Y. (1982). Antibodies to horseradish peroxidase as specific neuronal markers in Drosophila and in grasshopper embryos (neural development/segmentation mutants/differentiation antigen/pioneer neurons). In *Proc. NatL Acad. Sci. USA* (Vol. 79).

Yi, Y., Xu, W., Fan, Y., & Wang, H. X. (2021). Drosophila as an emerging model organism for studies of food-derived antioxidants. *Food Research International*, *143*(68), 110307. https://doi.org/10.1016/j.foodres.2021.110307

Yildirim, K., Petri, J., Kottmeier, R., & Klämbt, C. (2019). Drosophila glia: Few cell types and many conserved functions. *Glia*, *67*(1), 5–26. https://doi.org/10.1002/glia.23459

Zhang, S. H., Shurin, G. V, Khosravi, · Hasan, Kazi, R., Kruglov, O., Shurin, M. R., & Bunimovich, Y. L. (2020). Immunomodulation by Schwann cells in disease. *Cancer Immunology, Immunotherapy*, *69*, 245–253. https://doi.org/10.1007/s00262-019-02424-7

Zhou, J., Valentini, E., & Boutros, M. (2021). Microenvironmental innate immune signaling and cell mechanical responses promote tumor growth. *Developmental Cell*, *56*(13), 1884-1899.e5. https://doi.org/10.1016/j.devcel.2021.06.007

9. SUPPLEMENTS

Table 9.1 Statistics

Figure 4.1. Fat Body Relish Nuclear/Cytosolic Ratio				
Genotype/Condition	n(animals;nuclei)	Normality	Test Used	Mean ± SEM
Ppl>RelishYFP Uninfected	6/ 61	Yes	Mann-Whitney test	0,996±0.016
Ppl>RelishYFP Infected 30+30	6/ 58	No		1.183±0.043

	significant?	P value
Uninfected Vs Infected	**	0,0026

Figure 4.2. Muscles Relish Nuclear/Cytosolic Ratio				
Genotype/Condition	n(animals;nuclei)	Normality	Test Used	Mean ± SEM
Mhc>RelishYFP Uninfected	5/225	No	Mann-Whitney test	1.775±0.033
Mhc>RelishYFP Infected 30+30	7/385	No		2.339±0.029

	significant?	P value
Uninfected Vs Infected	***	<0,0001

Figure 4.3. Glia Relish Nuclear/Cytosolic Ratio				
Genotype/Condition	n(animals;nerves)	Normality	Test Used	Mean ± SEM
Repo>RelishYFP Uninfected	15/60	Yes	Mann-Whitney test	1.000±0.042
Repo>RelishYFP Infected	18/60	Yes		1.652±0.067

	significant?	P value
Uninfected Vs Infected	***	<0,0001

Figure 4.4. Glia Relish Nuclear/Cytosolic Ratio				
Genotype/Condition	n(animals;nuclei)	Normality	Test Used	Mean ± SEM
Repo>RelishYFP Uninfected	24/96	No	OVA Kruskal-Wallis	1,000±0.025
Repo>RelishYFP Infected 30'	15/45	No		1.919±0.127
Repo>RelishYFP Infected 1h	18/55	No		2.346±0.116
Repo>RelishYFP Infected 1h30	19/57	No		2.148±0.132

	significant?	P value
Uninfected Vs Infected 30'	***	<0,0001
	significant?	P value
Uninfected Vs Infected 30'+30'post	***	<0,0001
	significant?	P value
Uninfected Vs Infected 30'+1h post	***	<0,0001

	significant?	P value
Infected 30' Vs Infeceted 30'+30' post	ns	0,1216
	significant?	P value
Infected 30' Vs Infeceted 30'+ 1h post	ns	>0,9999
	significant?	P value
Infected 30'+30' post Vs Infeceted 30'+1h post	ns	0,8822

Figure 4.5. Glia (Pannel D) Flurescence Variation				
Genotype/Condition	n(animals;nerves)	Normality	Test Used	Mean ± SEM
Repo>RelishYFP Uninfected 1st	8/8	Yes	Mann whitney test	-0.008±0.050
Repo>RelishYFP Infected	6/6	No		0.888±0.346
Repo>RelishYFP Uninfected 2nd	8/8	Yes	Mann whitney test	0.023±0.085
Repo>RelishYFP Infected	6/6	No		0.695±0.257
Repo>RelishYFP Uninfected 3rd	7/7	Yes	Unpaired t-test	0.096±0.223
Repo>RelishYFP Infected	4/4	Yes		0.223±0.196

	significant?	P value
1st Uninfected Vs Infected	***	0,0007
	significant?	P value
2nd Uninfected Vs Infected	**	0,0047
	significant?	P value
3rd Uninfected Vs Infected	ns	0,3093

Figure 4.9. Perineurial Glia (Pannel B') Relish Nuclear/Cytosolic Ratio				
Genotype/Condition	n(animals;nerves)	Normality	Test Used	Mean ± SEM
Bsg>RelishYFP Unstim	2/4	Yes	Unpaired t test	1.000±0.125
Bsg>RelishYFP Infected 30+30	3/6	Yes		0.847±0.146

	significant?	P value
Uninfected Vs Infected	ns	0,5332

Figure 4.9. Subperineurial Glia (Pannel C') Relish Nuclear/Cytosolic Ratio				
Genotype/Condition	n(animals;nerves)	Normality	Test Used	Mean ± SEM
Mdr>RelishYFP Uninfected	8/11	Yes	Unpaired t-test	1,009±0.09645
Mdr>RelishYFP Infected	8/13	Yes		2.459±0.2107

	significant?	P value
Uninfected Vs Infected	***	<0,0001

Figure 4.9. Wrapping Glia (Pannel D') Relish Nuclear/Cytosolic Ratio				
Genotype/Condition	n(animals;nerves)	Normality	Test Used	Mean ± SEM
Nrv2>RelishYFP Uninfected	8/22	No	Mann-Whitney test	1,000±0.06583
Nrv2>RelishYFP Infected	8/24	Yes		2.266±0.1381

	significant?	P value
Uninfected Vs Infected	***	<0,0001

Figure 4.11. Ghost Boutons				
Genotype/Condition	n(animals;NMJs)	Normality	Test Used	Mean ± SEM
WIII8 Uninfected	29/111	No	Mann whitney test	1,658±0.193
WIII8 Infected	39/116	No		2,491±0.248

	significant?	P value
Uninfected Vs Infected	**	0,0044

Figure 4.12. Debris Area				
Genotype/Condition	n(animals;NMJs)	Normality	Test Used	Mean ± SEM
WIII8 Uninfected	12/43	No	Kruskal-Wallis test	0.01891±0.00285
WIII8 Infected 300	16/49	No		0.05159±0.00502
WIII8 Infected 600	7/18	No		0.07976±0.01121

	significant?	P value
Uninfected Vs Infected 300	***	<0,0001
Uninfected Vs Infected 600	***	<0,0001
Infected 300 Vs Infected 600	ns	0,1146

Figure 4.12. Debris Intensity				
Genotype/Condition	n(animals;NMJs)	Normality	Test Used	Mean ± SEM
WIII8 Uninfected	12/43	Yes	Kruskal-Wallis test	32.04±2.030
WIII8 Infected 300	16/49	No		54.50±3.669
WIII8 Infected 600	7/18	No		64.09±7.501

	significant?	P value
Uninfected Vs Infected 300	***	<0,0001
Uninfected Vs Infected 600	***	<0,0001
Infected 300 Vs Infected 600	ns	0,7887

Figure 4.13. NMJ Glial processes Overall Glia Area				
Genotype/Condition	n(NMJs)	Normality	Test Used	Mean ± SEM
Repo>CD4GFP Uninfected	4/13	Yes	Unpaired t test	261,4 ±29.22
Repo>CD4GFP Infected	4/13	Yes		214±16.58

	significant?	P value
Uninfected Vs Infected	ns	0,1708

Figure 4.13. NMJ Glial processes Glia Area Processes				
Genotype/Condition	n(NMJs)	Normality	Test Used	Mean ± SEM
Repo>CD4GFP Uninfected	4/13	Yes	Unpaired t test	74.78±11.77
Repo>CD4GFP Infected	4/13	Yes		50.17±6.11

	significant?	P value
Uninfected Vs Infected	ns	0,0757

Figure 4.13. NMJ Glial processes Number of Processes				
Genotype/Condition	n(NMJs)	Normality	Test Used	Mean ± SEM
Repo>CD4GFP Uninfected	4/13	Yes	Unpaired t test	6.615 ±0.626
Repo>CD4GFP Infected	4/13	Yes		7.917±0.892

	significant?	P value
Uninfected Vs Infected	ns	0,2386

Figure 4.14. NMJ Subperineurial Glia Glia Processes Area				
Genotype/Condition	n(animals;NMJs)	Normality	Test Used	Mean ± SEM
Mdr>CD4GFP Uninfected	/32	No	Mann-Whitney test	12.57±2.403
Mdr>CD4GFP Infected	/17	No		9.46±2.138

	significant?	P value
Uninfected Vs Infected	ns	0,7752

Figure 4.14. NMJ Subperineurial Glia Overall Area				
Genotype/Condition	n(animals;NMJs)	Normality	Test Used	Mean ± SEM
Mdr>CD4GFP Uninfected	/32	Yes	Mann-Whitney test	300.2±30.64
Mdr>CD4GFP Infected	/17	No		247.0±36.08

	significant?	P value
Uninfected Vs Infected	ns	0,1915

Figure 4.14. NMJ Subperineurial Glia Number of processes				
Genotype/Condition	n(animals;NMJs)	Normality	Test Used	Mean ± SEM
Mdr>CD4GFP Uninfected	/32	No	Mann-Whitney test	12.33±1.401
Mdr>CD4GFP Infected	/17	Yes		14.40±1.644

	significant?	P value
Uninfected Vs Infected	ns	0,208

Figure 4.16. All Glia (Pannel C) Relish Nuclear/Cytosolic Ratio				
Genotype/Condition	n(animals;nerves)	Normality	Test Used	Mean ± SEM
Repo>RelishYFP Control Basal	12/42	Yes	Kruskal-Wallis test	1,00±0,057
Repo>RelishYFP Asp Basal	13/55	No		0,99±0,065
Repo>RelishYFP Pyr-Sul Basal	12/64	No		1,00±0,068

	significant?	P value
Control vs. Aspirin	ns	>0,9999
Control vs. Pyr-Sul	*	0,0396
Aspirin vs. Pyr-Sul	*	0,0282

Figure 4.17. Subperineurial Glia (Pannel B) Relish Nuclear/Cytosolic Ratio				
Genotype/Condition	n(animals;nerves)	Normality	Test Used	Mean ± SEM
Mdr>RelishYFP Control Basal	5/21	Yes	Ordinary one-way ANOVA	1,00±0,057
Mdr>RelishYFP Asp Basal	5/15	Yes		0,99±0,065
Mdr>RelishYFP Pyr-Sul Basal	5/19	Yes		1,00±0,068

	significant?	P value
Control vs. Aspirin	ns	0,9935
Control vs. Pyr-Sul	ns	0,9992
Aspirin vs. Pyr-Sul	ns	0,9891

Figure 4.17. Wrapping Glia (Pannel D) Relish Nuclear/Cytosolic Ratio				
Genotype/Condition	n(animals;nerves)	Normality	Test Used	Mean ± SEM
Nrv2>RelishYFP Control Basal	6/15	Yes	Ordinary one-way ANOVA	1,000±0,043
Nrv2>RelishYFP Asp Basal	6716	Yes		0,796±0,038
Nrv2>RelishYFP Pyr-Sul Basal	6723	Yes		0,907±0,038

	significant?	P value
Control vs. Aspirin	**	0,0046
Control vs. Pyr-Sul	ns	0,2354
Aspirin vs. Pyr-Sul	ns	0,1243

Figure 4.18. Glia
(Pannel B)
Relish Nuclear/Cytosolic Ratio

Genotype/Condition	n(animals;nerves)	Normality	Test Used	Mean ± SEM
Repo>RelishYFP Control Uninfected	5/14	Yes	Kruskal-Wallis test	1,123±0.112
Repo>RelishYFP Control Infected	5/8	Yes		2,259±0.231
Repo>RelishYFP Asp Uninfected	7/36	No		1,112±0.066
Repo>RelishYFP Asp Infected	5/15	Yes		1,241±0.139
Repo>RelishYFP Pyr-Sul Uninfected	7/39	No		1,118±0.072
Repo>RelishYFP Pyr-Sul Infected	7/39	Yes		1,401±0.071

	significant?	P value
Control Uninfected vs. Control Infected	**	0,0068
Control Uninfected vs. Aspirin Uninfected	ns	>0,9999
Control Uninfected vs. Aspirin Infected	ns	>0,9999
Control Uninfected vs. PyrSul Uninfected	ns	>0,9999
Control Uninfected vs. PyrSul Infected	ns	>0,9999
Control Infected vs. Aspirin Uninfected	***	0,0004
Control Infected vs. Aspirin Infected	*	0,0208
Control Infected vs. PyrSul Uninfected	***	0,0002
Control Infected vs. PyrSul Infected	*	0,0244
Aspirin Uninfected vs. Aspirin Infected	ns	>0,9999
Aspirin Uninfected vs. PyrSul Uninfected	ns	>0,9999
Aspirin Uninfected vs. PyrSul Infected	ns	0,059
Aspirin Infected vs. PyrSul Uninfected	ns	>0,9999
Aspirin Infected vs. PyrSul Infected	ns	>0,9999
PyrSul Uninfected vs. PyrSul Infected	*	0,0352

Figure 4.19. Subperineurial Glia
(Pannel B)
Relish Nuclear/Cytosolic Ratio

Genotype/Condition	n(animals;nerves)	Normality	Test Used	Mean ± SEM
Mdr>RelishYFP Control Uninfected	5/8	Yes	Ordinary one-way ANOVA	1,000 ± 0,083
Mdr>RelishYFP Control Infected	513	Yes		1,775 ± 0,135
Mdr>RelishYFP Asp Uninfected	5/18	Yes		1,477 ± 0.110
Mdr>RelishYFP Asp Infected	5/12	Yes		1,329 ± 0,103
Mdr>RelishYFP Pyr-Sul Uninfected	5/12	Yes		1,150 ± 0,098
Mdr>RelishYFP Pyr-Sul Infected	5/7	Yes		1,407 ± 0.167

	significant?	P value
Control Uninfected vs. Control Infected	***	<0,0001
Control Uninfected vs. Aspirin Uninfected	*	0,0106
Control Uninfected vs. Aspirin Infected	ns	0,2749
Control Uninfected vs. PyrSul Uninfected	ns	0,9229
Control Uninfected vs. PyrSul Infected	ns	0,2406
Control Infected vs. Aspirin Uninfected	ns	0,3581
Control Infected vs. Aspirin Infected	ns	0,0864
Control Infected vs. PyrSul Uninfected	**	0,004
Control Infected vs. PyrSul Infected	ns	0,4066
Aspirin Uninfected vs. Aspirin Infected	ns	0,9284
Aspirin Uninfected vs. PyrSul Uninfected	ns	0,2838
Aspirin Uninfected vs. PyrSul Infected	ns	0,9989
Aspirin Infected vs. PyrSul Uninfected	ns	0,8932
Aspirin Infected vs. PyrSul Infected	ns	0,9987
PyrSul Uninfected vs. PyrSul Infected	ns	0,7773